Membrane lipids of the (hyper)thermophilic, methanogenic archaea *Methanothermobacter marburgensis*, *Methanocaldococcus villosus* and *Methanothermococcus okinawensis* and their geobiological and astrobiological relevance

Dissertation
zur Erlangung des Doktorgrades der Naturwissenschaften
an der Fakultät für Mathematik, Informatik und Naturwissenschaften
Fachbereich Geowissenschaften
der Universität Hamburg

vorgelegt von Lydia Baumann
aus Scheibbs, Österreich

Hamburg, 2020

Als Dissertation angenommen am Fachbereich Geowissenschaften

Tag des Vollzugs der Promotion:	16.06.2020
Gutachter/Gutachterinnen:	Prof. Dr. Jörn Peckmann
	Dr. Daniel Birgel
Vorsitzender des Fachpromotionsausschusses Geowissenschaften:	Prof. Dr. Dirk Gajewski
Dekan der Fakultät MIN:	Prof. Dr. Heinrich Graener

I. Table of contents

II. Lists of figures and tables

II.1 Figures

II.2 Tables

II.3 Supplementary Figures

II.4 Supplementary Tables

III. Acknowledgments

First of all, many thanks to my doctor fathers and supervisors Jörn Peckmann and Daniel Birgel, who made this dissertation possible. I am deeply grateful for your superior support, your availability, and patience during the meanwhile almost seven years we are working together. You two managed to create a pleasant and respectful working atmosphere, an atmosphere in which I felt to meet you at the same level. I never took this amount of effort for granted. Second, I thank Ruth-Sophie Taubner and Simon K.-M. R. Rittmann from the University of Vienna as our closest project partners for design of the experimental settings, for cultivation, analysis of amino acids, and for countless and fruitful consultations. Further, I express my gratitude to Sabine Beckmann. Without your technical support, the lipid extraction, measurements and data evaluation would have been substantially more difficult, if not impossible. Sabine, thanks for all the advice, frankness, and kindness, even and especially in the most difficult moments. I cannot put into words what all of this meant to me.

Other researchers and technicians contributed as well to this doctoral thesis. Thanks to Thorsten Bauersachs from the University of Kiel for HPLC-APCI-MS/MS measurements to confirm the identification of the detected lipids, for measurements and data evaluation of intact polar lipids, and for thorough proofreading of manuscripts. I also acknowledge Elisabeth L. Clifford, Barbara Mähnert, Barbara Reischl, and Sibylle Spann-Birk from the University of Vienna. Elisabeth L. Clifford developed the method for amino acid measurements, helped with interpretation of amino acid data, and helped writing the respective article. Barbara Mähnert helped measuring the amino acids, and Barbara Reischl helped to evaluate amino acid data. Sibylle Spann-Birk helped with the graphical design of Figure 1a. Richard Seifert from the University of Hamburg is thanked for extensive advice, discussions, and proofreading.

There are also several Master and Bachelor students, who contributed to this thesis and whom I want to thank here. Michael Steiner helped cultivate the Archaea at the University of Vienna. Jan Kruse, Khushi Sahu, Ann-Cathrin Rohrweber, Matthias Thiele, and Kordian Korynt helped me with lipid extraction, and partly also with data evaluation and interpretation at the University of Hamburg. I appreciate your trust, your extraordinary ambition, carefulness, your cheerful minds, and your feedback. I feel really lucky to had the opportunity to work together with you. I also feel lucky to have worked together with Marcello Natalicchio and with Kinga Oláh. Marcello Natalicchio was here in Hamburg as a postdoc for two years, spreading good mood and cheering me up when I was fighting with the HPLC-MS. Kinga Oláh was a doctoral student at the University of Vienna, and she impressed me with her abilities as a team player, her strong will, and her kindness, even in the face of severe obstacles.

Life at university was much more joyful with my colleagues and loyal friends Sabine Prader, Mathia Sabino, Alexmar Cordova-Gonzalez, Yu Pei, Nicole and Jörg Burdanowitz, Nicola Krake, Simon Rouwendaal, and Hatice Demirbay. Thanks for spending time together, at university and outside, thanks for eating and cooking together, going to science slams, and thanks for sharing sorrows and happiness.

As in the last part of my doctoral studies I was not employed at the university any more, I needed another source of income, which I finally found. I found it thanks to Christina Leo, who was my charming and ambitious job coach, and thanks to Rudi Siegfried Krengel, a personnel consultant, who had the right idea in the right moment and gave me the job I needed in that truly special situation. Ms. Leo and Mr. Krengel, I know I was and I am by no means a standard

client for you. Nevertheless, you supported me much more than you had to. Due to you it was financially possible for me to complete this dissertation. Thank you so much for that.

Luckily, I still had, and have, a life apart from university and people around me, who gave me the necessary support, motivation, inspiration, and distraction, to keep on track, while not loosing myself in this long-term endeaveor. Therefore, I want to thank my parents Christine and Alfred Baumann, my grandparents Christine and Anton Hintersteiner, and my brothers Georg and Alexander Baumann, who I am happy to also call my friends. Both, my family and my close friends from Austria, Barbara Reisinger, Sandra Watschka, Hermann Sandberger, Katharina Böhm, Gregor Hofer, Christine Peters, Birgit Steininger, and Nicolas Robisch were incredibly supportive, compassionate, frank, and generous. Although we could not see often within the last years, you have been always there for me, just one call away, and visiting me, whenever possible. And when I was visiting you in Austria (or Amsterdam, or Zurich), I felt instantaneously at home and welcome, like no time would have passed by. Many, many thanks to you wonderful people.

I also say thank you to my friends in Portugal, Flávia Silva, André Martins, and João Marques for great moments in and around Lisbon; and to the friends I got to know in Hamburg, Martin Busch, Isabel Martin, Yasmin Fede Schwietzer, Diana Dahms, Thomas Brandenburg, and Jan Sikora. I feel so grateful for the time we had together, and for your understanding, when we could not spend time together. You stepped into my life recently, and by doing so, made it a lot richer, each of you in her / his way. Josephine Osakwe, Mihai Chira, and Scott Konetzny accompanied me on a part of my journey through this doctorate. Thank you for the unusual we experienced together, and thank you, Scott Konetzny, for bringing Patrick Macanga into my life. Patrick, you have been at my side for almost the entire doctoral studies. You helped me think and being creative, when my creativity seemed exhausted, you were there for me in my sadest moments, and celebrated with me the very best ones, and you were brave enough to connect your life with the one of a junior scientist. Thank you, Patrick.

IV. List of Abbreviations

DoE …… Design of Experiment
DFAA …… Dissolved Free Amino Acids
Ala …… Alanine
Arg …… Arginine
Asn …… Asparagine
Asp …… Aspartic acid
Cys …… Cysteine
GABA …… Gamma-Amino Butyric Acid
Gln …… Glutamine
Glu …… Glutamic acid
Gly …… Glycine
His …… Histidine
Ile …… Isoleucine
Leu …… Leucine
Lys …… Lysine
Met …… Methionine
Phe …… Phenylalanine
Ser …… Serine
Tau …… Taurine
Thr …… Threonine
Trp …… Tryptophane
Tyr …… Tyrosine
Val …… Valine
H_2O …… Water
H_2 …… Molecular hydrogen
CO …… Carbon monoxide
CO_2 …… Carbon dioxide
CH_4 …… Methane
C_2H_4 …… Ethene
CH_2O …… Formaldehyde
CH_3OH ….. Methanol
NH_3 …… Ammonia
NH_4Cl …… Ammonium chloride
-OH …… Hydroxyl group
$-NH_2$ …… Amine group
-COOH ….. Carboxyl group
DAGE $C_{16:16}$ 1,2-Di-*O*-hexadecyl-*rac*-glycerol diether
DAGE $C_{18:18}$ 1,2-Di-*O*-octadecyl-*rac*-glycerol diether
DCM …… DiChloroMethane
HCl …… HydroChloric acid
HCO_2H ..… Formic acid
NaH_2PO_4 .. Monosodium phosphate
OPA …… O-PhthalAldehyde
N_2 …… Dinitrogen
GC …… Gas Chromatography
HPLC …… High Performance Liquid Chromatography
FID …… Flame Ionization Detection
MS …… Mass Spectrometry

MS/MS ..… Tandem Mass Spectrometry
APCI …… Atmospheric Pressure Chemical Ionization
ESI …… ElectroSpray Ionization
PTFE …… PolyTetraFluoroEthylene
UI …… Ultra Inert
TLE …… Total Lipid Extract
IPL …… Intact Polar Lipid
1G …… MonoGlycosidic (head group)
2G …… DiGlycosidic (head group)
PG …… PhosphoGlycosidic (head group)
AR …… Archaeol
MAR …… Macrocyclic Archaeol
Arch. …… Archaeol
Macr. …… Macrocyclic Archaeol
GDGT …… Glycerol Dialkyl Glycerol Tetraether
GMGT…… Glycerol Monoalkyl Glycerol Tetraether
GTGT …… Glycerol Trialkyl Glycerol Tetraether
GDD …… Glycerol Dialkyl Diether
GMD …… Glycerol Monoalkyl Diether
BDGT …… Butanetriol Dialkyl Glycerol Tetraether
PDGT …… Pentanetriol Dialkyl Glycerol Tetraether
OD …… Optical density (OD_{max} = maximum OD; OD_{end} = OD at end of cultivation)
rRNA …… ribosomal Ribose Nucleic Acid
rDNA …… ribosomal Desoxyribose Nucleic Acid

V. Abstract

The membrane core lipid and the intact polar lipid inventory of *Methanocaldococcus villosus* (DSM 22612^T) and *Methanothermococcus okinawensis* (DSM 14208^T), two strains of (hyper)thermophilic, methanogenic archaea isolated from deep-sea hydrothermal vents, is described here for the first time. Both strains reveal abundant mono- and diglycosidic head groups, with *M. okinawensis* also having minor phosphoglycosidic head groups. They exhibit an identical core lipid inventory, but can be distinguished by the different relative proportions of core lipids produced. The by far most abundant lipids are the diether lipids archaeol and macrocyclic archaeol. The latter is most likely the most specific membrane lipid for these archaea. A novelty was the detection of two isomers of GMGT-0a, which have never been detected in any organism before. GMGTs and GTGTs have not been found previously in any species of these two genera.

M. villosus and *M. okinawensis* were not only cultured under their optimal conditions. The two strains and the thermophilic *Methanothermobacter marburgensis* (DSM 2133^T), a methanogen isolated from anaerobic sewage sludge, were grown under varying temperature and nutrient supply. *M. okinawensis* was also cultured under varying concentrations of substances, which are usually regarded as inhibitors for life: ammonium chloride, formaldehyde, and methanol. These three potential inhibitors have been found in the plume of Saturn's icy moon Enceladus. After cultivation with these inhibitors, core lipids and amino acids of *M. okinawensis* were analyzed to find biomarker patterns, which could be useful not only to study life on Earth, but also for the search for extraterrestrial life in the Solar System. Depending on the amount of ammonium chloride, formaldehyde, and methanol in the growth medium *M. okinawensis* reveals different patterns of growth, lipid production, and amino acid excretion. Ammonium chloride and formaldehyde had a strong impact on these parameters, while methanol did not markedly affect them.

When exposed to varying temperatures, volumes (25 mL, 50 mL, or 75 mL in ~120 mL serum bottles), and composition of liquid medium, or gas exchange frequency, *M. marburgensis*, *M. villosus*, and *M. okinawensis* also adapted their core lipid compositions. *M. marburgensis* has a different core lipid inventory than the more closely related *M. villosus* and *M. okinawensis*, revealing no macrocyclic archaeol, but instead GDGTs and GMGTs with additional methylations in their isoprenoid chains. Nevertheless, the lipid response to varying growth conditions is similar in all three organisms. Temperature had the strongest effect on lipid composition in all three strains. *M. villosus* showed the overall weakest response of lipid patterns to changing culture parameters. In contrast, *M. okinawensis* revealed the strongest and clearest response, with archaeol and GTGT-0a being most abundant at 50°C and 25 mL of liquid medium, and macrocyclic archaeol and the GMGTs being most abundant at 60°C and 75 mL. Except for macrocyclic archaeol, *M. marburgensis* showed a similar response, and in *M. villosus* macrocylic archaeol and the GMGTs are more abundant at 80°C than at 65°C. In all three strains, those lipids, which are considered more specific to these methanogens and considered to build up more rigid membranes, namely macrocyclic archaeol, certain GDGTs and GMGTs are more abundant at or slightly below temperature optimum. On the other hand, the comparably unspecific and supposedly less rigidifying lipids archaeol and GTGT-0a have their highest abundance about 15°C below the optimum temperature and at 25 mL of liquid medium.

The outcomes of this thesis might improve our understanding of the adaptations of the cell membrane of presumably primordial life forms to environmental changes and might

complement the biomarker concept for the terrestrial, and perhaps, the extraterrestrial application.

VI. Kurzfassung

Das Inventar an Membran-Core-Lipiden und intakten polaren Lipiden von *Methanocaldococcus villosus* (DSM 22612^T) und *Methanothermococcus okinawensis* (DSM 14208^T), zwei Stämmen (hyper)thermophiler, methanogener Archaeen, die von Hydrothermalquellen in der Tiefsee isoliert wurden, wird hier zum ersten Mal beschrieben. Beide Stämme weisen hauptsächlich mono- und diglycosidische Kopfgruppen auf, wobei *M. okinawensis* zudem geringfügig phosphoglycosidische Kopfgruppen beinhaltet. Sie haben dasselbe Inventar an Core-Lipiden, können aber voneinander unterschieden werden durch die unterschiedlichen relativen Anteile der Core-Lipide. Die mit Abstand häufigsten Lipide sind die Dietherlipide Archaeol und makrozyklisches Archaeol. Letzteres ist höchstwahrscheinlich das spezifischte Membranlipid dieser Archaeen. Völlig neu war der Nachweis von zwei Isomeren von GMGT-0a, die bisher noch in keinem anderen Organismus gefunden wurden. GMGTs und GTGTs wurden vor dieser Arbeit noch in keiner anderen Spezies dieser beiden Gattungen nachgewiesen.

M. villosus und *M. okinawensis* wurden nicht nur unter ihren Optimalbedingungen kultiviert. Die beiden Stämme und der thermophile *Methanothermobacter marburgensis* (DSM 2133^T), ein Methanogener, der aus anaerobem Klärschlamm isoliert wurde, wurden variierender Temperatur und Nährstoffzufuhr ausgesetzt. *M. okinawensis* wurde außerdem unter variierenden Konzentrationen von Substanzen kultiviert, die für gewöhnlich als Inhibitoren für Lebewesen angesehen werden: Ammoniumchlorid, Formaldehyd und Methanol. Diese drei potentiellen Inhibitoren wurden im Plume von Saturns Eismond Enceladus nachgewiesen. Nach der Kultivierung mit diesen drei Inhibitoren wurden die Core-Lipide und Aminosäuren von *M. okinawensis* untersucht um Muster der Biomarker zu finden, die nützlich sein könnten, nicht nur um das Leben auf der Erde zu studieren, sondern auch für die Suche nach extraterrestrischem Leben im Sonnensystem. In Abhängigkeit von der Menge an Ammoniumchlorid, Formaldehyd und Methanol im Wachstumsmedium zeigte *M. okinawensis* unterschiedliche Muster in Wachstumsrate, Lipidproduktion und Aminosäurenexkretion. Ammoniumchlorid und Formaldehyd hatten einen starken Effekt auf die genannten Parameter, während Methanol sie nicht merklich beeinflusste.

Wenn sie variierenden Temperaturen, Volumina (25 mL, 50 mL, oder 75 mL in ~120 mL Serumflaschen) und Zusammensetzungen des Flüssigmediums, oder unterschiedlichen Frequenzen des Gasaustauschs ausgesetzt waren, passten *M. marburgensis*, *M. villosus*, und *M. okinawensis* ihre Core-Lipid-Zusammensetzungen an. *M. marburgensis* hat ein anderes Core-Lipid-Inventar als die beiden näher miteinander verwandten *M. villosus* und *M. okinawensis. M. marburgensis* weist kein makrozyklisches Archaeol auf, stattdessen produziert es GDGTs und GMGTs mit zusätzlichen Methylgruppen in deren Isoprenoidketten. Nichtsdestotrotz ist die Reaktion auf die variierenden Wachstumsbedingungen ähnlich in allen drei Organismen. Temperatur hatte den stärksten Effekt auf die Lipidzusammensetzung in allen drei Stämmen. *M. villosus* zeigte insgesamt die schwächste Reaktion der Lipidmuster auf die sich ändernden Kultivierungsparameter. Im Gegensatz dazu zeigte *M. okinawensis* die stärksten und eindeutigsten Reaktionen. Archaeol und GTGT-0a sind am häufigsten bei 50°C und 25 mL

Flüssigmedium, und makrozyklisches Archaeol und die GMGTs sind am häufigsten bei 60°C und 75 mL. Außer beim makrozyklischen Archaeol zeigte *M. marburgensis* sehr ähnliche Reaktionen, und in *M. villosus* waren makrozyklisches Archaeol und die GMGTs häufiger bei 80°C verglichen zu 65°C. In allen drei Stämmen waren jene Lipide, die als spezifischer für diese Methanogenen betrachtet werden, und jene, die als solche gelten, die stabilere Membranen aufbauen, nämlich makrozyklisches Archaeol, bestimmte GDGTs und GMGTs, häufiger beim oder etwas unter dem Temperaturoptimum. Andererseits waren die vergleichsweise unspezifischen und wahrscheinlich weniger membranstabilisierenden Lipide Archaeol und GTGT-0a am häufigsten bei ca. 15°C unter dem Temperaturoptimum und bei 25 mL Flüssigmedium.

Die Ergebnisse dieser Doktorarbeit könnten das Verständnis verbessern von den Anpassungen der Zellmembran vermutlich ursprünglicher Lebensformen an Umweltveränderungen und könnten das Biomarkerkonzept ergänzen, für die terrestrische, und möglicherweise die extraterrestrische, Anwendung.

1. Introduction

Methanogenic archaea are the only known group of organisms producing methane. By doing this, they fulfill important ecological roles and degrade the most recalcitrant organic molecules, such as methanol, methylated sulfides, methylamines, acetate, and formate in zones devoid of sufficient potent electron acceptors such as oxygen or sulfate (Liu and Whitman, 2008). These zones can be anoxic sediments, soils, swamps, peat bogs, or rice paddies, biogas plants, and the gastrointestinal tracts of various kinds of animals, such as termites, ruminants, and also humans (e.g. Liu and Whitman, 2008; Thauer et al., 2008; Offre et al., 2013). Not all, but many methanogens are thermophilic to different degrees and thrive at hydrothermal vent sites on land and in the deep sea, where they use molecular hydrogen and carbon dioxide as substrates (Corliss et al., 1979; Baross et al., 1982; Jones et al., 1983; Liu and Whitman, 2008). Some authors state that this is a very, if not the most, primordial way of living for Archaea (e.g. Ueno et al., 2006; Martin et al., 2008; Russell et al., 2010; Brochier-Armanet et al., 2011; Taubner et al., 2015, 2018; Borrel et al., 2016). Understanding the physiology of these intriguing organisms can thus be crucial for research including geobiology (e.g. Bradley et al., 2009), astrobiology (e.g. Taubner et al., 2015, 2018; Taubner and Baumann et al., 2019), and biotechnology (e.g. Patel and Sprott, 1999; Rittmann et al., 2015). Hence, this thesis aims to contribute to study further the lipid and amino acid inventory and the physiology of methanogenic archaea.

An important tool to identify many organisms and also methanogens on a wider taxonomic level is the analysis of their membrane lipids, which constitute their cell membranes. Archaea have generally rather special lipids, where isoprenoid alcohols are bound to the glycerol moiety via ether bonds at the *sn*-2 and *sn*-3 positions. However, recently it has been shown that some Lokiarchaea from a salt lagoon in Mexico might have the genes to synthesize not only typical archaeal-like, but also bacterial and eukaryotic-type membrane lipids or even chimeric membrane lipids (Manoharan et al., 2019). Further, beside diether lipids Archaea possess bipolar tetraether lipids, so-called GDGTs, which span the membrane to form a membrane monolayer (e.g. De Rosa and Gambacorta, 1988; Koga and Morii, 2007, Schouten et al., 2013). Many of these lipids, and especially their hydrophobic cores, are sufficiently durable to serve not only as tracers of living and recent biomass, but also as molecular fossils. As such, these lipid biomarkers make it possible to trace back the existence of various groups of Archaea in time (e.g. De Rosa and Gambacorta, 1988; Koga et al., 1993; Birgel et al., 2008; Schouten et al., 2013; Schinteie and Brocks, 2017). The hydrophobic cores of lipids are hydrocarbon “tails” bound to glycerol. These make up the central part of a cell membrane. IPLs include core lipids and hydrophilic, polar head groups. The latter consist for example of sugars and/or phosphate groups. The polar head groups form the outer part of the cell membrane facing either into the cell interior or exterior. Head groups can be specific for certain groups and even strains of organisms and may thus provide additional taxonomic information. However, they make IPLs chemically less stable than membrane core lipids, which reduces their preservation potential in more ancient sediments or rocks (e.g. Sturt et al., 2004; Koga and Morii, 2005; Gibson et al., 2013; Lengger et al., 2014).

Lipids typical for methanogens are isoprenoid hydrocarbons such as squalene, archaeol and macrocyclic archaeol, and GDGTs mostly devoid of ring structures (cyclopentane or cyclohexane moieties; Koga et al., 1998; Schouten et al., 2013). GDGT-0 is often reported as the most common tetraether lipid in methanogenic archaea. GMGTs have previously been found in cultures of (hyper)thermophilic archaea, including methanogens, but also in temperate environments such as soils (e.g. Tornabene et al, 1979; De Rosa and Gambacorta, 1988; Koga et al., 1993; Koga et al., 1998; Morii et al., 1998; Koga and Morii, 2005; Schouten et al., 2008a,

2013; Naafs et al., 2018). Methanogens with exceptional lipid inventories are *Methanosphaera stadtmanae*, which produces minor amounts of ring-containing GDGTs (Bauersachs et al., 2015) and the recently discovered *Methanomassiliicoccus luminyensis*, the only cultured representative of the Methanomassiliicoccales (e.g. Dridi et al., 2012; Paul et al., 2012; Becker et al., 2016). *M. luminyensis* is just distantly related to other methanogens and comprises very unusual membrane lipids. Some of these lipids, such as extended and di-extended archaeol, are typical for halophiles rather than methanogens (e.g. Teixidor et al., 1993; Dawson et al., 2012), while others such as the BDGTs and PDGTs have not been identified until recently by Becker et al. (2016) in marine sediments. Unfortunately, still little is known about lipid biomarker inventory changes of thermophilic methanogens at different environmental sites, especially hydrothermal vent sites (Blumenberg et al., 2007, 2012; Jaeschke et al., 2014; Reeves et al., 2014).

Proteins consist of amino acids, which are defined as having at least one NH_2 and at least one COOH group as functional groups and further a side chain (R group), which is specific to each amino acid. There are D- ("right-handed") and L-stereoisomers ("left-handed"). L-amino acids, which have both, the amine as well as the carboxyl group attached to the first (alpha-) carbon of the side chain are called L-*α*-amino acids. The L-*α*-amino acids make up most of the natural amino acids and include the 22 proteinogenic amino acids, which are incorporated biosynthetically into proteins during translation (Weber and Miller, 1981; Lu and Freeland, 2006). Twenty of these are encoded by the universal genetic code and called "standard" or "canonical" amino acids. The additional two do not have a dedicated codon, but are added in place of a stop codon, when a specific sequence is present. Non-proteinogenic amino acids are all other amino acids, of which hundreds are known so far. As more than 140 amino acids are found in natural proteins, some of them are also part of proteins (Ambrogelly et al., 2007). In this case, they are formed by modification of standard amino acids in already synthesized proteins (Park, 2006). Beside that, non-proteinogenic amino acids can also be intermediates and products of biosynthesis (Lu and Freeland, 2006), components of neurotransmitters (Li and Xu, 2008), osmolytes (Robertson et al., 1990; 1992) or toxins (Dasuri et al., 2011). Amino acids can further be classified by pH level, polarity and side chain group type. Miller and Urey demonstrated in 1953 with the aid of electric discharge, to simulate atmospheric lightning that proteinogenic amino acids like glycine (Gly), alanine (Ala), and aspartic acid (Asp) could have been produced from simpler organic and inorganic precursors like water (H_2O), methane (CH_4), ammonia (NH_3), and molecular hydrogen (H_2), which were considered to dominate the atmosphere of the early Earth (Miller, 1953). Abiotic amino acids could have been also synthesized at submarine hydrothermal systems or brought to Earth by extraterrestrial input (Kitadai and Maruyama, 2018). There are just two articles known by the author so far about amino acid excretion by methanogens. First, it was shown that the methanogenic strains *Methanogenium cariaci* and *Methanothermococcus thermolithotrophicus* accumulate four different and partly rare amino acids (L-α-glutamate, β-glutamate, N^{ε}-acetyl-β-lysine, and betaine) as a response to osmotic stress (Robertson et al., 1992). Second, β-glutamate was also found in the marine strains *Methanocaldococcus jannaschii* JAL-1, *Methanococcus igneus*, and *Methanogenium anulus* AN9 (Robertson et al., 1990).

Genomic data indicate that the last common ancestor of all archaea was a methanogen (Brochier-Armanet et al., 2011; Borrel et al., 2016); and the ancestors of all modern methanogens most likely inhabited hydrothermal vent environments (Martin et al., 2008; Russell et al., 2010). Methanogens thriving in such environments are thermophiles or hyperthermophiles to different degrees, and typically gain their energy by converting carbon dioxide and molecular hydrogen (thereafter just called "hydrogen"), emanating from vents, to biomass, methane, and water (Corliss et al., 1979; Baross et al., 1982; Jones et al., 1983; Liu

and Whitman, 2008). Ultramafic rock-hosted hydrothermal fields, such as the Lost City (Kelley et al., 2001; Bradley et al., 2009; Méhay et al., 2013), the Rainbow (e.g. Charlou et al., 2002; Gibson et al., 2013), and the Logatchev hydrothermal fields (Perner et al., 2007), generate fluids with less hydrogen sulfide, more hydrogen and methane and at the Lost City and Logatchev fields, also a higher pH compared to basalt-hosted hydrothermal fields. Ultramafic rock-hosted hydrothermal fields, driven by serpentinization of ultramafic rocks, are particularly interesting for early-life-studies, because they could represent an analogue to early Earth hydrothermal fields (e.g. Kelley et al., 2001; Bradley et al., 2009; Russell et al., 2010; Zwicker et al., 2018). The fact that methanogenic archaea occur at such sites is consequently another indicator for the antiquity of this metabolism. Hence, methanogenesis could constitute the root of "life as-we-know-it", as life on Earth is also called (Ueno et al., 2006; Martin et al, 2008).

Beside their relevance for Early Life research, methanogens also have great potential for astrobiology. Some species of methanogens could in principle survive under Mars- or Enceladus-like conditions as recent simulation studies showed (Kral et al., 2016; Moissl-Eichinger et al., 2016; Taubner et al., 2018). Studies using terrestrial Mars analogues like natural acid streams (Tan et al., 2018) have demonstrated that organic matter can be preserved over long periods of time in environments as hostile to life as Martian soils and rocks. The preservation potential of molecular fossils on Mars thus seems promising, but icy moons like Europa or Enceladus seem to be far better suited for potentially hosting extraterrestrial life. Hydrothermal vents were indirectly found at Enceladus' ocean floor (Hsu et al., 2015); and many different organic and inorganic molecules, also complex macromolecular organic material with molecular masses >200 Da, were detected in its plume (Waite et al., 2009; Postberg et al., 2018). These molecules could act both as potential substrates for life (H_2O, H_2, CO_2, etc.) or as its inhibitors (CO, C_2H_4, etc.). Three methanogenic strains (*Methanothermobacter marburgensis* DSM 2133, *Methanocaldococcus villosus* DSM 22612, and *Methanothermococcus okinawensis* DSM 14208) were tested on their tolerance regarding the potential inhibitors CO and C_2H_4 (Taubner et al., 2018). Among these, *M. okinawensis* was the only one which tolerated the above-mentioned components and even grew and released a substantial amount of CH_4, when high amounts of the additional inhibitiors H_2CO, NH_4Cl, and CH_3OH were added to the culture medium (Taubner et al., 2018).

H_2CO, NH_4Cl, and CH_3OH also belong to the potential inhibitors and precursor molecules of life. These three components are known as constituents of the organic matter of meteorites, comets, and molecular clouds (e.g. Cheung et al., 1968; Snyder et al., 1969; Kvenvolden et al., 1970; Lees and Haque, 1974; Ehrenfreund and Charnley, 2000; Cooper et al., 2001; Gibb et al., 2001; 2004) and were among the first molecules found in the interstellar medium (Cheung et al., 1968; Snyder et al., 1969; Lees and Haque, 1974; Woodman et al., 1977; Ho and Townes, 1983). The Late Heavy Bombardment period about 4-3.85 billion years ago could have brought H_2CO, NH_4Cl, and CH_3OH to the young Earth (Bottke and Norman, 2017; Deienno et al., 2017), when the atmosphere was dense enough to slow down the impactors. Alternatively, they could have been formed directly on Earth or in its early atmosphere (Schlesinger and Miller, 1983). It is possible that H_2CO has been produced photochemically by UV irradiation in a CO_2- and/or CO- and water vapour-containing atmosphere (Schlesinger and Miller, 1983; Sutherland, 2016). Regardless of whether these components were produced on early Earth or they came from extraterrestrial sources, H_2CO, NH_4Cl, and CH_3OH could have been crucial for prebiotic chemistry.

In the present thesis, the IPL and the core lipid inventory of two members of the Methanococcales, the deep-sea hydrothermal vent methanogens *M. villosus* and *M. okinawensis* is described (Baumann and Taubner et al., 2018; Takai et al., 2002; Bellack et

al., 2011). So far, very few members of the order Methanococcales have been investigated for their lipid biomarker inventory, and in particular for their intact polar lipid compositions (Tornabene and Langworthy, 1979; Comita and Gagosian, 1983; Comita et al., 1984; Ferrante et al., 1986; Sprott et al., 1991; Trincone et al., 1992; Liu et al., 2012a). Here, also the lipids of *M. marburgensis* were analyzed, but its lipid inventory was already known previously (Gräther, 1994)

Further, this work demonstrates the effect of the afore-mentioned potential inhibitors NH_4Cl, H_2CO, and CH_3OH found in the Enceladian cryovolcanic plume on the growth, membrane lipid composition and amino acid excretion patterns of *M. okinawensis*. The three potential inhibitors were chosen to perform an experiment based on a multivariate design space setting (DoE) as described in Taubner et al. (2018). Varying amounts of H_2CO, CH_3OH, and NH_3 (replaced by NH_4Cl) in the range of the upper limit of the amount expected to be present on Enceladus were added to the culture medium for the DoE. Although life on Enceladus has most likely not emerged yet, and would probably use different biomolecules, lipids and amino acids could in principal act as biomarkers for methanogenic life on the icy moons of our Solar system and beyond. The possibilities of biomolecules for life are vast and need not match those of life as-we-know-it. Life as-we-know-it is very selective and uses just a few out of the thousands of biomolecules possible (Schulze-Makuch and Irwin, 2018). However, it is considered likely that other life forms are very selective too and could generate recognizable patterns with similar or completely different biomolecules (Dorn et al., 2011; Georgiou and Deamer, 2014; Georgiou, 2018; Schulze-Makuch and Irwin, 2018). Therefore, the focus here does not lie on the existence of single amino acids or lipids, but on a pattern that could be characteristic for life. This may yield implications for biomarker search as part of future space missions.

In the environment, organisms are unavoidably exposed to changing conditions, such as changing temperature, pressure, pH, salinity, humidity, irradiation, and micro- as well as macronutrient availability. Organisms had to develop mechanisms to cope with these everlasting changes, otherwise they could not survive. Microorganisms do that, for instance, by adapting their lipid inventories (e.g. Sprott et al., 1991; Yoshinaga et al., 2015). Therefore, the same three strains of (hyper)thermophilic, hydrogenotrophic methanogens were grown in pure cultures under varying temperatures and nutrient supply. These are again *M. villosus* and *M. okinawensis*, but also *M. marburgensis* from the order Methanobacteriales, which was isolated from sewage sludge (Wasserfallen et al., 2000). Thereafter, changes in amounts and proportions of core lipids were evaluated. By doing this, the author wants to gain more insight into the effect of varying temperature and nutrient supply on the expression of lipids. There are already several studies about lipid biomarkers under changing temperature, pressure, and pH (e.g. Sprott et al., 1991; Kaneshiro and Clark, 1995; Koga, 2012; Siliakus et al., 2017), but very few under changing nutrient supply (e.g. Yoshinaga et al., 2015). The present thesis aims to contribute to fill this gap.

2. Materials and methods

2.1 Archaeal strains and culture conditions

Methanothermobacter marburgensis strain DSM 2133^T (Wasserfallen et al., 2000), *Methanocaldococcus villosus* strain DSM 22612^T (Bellack et al., 2011) and *Methanothermococcus okinawensis* strain DSM 14208^T (Takai et al., 2002) are anaerobic, hydrogenotrophic methanogens. *M. marburgensis* belongs to the order Methanobacteriales and has originally been isolated from anaerobic, mesophilic sewage sludge (Wasserfallen et al., 2000). It is thermophilic with an optimum temperature of 65°C. *M. villosus* and *M. okinawensis* belong to the order Methanococcales and have initially been isolated from hydrothermal vent systems. *M. villosus* was isolated from a submarine hydrothermal vent system at the Kolbeinsey Ridge, north of Iceland (Bellack et al., 2011). Kolbeinsey Ridge forms a part of the Mid-Atlantic Ridge, and no ultramafic rocks are present at this site. Sampling was conducted at a water depth of 105 m on a rocky seafloor next to effusing fluids, with a water temperature of up to 89°C, and containing hydrogen sulfide, helium, manganese and silicon dioxide (Fricke et al., 1989; Bellack et al., 2011). *M. villosus* is a hyperthermophilic methanogen with an optimum growth temperature of 80°C. *M. okinawensis* was isolated from the tip of a black smoker chimney in 972 m water depth at the Iheya Ridge in the Okinawa Trough, Japan (Takai et al., 2002). The Iheya Ridge is an arc-backarc hydrothermal vent system with hot (more than 300°C) fluids rich in carbon dioxide, methane and hydrogen sulfide (Takai and Horikoshi, 2000; Takai et al., 2002). *M. okinawensis* is thermophilic, with an optimum growth temperature of 60–65°C. All three strains were obtained from the *Deutsche Stammsammlung von Mikroorganismen und Zellkulturen GmbH (DSMZ)*, Braunschweig, Germany, and grown as described below. The experimental setting was designed by Simon K.-M. R. Rittmann and Ruth-Sophie Taubner. Culturing was done by Simon K.-M. R. Rittmann, Ruth-Sophie Taubner and Michael Steiner at the University of Vienna.

Cultivation was performed in 120 mL serum bottles (La-Pha-Pack, Langerwehe, Germany) with either 25 mL, 50 mL, or 75 mL of chemically defined liquid medium (25 mL and 75 mL just for the experiments described in chapter 3.3). *M. marburgensis* grew in a different medium than *M. villosus* and *M. okinawensis* (Taubner and Rittmann, 2016; Taubner et al., 2018). The medium of *M. marburgensis* is described in detail in Taubner and Rittmann (2016) with the modification that in some experiments the carbonate was omitted. DSMZ medium 282 was modified for *M. villosus* and *M. okinawensis* (Taubner and Rittmann, 2016; Baumann and Taubner et al., 2018). For the DoE and extreme value experiments with *M. okinawensis* the inhibitors, NH_4Cl, H_2CO, and CH_3OH, were added to the bottles before autoclaving (Taubner and Baumann et al., 2019; for exact preparation and composition see Supplementary Table 8 in Taubner et al.; 2018). After sealing the serum bottles, they were degassed and autoclaved. Vitamin solution (only in some cultures), $Na_2S{\cdot}9H_2O$, $_L$-Cystein-HCl solution, and $NaHCO_3$ solution, were added to the bottles in an anaerobic chamber (Coy Laboratory Products, Grass Lake, USA) for *M. villosus* and *M. okinawensis*. Only $Na_2S{\cdot}9H_2O$ was added to the bottles for *M. marburgensis* (Taubner and Rittmann, 2016). The vitamin solution was originally used for *M. villosus* and *M. okinawensis*, because it is part of the DSMZ instructions for cultivation of them. However, after it was observed that these organisms exhibited the same growth with and without the vitamin solution, vitamin addition was suspended. Afterwards, the serum bottles were inoculated with 1 mL (2 vol%) of the respective pre-culture in exponential growth phase. All cultures were performed in triplicates (or quadruplicates, described below) plus two negative controls. The negative controls were inoculated with 1 mL of fresh medium. *M. villosus* was incubated in an air bath with a serum bottle head space pressure of 2.5–3.0 bar

(or 1.5–2.0 barg); *M. marburgensis* and *M. okinawensis* in a water bath with a serum bottle head space pressure of 2.4–3.0 bar (or 1.4–2.0 barg; *M. marburgensis*) and 2.4–2.7 bar (or 1.4–1.7 barg; *M. okinawensis*). The water bath is gently shaking the serum bottles, while the air bath is not shaking them. All three strains were incubated in the dark at their respective optimal growth temperatures (65°C for *M. marburgensis*, 80°C for *M. villosus*, and 65°C for *M. okinawensis*) or the alternative culture temperatures (see chapter 3.3) with a variation of no more than 2°C. The generated methane was replaced in regular intervals with a mixture of carbon dioxide and hydrogen (20 vol % carbon dioxide in hydrogen) of approximately 2 bar relative pressure. *M. marburgensis* received carbon dioxide/hydrogen gas once per day, whereas *M. villosus* and *M. okinawensis* either once or twice per day, depending on culture condition, approximately every twelve or 24 hours. Growth was recorded via optical density (OD) measurements (λ = 578 nm, blanked with Milli-Q water, spectrometer: DU800, Beckman Coulter, USA) and H_2/CO_2 to CH_4 conversion and turnover rate[1] via head space pressure measurements of the serum bottles (digital manometer LEO1-Ei, −1...3 bar, Keller, Germany), approximately every twelve hours. For OD measurements ca. 0.75 mL per bottle were removed each time. On average, an experiment with *M. marburgensis* lasted approximately 7–10 days, an experiment with *M. villosus* 2–5 days, and one with *M. okinawensis* 5–8 days. The duration of an experiment tended to be longer at a higher volume of liquid medium. After finishing each experiment, biomass and supernatant were harvested. For this, each culture was centrifuged for 20 minutes at 4500 rpm (3328 rcf) and 4°C in 50 mL Greiner tubes (Hettich Universal 320R). The cell pellets and 3 mL of supernatant of each experiment were then separately stored in sterile Eppendorf tubes at -20°C. The cell pellets were subsequently freeze-dried in a Martin Christ Alpha 1-4 or a Martin Christ Gamma 1-16 LSC Plus freeze-dryer at 0.370 mbar and 0°C footprint temperature for 1–3 days.

2.1.1 Design of Experiment (DoE)

A central composite design with a spherical design space with a normalized radius equal to one was selected for the inhibition studies with *M. okinawensis* (Taubner et al., 2018; Taubner and Baumann et al., 2019). The theoretical setting of the DoE experiment is depicted in Fig. 1a, while Fig. 1b shows the maximum optical density (OD_{max}) of the respective cultures. Except for the central point "O", which represents the center of the sphere, all points displayed in Fig. 1a are positioned on the surface of the sphere. Experiments with triplicates were performed for each of these points, and for point "O" even quintuplicates. The concentration of NH_4Cl, H_2CO, and CH_3OH added to the standard medium of *M. okinawensis* for the DoE experiments is given in Taubner et al., 2018 (see Supplementary Table 1). Two datapoints of setting "O" and one of setting "F" had to be excluded due to low growth (statistically excluded). Due to fluctuations of the performance of HPLC–APCI–MS (High Performance Liquid Chromatography – Atmospheric Pressure Chemical Ionization – Mass Spectrometry) during lipid analysis, one datapoint of each setting "E", "J", and "N" had to be excluded. Further information about the experimental setting is provided in Taubner et al. (2018).

[1] The turnover rate is equal to the conversion rate per hour of incubation. It was determined via the decrease in headspace pressure in each bottle after each incubation period.

2.1.2 Extreme value experiments

Here, and as described in Taubner and Baumann et al. (2019) the growth, amino acid and lipid production of *M. okinawensis* was tested when exposed to a maximum amount of one certain inhibitor (i.e., 210.91 µL/L 37% H_2CO (ROTIPURAN, Roth, Karlsruhe, Germany)) (7.656 mmol/L), 210.91 µL/L CH_3OH (98%, Sigma-Aldrich, Taufkirchen, Germany) (5.207 mmol/L), or 14.06 g/L NH_4Cl (99.5%, Sigma-Aldrich, Taufkirchen, Germany) (0.263 mol/L), respectively) while the other two inhibitors were added at a minimal amount (i.e., 9.09 µL/L (0.330 mmol/L) H_2CO, 9.09 µL/L (0.224 mmol/L) CH_3OH, and 1.44 g/L NH_4Cl (0.027 mol/L), respectively). In the following, the four different settings will be called "Min" (all amounts at minimum), "Me" (high in CH_3OH), "Am" (high in NH_4Cl), and "Fo" (high in H_2CO). The H_2CO (37 Vol.-%) solution also contained minor amounts of CH_3OH. However, these amounts are as small as the statistical error and are negligible for the current application. All experiments were performed in quadruplicates together with an additional zero control.

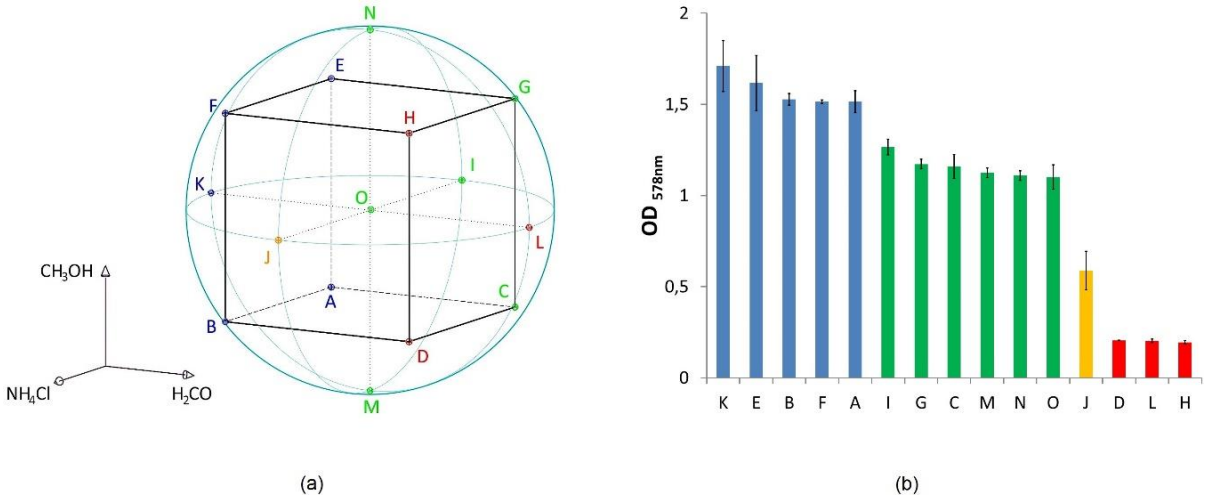

Figure 1 (a): Illustration of the central composite design for the DoE. For the exact concentration of the three inhibitors at the different points tested, see Supplementary Table 1 in Taubner et al., 2018. The colors are in relation to the grouping observed in the OD_{max} bar chart; **(b):** OD_{max} bar chart of the different datapoints (n = 2 for "F", n = 3 for all other points , mean values are shown, error = standard deviation). Figure from Taubner et al. (2018), and Taubner and Baumann et al. (2019).

2.2 Extraction and derivatization of core lipids

All glassware for lipid extraction was combusted at 450°C for 4 h before use (Baumann and Taubner et al., 2018). As internal standards 5-α-cholestane (CAS 481-21-0), DAGE $C_{16:16}$ (CAS 13071-60-8), and DAGE $C_{18:18}$ (CAS 6076-38-6) were added prior extraction. An aliquot of 0.1 to 15 mg of the freeze-dried cells was subjected to acid hydrolysis with HCl (10%) at 110°C for 2 h. Thereafter, lipids were extracted four times with *n*-hexane/DCM (4:1 v:v) to gain the total lipid extract (TLE). For GC–MS and GC–FID analyses, an aliquot of the extract was derivatized with acetic anhydride and pyridine (1:1 v:v) at 60°C for 1 h and at room temperature (ca. 20°C) overnight.

2.3. Gas Chromatography – Mass Spectrometry (GC–MS) and Gas Chromatography – Flame Ionization Detection (GC–FID)

GC–MS was used for identification and GC–FID was used for quantification of diether lipids as a control for HPLC-APCI-MS measurements (compare Baumann and Taubner et al., 2018; Taubner and Baumann et al., 2019). The GC-MS was a Thermo Scientific Trace GC Ultra coupled to a Thermo Scientific DSQ II mass spectrometer and the GC–FIDs used were a Fisons Instruments GC 8000 series and a Fisons Instruments HRGC MEGA 2 series. For both, GC–MS and GC–FID measurements, acetylated aliquots of the acid hydrolysis derived TLEs were used. Injection mode was PTV and carrier gas was helium for the GC–MS analysis. For GC–FID the injection mode was on-column, the carrier gas was hydrogen, the fuel gases were hydrogen and compressed air and the make-up gas was nitrogen (N_2). For these three devices, an Agilent DB-5MS UI and an Agilent HP-5MS UI fused silica column with a length of 30 m, a diameter of 0.25 mm and a film thickness of 0.25 µm, were used. The GC temperature program at the GC–MS and the Fisons Instruments GC 8000 was: 50°C for 3 min to 230°C at 25°C/min, held at 230°C for 2 min and heated to 325°C at 6°C/min and held for 20 min. The temperature program used at the Fisons Instruments HRGC MEGA 2 series was as follows: 50°C for 3 min to 230°C at 15°C/min, then held at 230°C for 2 min and to 325°C at 6°C/min and held for 20 min. This modification was due to the limited heating speed of this GC. The retention time of the components was therefore different on the two GC–FIDs, but this did not affect the quantification. The response factor between 5-α-cholestane and DAGE $C_{18:18}$ was 1.6:1 on both GC–FIDs.

2.4. High Performance Liquid Chromatography – Atmospheric Pressure Chemical Ionization – Mass Spectrometry (HPLC–APCI–MS)

Archaeal di- and tetraether lipids were identified and quantified based on the method of Hopmans et al. (2000) using a Varian MS Workstation 6.91 HPLC system coupled to a Varian 1200L triple quadrupole mass spectrometer (Baumann and Taubner et al., 2018). Prior to injection, underivatized and unfiltered dry aliquots of the TLEs (5%-20% of TLE) were dissolved in *n*-hexane with 12 mg/L C_{46} GDGT as internal standard (Huguet et al., 2006). To avoid overload of the MS, the injection volume was adapted to the initial weight of the biomass and varied between 5 µL and 25 µL to not exceed 25 µg/mL injection concentration per component. Separation was achieved on a Grace Prevail Cyano column (150 mm × 2.1 mm; 3 µ particle size) and a guard column of the same material. Both columns were held at a temperature of 30°C. Archaeal lipids were eluted with the following gradient program modified after Liu et al. (2012c): linear change from 97.5% A (100% *n*-hexane) and 2.5% B (90% *n*-hexane: 10% 2-propanol; v:v) to 75% A and 25% B from 0 to 35 min; then linearly to 100% B in 5 min and held for 8 min. Thereafter, the column was re-equilibrated with 97.5% A and 2.5% B for 12 min. Total run time was 60 min. The solvent flow was constant at 0.3 mL/min during the entire run time. The mass spectrometer was equipped with an APCI interface operated in positive ion mode. The nebulizing gas was N_2 with a pressure of 60 psi. The manifold temperature was fluctuating between 35°C and 40°C, the manifold pressure was 0.66 Pa; the APCI housing temperature was 50°C, the APCI main gas had a pressure of 80 psi; the APCI drying gas temperature was 200°C, the pressure was 12 psi; the APCI auxiliary gas temperature was 400°C, and the pressure was 18 psi. The mass spectral scan range was set at *m/z* 500 to 750 and 950 to 1500. The response factors between archaeal di- and tetraether lipids were constantly evaluated using a standard mixture, injected after every 4–5 samples. The

standard mixture from synthetic archaeol (1,2-Di-*O*-phytanyl-*sn*-glycerol; CAS 99341-19-2), DAGE $C_{18:18}$ (CAS 6076-38-6), DAGEs $C_{18:18}$-4ene (1,3-Dilinoleoyl-*rac*-glycerol; CAS 15818-46-9), and the aforementioned C_{46} GDGT (CAS 138456-87-8) was prepared by Sabine Beckmann at the University of Hamburg. The response factor between synthetic archaeol and C_{46} GDGT was usually around 1.5:1 and the response factor between DAGE $C_{18:18}$ and C_{46} GDGT was usually between 1.5:1 and 2:1. The response factor between the diester DAGEs $C_{18:18}$-4ene and C_{46} GDGT was not used for this thesis, but it is part of the standard mixture as this mixture is also used for samples, which potentially include diester lipids. The response factor between C_{46} GDGT and the glycerol dialkyl diethers GDD-0 and GMD-0 (see below) could not be determined since there was no standard available. A similar response factor as for the tetraether lipids was assumed. Therefore, the quantities of GDD-0 and GMD-0 include possible errors and must be taken cautiously. Relative lipid abundances were determined by selecting individual base peaks with the target mass *m/z*, including ions symmetrically with ±1.0 of target *m/z*.

2.5. High Performance Liquid Chromatography – Atmospheric Pressure Chemical Ionization – tandem Mass Spectrometry (HPLC–APCI–MS/MS)

Structural identification of archaeal ether lipids was conducted by Thorsten Bauersachs at the University of Kiel using HPLC–APCI–MS/MS (Baumann and Taubner et al.; 2018). Briefly, aliquots of the TLEs derived from the acid hydrolysis of archaeal cell material were dissolved in *n*-hexane/2-propanol (99:1, v:v) to a concentration of 1 mg/mL and filtered through a 0.45 µm polytetrafluoroethylene (PTFE) filter prior to analysis. Normal-phase HPLC was performed using a Waters Alliance 2690 HPLC system fitted with a Grace Prevail Cyano column (150 × 2.1 mm i.d., 3 µm particle size) and a security guard column cartridge of the same material. Separation of target compounds was achieved at a constant 30°C with a flow rate of 0.2 mL/min and the following binary gradient profile: 90% A and 10% B for 5 min; linear gradient to 19% B in 20 min; linear gradient to 100% B in 35 min; held at 100% B for 5 min; returning to initial conditions within 1 min and holding for 15 min to re-equilibrate the column (where A = 100% *n*-hexane and B = 90% *n*-hexane/10% 2-propanol). MS/MS experiments were performed using a Micromass Quattro LC triple quadrupole mass spectrometer equipped with an APCI interface operated in positive ion mode. Source settings were as follows: source 150°C, vaporizer 500°C, corona 30 µA, cone voltage 35 V, desolvation gas (N_2) 490 L/h, cone gas (N_2) 70 L/h. Product ion spectra of archaeal ether lipids were recorded using a collision energy of 43 eV and scanning from *m/z* 450 to 1350 (in 1.9 s). Structural assignments of archaeal lipids were based on comparison with published mass spectra (Knappy et al., 2009, 2015; Liu et al., 2012c; Bauersachs and Schwark, 2016).

2.6. Extraction of IPLs and High Performance Liquid Chromatography – ElectroSpray Ionization – tandem Mass Spectrometry (HPLC–ESI–MS/MS)

Before extraction, 1.9–8.8 mg of the freeze-dried cells were homogenized and 5-α-cholestane and DAGE $C_{18:18}$ were added as internal standards. A modified Bligh and Dyer protocol (Rütters et al., 2002) was applied as follows: 7 mL of CH_3OH:DCM:phosphate buffer (2:1:0.8 v:v:v:v) were added and lipids were extracted thrice with an ultrasonic bath (Baumann and Taubner et al., 2018). Subsequently, DCM and phosphate buffer were added to the combined extracts to achieve a solvent ratio of 1:1:0.9 (v:v:v), which induced a phase separation. The organic-rich bottom layer was collected and the aqueous phase re-extracted twice with DCM. The bulk of solvent was removed by rotatory evaporation and dried under a gentle stream of nitrogen. The IPLs were analyzed by Thorsten Bauersachs at the University of Kiel using high performance liquid chromatography coupled to electrospray ionization tandem mass spectrometry (HPLC–ESI–MS/MS) according to the protocol by Sturt et al. (2004) with some modifications. An aliquot of each Bligh and Dyer extract was re-dissolved in a solvent mixture of hexane:2-propanol (79:21, v:v) and injected in a Waters 2960 high performance liquid chromatograph equipped with a Phenomenex Luna NH_2 column (150 × 2 mm i.d., 3 µm particle size) and a guard column of the same material, which were both maintained at a temperature of 30°C. Separation of target compounds was accomplished using the following gradient with a flow rate of 0.2 mL/min: 90% A:10% B to 70% A:30% B in 10 min, hold for 20 min, then to 35% A:65% B in 15 min, hold for 35 min and returning to starting conditions to re-equilibrate the column for 15 min. Solvent A was *n*-hexane/2-propanol/HCO_2H/14.8 M NH_3 aq. (79:20:0.12:0.04; v:v:v:v) and solvent B was 2-propanol/water/HCO_2H/14.8 M NH_3 aq. (88:10:0.12:0.04; v:v:v:v). Detection of IPLs was achieved using a Micromass Quattro LC triple quadrupole mass spectrometer equipped with an electrospray ionization (ESI) interface operated in positive ion mode. Instrument parameters were tuned by directly infusing archaeal lipid extracts in a stream of 100% solvent A into the ESI source, which resulted in the following optimized settings: capillary voltage 3.8 kV, cone voltage 25 V, desolvation temperature 230°C, source temperature 100°C, desolvation gas flow 400 L/h, cone gas flow 70 L/h. Mass detection was performed in a data-dependent mode with two scan events, where a positive ion scan (*m/z* 400–2000) was followed by a product ion scan of the base peak of the mass spectrum of the first scan event. Identification and data evaluation of archaeal IPLs was accomplished by Thorsten Bauersachs by comparison of published mass spectra and characteristic fragment ions reported in the literature (Sturt et al., 2004; Schouten et al., 2008b; Sinninghe Damsté et al., 2012).

2.7 Amino acid analysis

Amino acids were measured by Ruth-Sophie Taubner and Barbara Mähnert at the University of Vienna (Taubner and Baumann et al., 2019). Samples were first diluted in Milli-Q water at a ratio of 1:4. Analyses were performed in technical triplicates on an Agilent 1260 Infinity Bioinert HPLC system, consisting of an autosampler, a quaternary pump, a column oven and a fluorescence detector (Taubner and Baumann et al., 2019). Derivatization was conducted in a robotic autosampler. 75 µL of borate buffer (0.4 N in water, pH = 10.2; Agilent Technologies) were added to 1 mL sample, and subsequently mixed. Thereafter, 5 µL OPA reagent (10 mg/mL OPA and 3-mercaptopropionic acid in 0.4 mol/L borate buffer; Agilent Technologies) were added and subsequently mixed as well. After 2 min of reaction time at 27°C, 100 µL of the reaction mixture were injected into the HPLC system. The separation of

the fluorescent derivatives (primary dissolved free amino acids) was achieved on a Zorbax ECLIPSE AAA column (4.6 x 150 mm, 3.5 µm particle size, Agilent Technologies) with a Zorbax ECLIPSE AAA guard cartridge (4.6 x 150 mm, 5 µm particle size, Agilent Technologies), with the column temperature set at 25°C and a flow rate of 0.8 mL/min. Excitation and emission wavelengths were 340 nm and 450 nm, respectively. Gain factors of 8 to 12 were used depending on the expected concentrations.

This method was developed by Elisabeth L. Clifford at the University of Vienna and is particularly established for samples with a much higher concentration of ammonia than of Dissolved Free Amino Acids (DFAA). Such conditions can make the quantification of DFAAs challenging due to the excess of sodium and interaction with the stationary phase, resulting in peak broadening. Hence, some of the DFAA cannot be quantified, since they are masked by the ammonia peak. For this reason, the gradient, the injection volume, and eluents had to be modified (Krömer et al., 2005) to reduce peak tailing and suppress matrix effects as described elsewhere (Clifford et al., 2017). To generally achieve a better separation of individual components, especially between Met and Val, tetrahydrofuran was used. Trifluoroacetic acid was added as an ion-pairing agent to reduce the broadening and thus improving peak shape. Instead of sodium acetate buffer, NaH_2PO_4 buffer was used, which also resulted in a better ammonia peak shape. The elution gradient is shown in Table S1 and examples of the separation of the dissolved free amino acids are shown in Figs. S1 and S2. For peak identification and quantification, a primary amino acid standard mix (AAS18, Sigma Aldrich) was prepared for each run in different concentrations according to the concentration range of the samples (100 nmol/L to 15 µmol/L). The five missing amino acids (Asn, Glu, GABA, Tau, Trp; all Sigma Aldrich) were added to the AAS18 standard mix in known concentrations. Data evaluation of amino acids was done by Ruth-Sophie Taubner and Barbara Reischl. Elisabeth L. Clifford helped with the interpretation of the data (Taubner and Baumann et al., 2019).

3. Results

3.1 Lipid inventories of *Methanothermobacter marburgensis*, *Methanocaldococcus villosus* and *Methanothermococcus okinawensis*

3.1.1 Archaeal core lipids

As described previously (Gräther, 1994), *M. marburgensis* reveals a range of diether and tetraether membrane lipids (mostly measured as core lipids). In this thesis, the nomenclature introduced by Knappy et al. (2015) for *Methanothermobacter thermautotrophicus*, a close relative of *M. marburgensis*, is used. The core lipids of *M. marburgensis* can be subdivided into three groups: isoprenoid hydrocarbons, isoprenoid diethers, and isoprenoid tetraethers. All compounds are displayed in Fig. 2. *M. marburgensis* produces predominantly archaeol as diether lipid, and very minor amounts of additional diethers, composed of two C_{40} alkyl chains, GDD-0a and -0b, both containing zero rings, GDD-0a without and GDD-0b with one additional methylation, as well as GMD-0a' (the second structural isomer; see below in the second paragraph of chapter 3.1.1) and GMD-0b' (the second structural isomer; see below in the second paragraph of chapter 3.1.1). The major tetraether lipids produced are GDGT-0a, -0b, and -0c (with a = zero, b = one, and c = two additional methylations), and GMGT-0a, -0a', -0b, -0b', -0c' (two isomers with zero and one, and one isomer with two additional methylations), plus the tetraether lipid GTGT-0. Chromatograms of these lipids can be found in Figs. 3 and 4 (actually only chromatograms of *M. villosus* and *M. okinawensis*, but the order of elution on HPLC-APCI-MS is the same for all three strains) and in Knappy et al. (2015).

The intact polar lipid and core lipid inventory of *M. villosus* and *M. okinawensis* has been revealed in the course of this work for the first time (Baumann and Taubner et al., 2018). For this reason, the lipid inventory of *M. villosus* and *M. okinawensis* is described here in much more detail, than the lipid inventory of *M. marburgensis*. *M. villosus* and *M. okinawensis* exhibit the same general membrane core lipid composition. The two strains have the diether lipids archaeol and macrocyclic archaeol, and minor amounts of GDD-0a, GMD-0a, and GMD-0a' (Figs. 2, 3, and 4). Their tetraether lipid inventory comprises GTGT-0a, GDGT-0a, GMGT-0a, and GMGT-0a' (Fig. 2). As two isomers of GMGT-0 occur, one might also suggest the presence of two isomers of GMD-0, but in the present work just one isomer of GMD-0 was found in *M. villosus* and none in *M. okinawensis* (Table 1). The occurrence of two isomers of GMGT-0 is confirmed by the MS/MS measurements (see Fig. S3). No diether or tetraether lipids with additional methylations, as found in *M. marburgensis*, were found in *M. villosus* or in *M. okinawensis*.

The only isoprenoid hydrocarbon found in in all three specimens is squalane, which occurs in only low abundance in these experiments. As squalane is the degradation product of squalene, squalene rather than squalane would be expected in fresh cultures of archaea (Tornabene et al., 1979). However, the applied acid hydrolysis possibly modified the original squalene composition. This could have been avoided by the application of a milder hydrolysis procedure (Cario et al., 2015), but as this work did not focus on isoprenoidal hydrocarbons, this was not conducted.

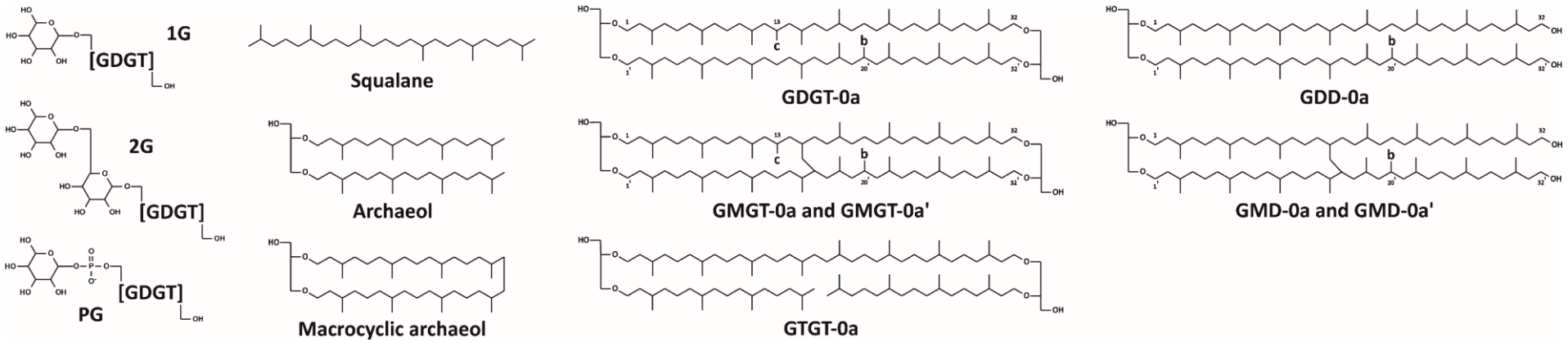

Figure 2: Structures of polar head groups and core lipids found in *Methanothermobacter marburgensis*, *Methanocaldococcus villosus*, and *Methanothermococcus okinawensis*. Abbreviations of polar head groups are: 1G (monoglycosidic), 2G (diglycosidic), and PG (phosphoglycosidic). Abbreviations of core lipids are: GDGT (glycerol dialkyl glycerol tetraether), GMGT (glycerol monoalkyl glycerol tetraether), GTGT (glycerol trialkyl glycerol tetraether), GDD (glycerol dialkyl diether), and GMD (glycerol monoalkyl diether). "0": zero rings in the alkyl chains; "a", "b" and "c": no, one and two additional methyl groups as indicated in the structures (cf., Knappy et al. 2015). Note that the exact positions of the covalent carbon-carbon bonds between the isoprenoid chains of GMGT-0 and GMD-0 are unknown. Figure modified from Baumann and Taubner et al. (2018).

Figs. 3 and 4 provide representative chromatograms, which show the diether and tetraether lipid distributions of *M. villosus* and *M. okinawensis*. Both chromatograms reveal two peaks for archaeol, which cannot be explained at this point. Two isomers or any compounds with the same molecular mass could also not be identified by GC-MS analyses. For this reason and because two peaks were also observed when measuring the synthetic archaeol standard, both peaks are assumed to correspond to archaeol. Table 1 shows the abundance of core ether lipids in each of the three samples of *M. villosus* and *M. okinawensis*. *M. villosus* contains about 3200 ng/mg dw (dry weight) on average, whereas the average lipid content of *M. okinawensis* is about 1600 ng/mg dw. Hence, *M. villosus* has roughly double the amount of lipids as *M. okinawensis* does. The diether lipids (i.e. archaeol and macrocyclic archaeol) are much more abundant than the tetraether lipids, constituting about 95% (weight %) of all lipids in both strains (Fig. 5).

There are several substantial differences in the core lipid patterns between the two strains. *M. villosus* synthesizes more macrocyclic archaeol (55%) than archaeol (39%) and more GMGT-0a' (1%) than GMGT-0a (0.1%). In contrast, *M. okinawensis* has 59% archaeol, 35% macrocyclic archaeol, 1% GMGT-0a, and 0.4% GMGT-0a' (Table 1; Fig. 5). GDGT-0a is the most abundant tetraether lipid in both organisms and comprises on average 4.3% in *M. villosus* and 3.7% in *M. okinawensis*. The second most abundant tetraether lipid is GMGT-0 with the two isomers constituting 1.1% in *M. villosus* and 1.4% in *M. okinawensis*. Both organisms exhibit 0.2% of GTGT-0a. GDD-0a and GMD-0a are the least abundant components and generally do not comprise more than 0.1% of all lipids. To verify the quantification performed with HPLC-APCI-MS, archaeol and macrocyclic archaeol of each sample were also quantified with GC-FID. Archaeol and macrocyclic archaeol were the only lipids, which could have been detected with GC-FID. The ratio of GC-FID/HPLC-APCI-MS was in the range of 1.09 to 1.33 for archaeol and 1.01 to 1.42 for macrocyclic archaeol (Table S2).

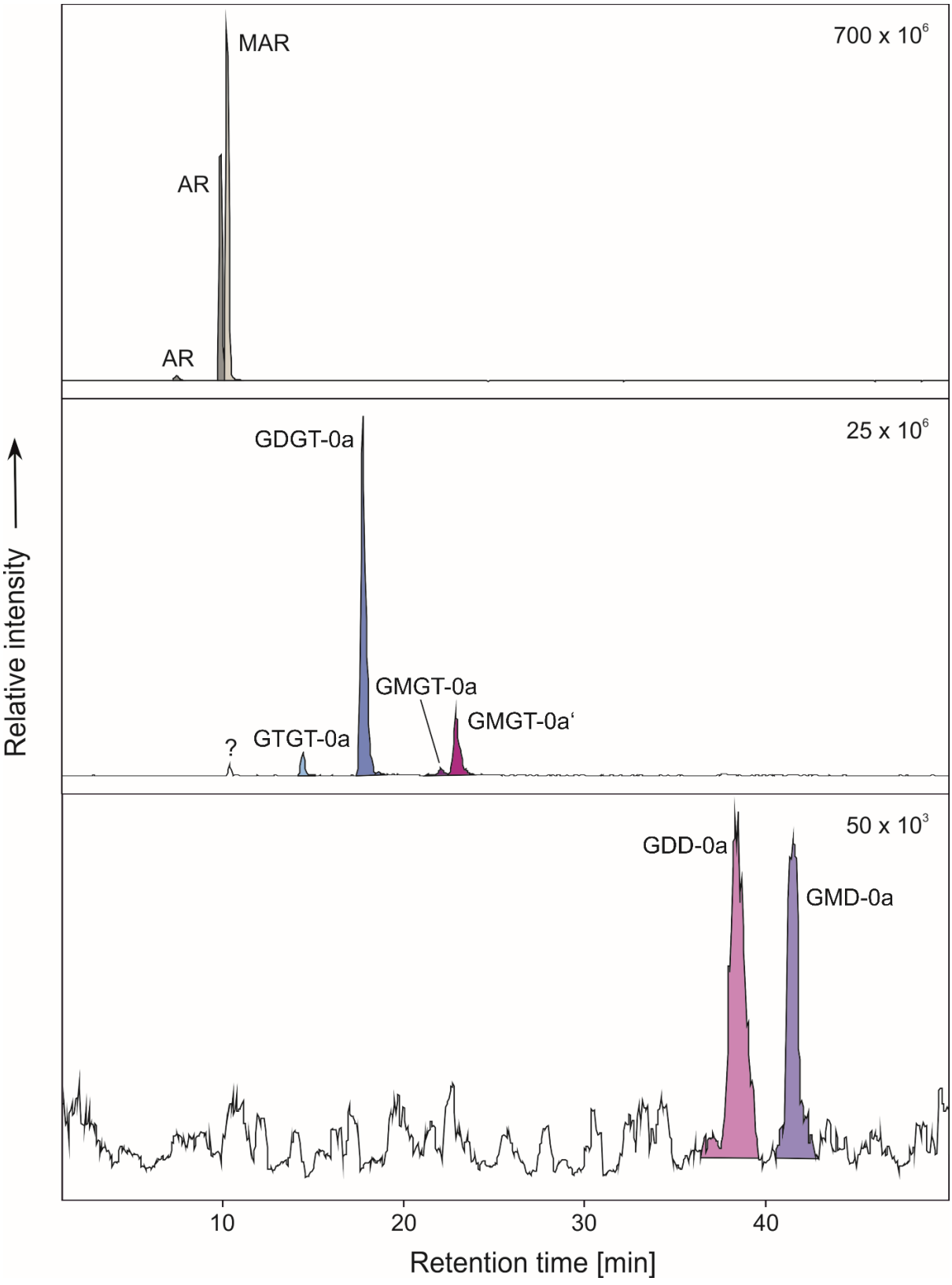

Figure 3: Representative base peak chromatograms showing the core lipid distribution of *M. villosus*. Abbreviations of lipids are: AR (archaeol), MAR (macrocyclic archaeol), GTGT (glycerol trialkyl glycerol tetraether), GDGT (glycerol dialkyl glycerol tetraether), GMGT (glycerol monoalkyl glycerol tetraether), GDD (glycerol dialkyl diether), and GMD (glycerol monoalkyl diether). Figure modified from Baumann and Taubner et al. (2018).

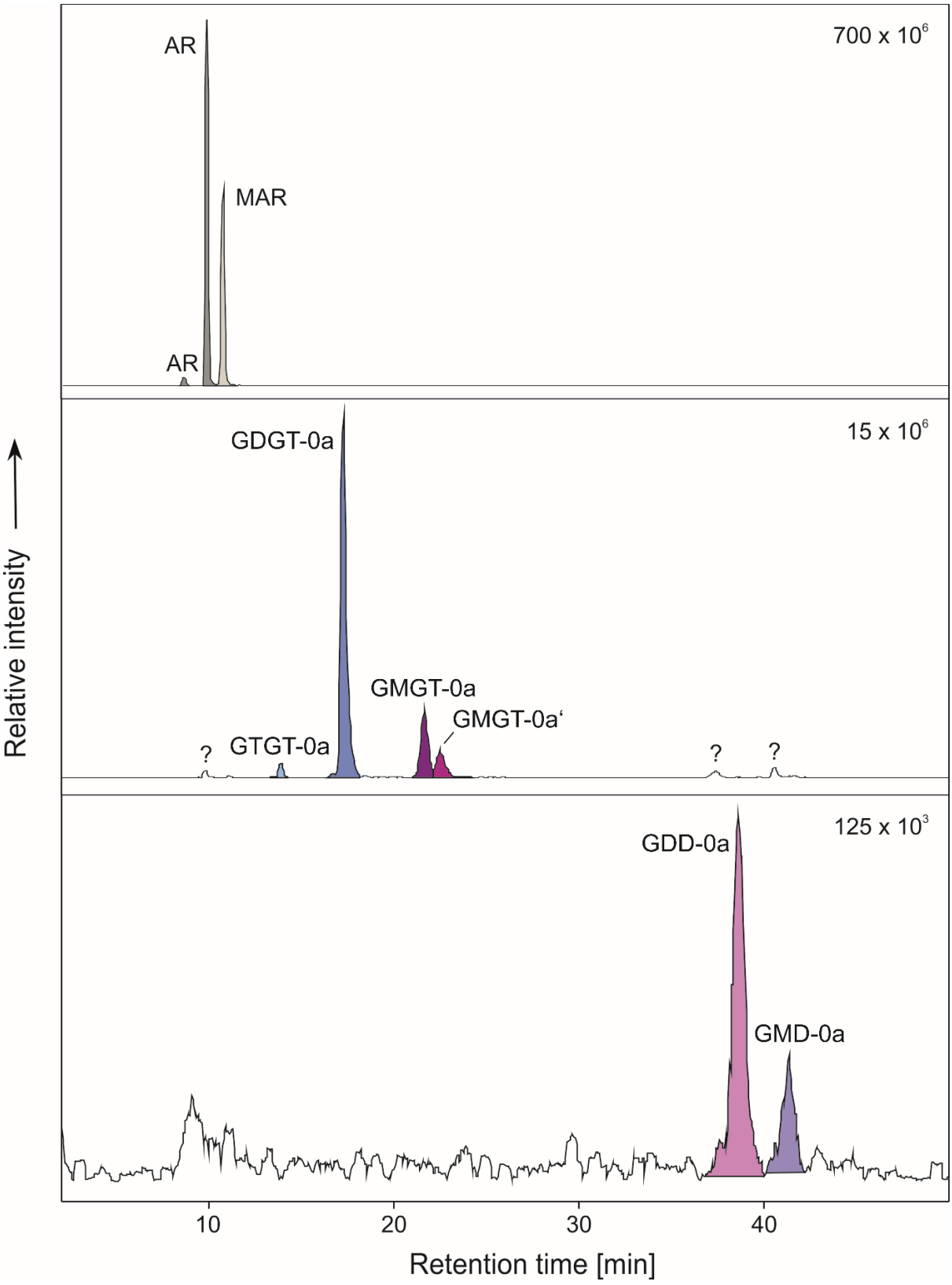

Figure 4: Representative base peak chromatograms showing the core lipid distribution of *M. okinawensis*. Abbreviations of lipids are: AR (archaeol), MAR (macrocyclic archaeol), GTGT (glycerol trialkyl glycerol tetraether), GDGT (glycerol dialkyl glycerol tetraether), GMGT (glycerol monoalkyl glycerol tetraether), GDD (glycerol dialkyl diether), and GMD (glycerol monoalkyl diether). Figure modified from Baumann and Taubner et al. (2018).

Table 1: Contents of core ether lipids in *M. villosus* and *M. okinawensis* in nanogram per milligram dry weight of biomass (ng/mg dw). "Mean v." = mean value; SD = standard deviation; Vil-1-3 = samples of *M. villosus* 1-3; Oki-1-3 = samples of *M. okinawensis* 1-3. Abbreviations of lipids are: Macr. archaeol = macrocyclic archaeol; GTGT (glycerol trialkyl glycerol tetraether), GDGT (glycerol dialkyl glycerol tetraether), GMGT (glycerol monoalkyl glycerol tetraether), GDD (glycerol dialkyl diether), and GMD (glycerol monoalkyl diether). Table modified from Baumann and Taubner et al. (2018).

	Methanocaldococcus villosus					***Methanothermococcus okinawensis***				
	Vil-1 [ng/mg dw]	**Vil-2** [ng/mg dw]	**Vil-3** [ng/mg dw]	**Mean v.** [ng/mg dw]	**SD** [ng/mg dw]	**Oki-1** [ng/mg dw]	**Oki-2** [ng/mg dw]	**Oki-3** [ng/mg dw]	**Mean v.** [ng/mg dw]	**SD** [ng/mg dw]
Archaeol	1045.7	1674.9	1120.6	1280.4	280.6	711.5	1589.2	588.5	963.1	445.6
Macr. archaeol	1772.7	1958.4	1597.4	1776.2	147.4	333.8	917.1	460.6	570.5	250.5
GTGT-0a	7.5	8.1	7.9	7.8	0.2	3.6	4.1	2.4	3.4	0.7
GDGT-0a	158.3	143.1	112.9	138.1	18.8	49.4	73.0	44.7	55.7	12.4
GMGT-0a	3.5	3.1	1.9	2.9	0.7	13.5	19.8	13.0	15.4	3.1
GMGT-0a'	30.3	32.5	29.1	30.6	1.4	5.2	8.9	4.8	6.3	1.9
GDD-0a	1.2	0.0	1.0	0.7	0.5	1.3	2.3	1.6	1.7	0.4
GMD-0a'	0.3	0.0	0.3	0.2	0.2	0.0	0.0	0.0	0.0	0.0
Sum	3019.4	3820.1	2871.1	3236.9	449.9	1118.2	2614.4	1115.5	1616.0	714.5

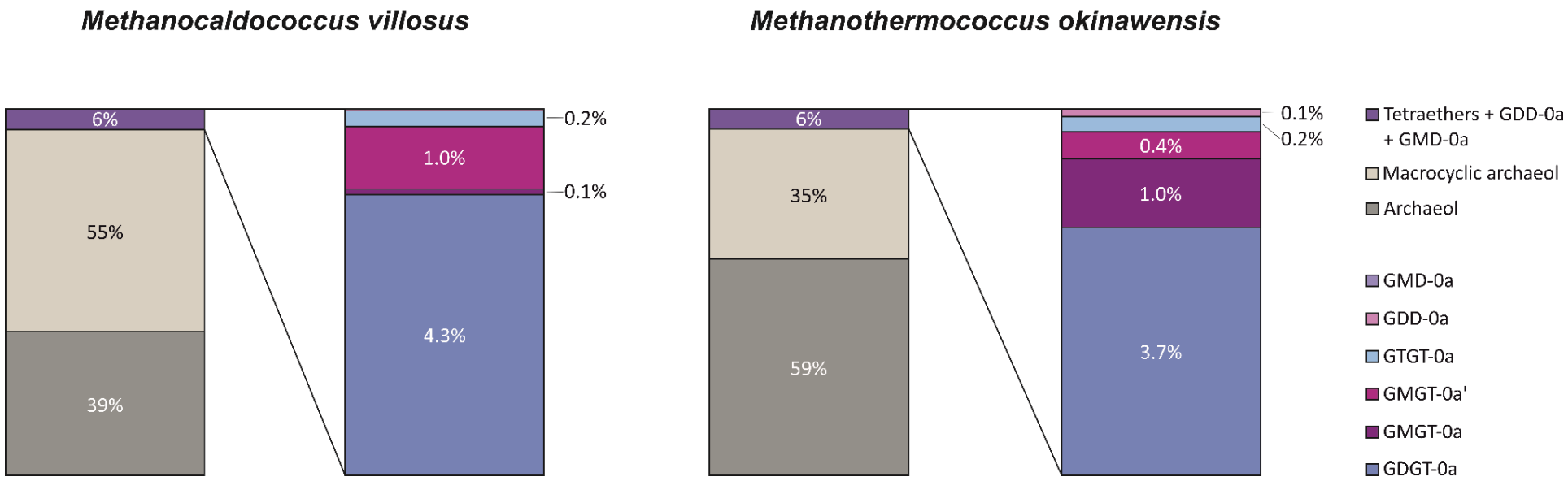

Figure 5: Relative abundance (%) of total core lipids of *M. villosus* and *M. okinawensis*. The bars represent average values (n = 3). Abbreviations of lipids are: GMD (glycerol monoalkyl diether), GDD (glycerol dialkyl diether), GTGT (glycerol trialkyl glycerol tetraether), GMGT (glycerol monoalkyl glycerol tetraether), and GDGT (glycerol dialkyl glycerol tetraether). Figure modified from Baumann and Taubner et al. (2018).

3.1.2 Archaeal intact polar lipids

The relative abundances (%) of the total intact polar lipids based on peak areas are given in Table 2 and in Fig. 6. As the separation of IPLs mainly depends on the polarity of the head group, the two isomers of intact polar GMGT-0a cannot be distinguished. *M. villosus* exhibits mono- (1G) and diglycosidic (2G), whereas *M. okinawensis* additionally contains phosphoglycosidic (PG) head groups (Fig. 2; Table 2). *M. villosus* contains about 6% 1G-archaeol and 5% 1G-macrocyclic archaeol, ca. 40% 2G-archaeol and 45% 2G-macrocyclic archaeol; 2% 2G-GDGT-0a and 1% 2G-GMGT-0a'. IPLs of other core lipids detected beforehand were below detection limit (Table 2). In summary, *M. villosus* is characterized by a clear dominance of diglycosidic over monoglycosidic head groups. In contrast, *M. okinawensis* has about 30% 1G-archaeol and 30% 1G-macrocyclic archaeol, and not more than 11% 2G-archaeol and 8% 2G-macrocyclic archaeol. *M. okinawensis* also contains 2-3% 1G-GTGT-0a, 1G-GDGT-0a, and 1G-GMGT-0a; about 10% 2G-GDGT-0a, 6% 2G-GMGT-0, and PG-GDGT-0a and PG-GMGT-0a on an order of ~1% (Table 2).

As *M. okinawensis*, *M. marburgensis* also reveals mono- and diglycosidic head groups and minor amounts of PG-GDGT-0. However, the PG-GDGT-0 makes up less than 0.01% of total intact polar lipids. *M. marburgensis* has 15% 1G-archaeol, 67% 2G-archaeol, 1% 1G-GDGT-0b with one methylation, 1% 1G-GMGT-0a, 2% 1G-GMGT-0b, 1% 1G-GMGT-0c, 2% 2G-GDGT-0a, 2% 2G-GDGT-0b, 1% 2G-GDGT-0c, 1% 2G-GMGT-0a, 3% 2G-GMGT-0b, and 2% 2G-GMGT-0c. Relative amounts of 1G-GDGT-0a, 1G-GDGT-0c, and PG-GDGT-0a were below 0.01% and the remaining intact polar lipids were all below detection limit.

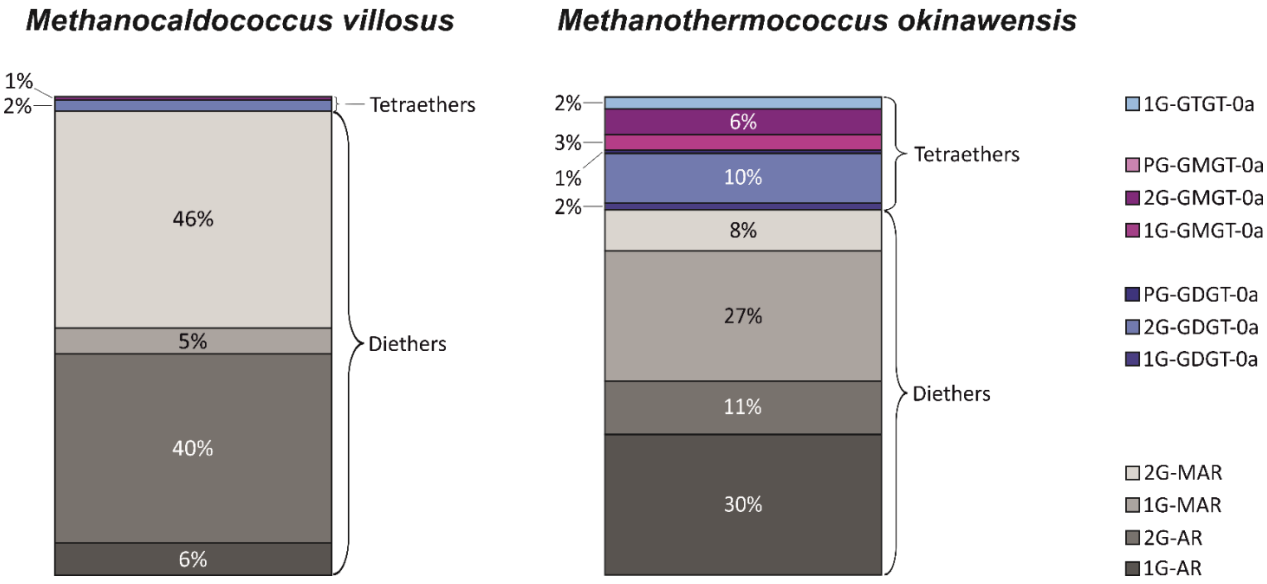

Figure 6: Relative abundance (%) of total intact polar lipids of *M. villosus* and *M. okinawensis*. Abbreviations of polar head groups are: 1G (monoglycosidic), 2G (diglycosidic) and PG (phosphoglycosidic). Abbreviations of core lipids are: AR (archaeol), MAR (macrocyclic archaeol), GTGT (glycerol trialkyl glycerol tetraether), GDGT (glycerol dialkyl glycerol tetraether), and GMGT (glycerol monoalkyl glycerol tetraether). Figure modified from Baumann and Taubner et al. (2018).

Table 2: Relative abundance (%) of total intact polar lipids in *M. villosus* and *M. okinawensis*. SD = standard deviation; n.d. = not detected. Abbreviations of polar head groups are: 1G (monoglycosidic), 2G (diglycosidic) and PG (phosphoglycosidic). Abbreviations of core lipids are: AR (archaeol), MAR (macrocyclic archaeol), GTGT (glycerol trialkyl glycerol tetraether), GDGT (glycerol dialkyl glycerol tetraether), and GMGT (glycerol monoalkyl glycerol tetraether). Table modified from Baumann and Taubner et al. (2018).

	Methanocaldococcus villosus		***Methanothermococcus okinawensis***	
	Mean value (rel)	**SD (rel)**	**Mean value (rel)**	**SD (rel)**
1G-AR	6%	2%	30%	15%
1G-MAR	5%	3%	27%	6%
2G-AR	40%	17%	11%	4%
2G-MAR	46%	13%	8%	5%
1G-GTGT-0a	n.d.	n.d.	2%	1%
1G-GDGT-0a	n.d.	n.d.	2%	1%
1G-GMGT-0a	n.d.	n.d.	3%	2%
2G-GDGT-0a	2%	2%	10%	5%
2G-GMGT-0a	1%	1%	6%	3%
PG-GDGT-0a	n.d.	n.d.	1%	0%
PG-GMGT-0a	n.d.	n.d.	traces	traces
Sum	100%		100%	

3.2 Results of the DoE and the extreme value settings mimicking the assumed Enceladian ocean

3.2.1 Lipid and amino acid production under the DoE setting

As demonstrated in Taubner et al. (2018), *M. okinawensis* is capable to grow in the presence of multivariate concentrations of the potential inhibitors NH_4Cl, H_2CO, and CH_3OH. Fig. 1a provides an overview of the DoE design space and Fig. 1b shows the mean values of OD_{max}, an indicator for growth. The core lipid inventory of *M. okinawensis* exposed to the multivariate concentrations of the potential inhibitors is unchanged compared to the optimal standard conditions (see chapter 3.1). The lipid inventory comprises archaeol, macrocyclic archaeol, GDGT-0a, GTGT-0a, and two isomers of GMGT-0a as well as traces of GDD-0a and GMD-0a in some samples. Table 3 shows the respective minimum, mean, and maximum values for different parameters (including lipid and amino acid concentrations, ratio of archaeal di- and tetraethers). The ratio of diethers/tetraethers is defined as (archaeol + macrocylic archaeol) / (GTGT-0a + GDGT-0a + GMGTs-0a). The mean values of each lipid species of all samples of one experiment in percent [%] of total lipids can be found in Table S3.

All cultures reached a maximum turnover rate of at least 0.086 h^{-1}, except for "D", "H", and "L" (all high H_2CO), which stayed below 0.031 h^{-1} for the entire experiment. Overall, the OD_{max} values and the concentration of total lipids in ng/mg dw show similar patterns as described in the following. The cultures "K", "E", "B", "F" and "A" (all low H_2CO) reveal the highest OD_{max} and "K", "A", and "E" show the highest contents of lipids. The cultures "D", "H" and "L" not only reveal the lowest OD_{max}, but also the lowest lipid content. Only the cultures "J" appear to show diverging OD_{max} and lipid patterns as they have a low OD_{max} compared to other cultures, but with the same or slightly higher amounts of lipids (compare cultures "C", "G", or "I"). When comparing single lipid species, the lipids archaeol and GTGT-0a are relative to the other lipids more abundant in cultures "C", "G", "J", "L", and partly also in "O" (Fig. 7). On the contrary, macrocyclic archaeol, GDGT-0a and the GMGTs-0a are relatively more abundant in cultures "A", "B", "E", "I", and "K" (Fig. 7).

Excreted amino acids show a different behavior than core lipids. Cultures "I" exhibit by far the most excreted amino acids, whereas cultures "H" showed just one tenth of that amount. Cultures with high NH_4Cl and medium to high H_2CO ("H", "D", "J", and "L") show the lowest amounts of excreted amino acids. Cultures "I" not only revealed the highest amounts of 15 of the 18 measured amino acids, but at the same time showed the lowest amount of Gln (0.40 ± 0.06 µmol/L). In total, 18 different excreted amino acids were detected, whereas the most prominent of them found in all cultures were Glu and Gly.

In summary, the different inhibitors were shown to affect *M. okinawensis* differently regarding lipid and amino acid production and excretion. While the lowest amounts of H_2CO (cultures K) favored growth (OD_{max}) and total lipid production, the lowest amounts of NH_4Cl (cultures I) favored total amino acid production (see Fig. 7 and Fig. 8).

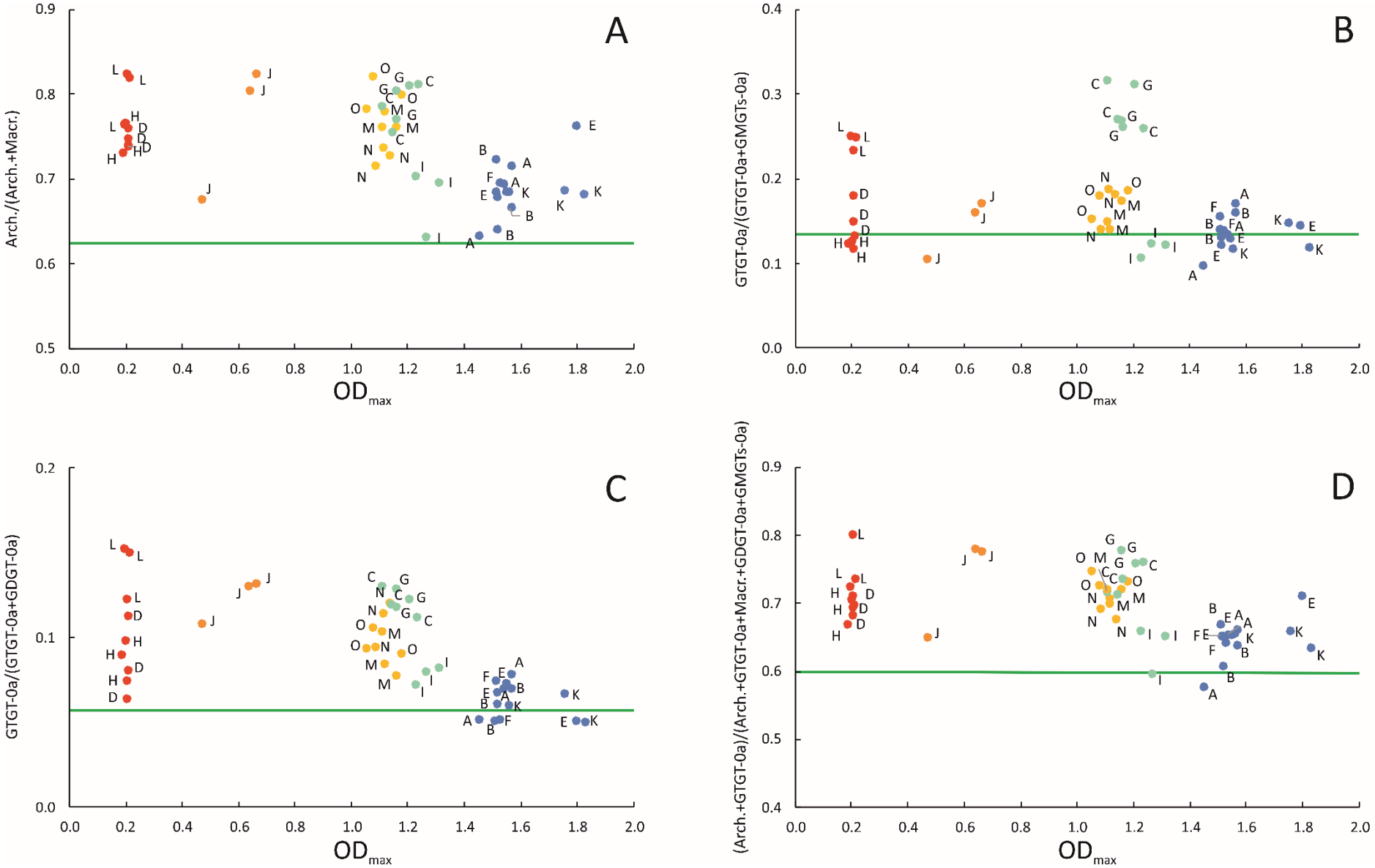
A
Arch./(Arch.+Macr.)
OD max
B
GTGT-0a/(GTGT-0a+GMGTs-0a)
OD max
C
GTGT-0a/(GTGT-0a+GDGT-0a)
OD max
D
(Arch.+GTGT-0a)/(Arch.+GTGT-0a+Macr.+GDGT-0a+GMGTs-0a)
OD max

Figure 7

Figure 7: Selected lipid ratios A, B, C, and D plotted against OD_{max} under the DoE setting. Color code is the same as established in Fig. 1. For comparison, the green line shows the lipid ratio at optimum conditions (data from chapter 3.1 and from Baumann and Taubner et al., 2018). "Arch." = archaeol; "Macr." = Macrocyclic archaeol; OD_{max} = OD_{end} in almost all cases except for two samples of "D" (OD_{end} = 0.1848; 0.1957), all three samples of "H" (OD_{end} = 0.1873; 0.1738; 0.1796), all three samples of "L" (OD_{end} = 0.1777; 0.1842; 0.1925) and one sample of "O" (OD_{end} = 0.2868).

Table 3: Minimum, mean, and maximum values (incl. standard deviation) of the DoE study for the parameters OD_{max}, turnover rate max, diethers [ng/mg dw], tetraethers [ng/mg dw], ratio diethers / tetraethers, total lipids [ng/mg dw], and total amino acids [µmol/L]. The capital letters in brackets next to the minimum and maximum values indicate the culture (see Fig. 1a). Table modified from Taubner and Baumann et al. (2019).

	Minimum value	**Mean value**	**Maximum value**
OD_{max}	0.20 ± 0.01 (H)	1.07 ± 0.05	1.71 ± 0.14 (K)
Turnover rate max [h^{-1}]	0.028 ± 0.003 (L)	0.082 ± 0.002	0.098 ± 0.000 (G)
Diethers [ng/mg dw]	198.41 ± 58.42 (L)	583.96 ± 68.73	883.79 ± 197.54 (K)
Tetraethers [ng/mg dw]	16.89 ± 15.16 (L)	42.50 ± 15.63	68.36 ± 7.04 (A)
Diethers/tetraethers	11.53 ± 2.14 (H)	15.31 ± 5.10	19.43 ± 7.00 (G)
Total lipids [ng/mg dw]	215.31 ± 73.42 (L)	626.46 ± 78.95	938.11 ± 228.19 (K)
Total amino acids [µmol/L]	62.08 ± 9.82 (H)	228.00 ± 34.27	663.58 ± 129.24 (I)

3.2.2 Lipid and amino acid production under the extreme value setting

Extreme value experiments were conducted to better understand and distinguish the effects of the three inhibitors. For this reason, one inhibitor was set at maximum, while the other two were set at minimum, or all three inhibitors were set at minimum concentrations. This makes in total four different conditions, whereas the tested data points do not lie within the design space of the DoE. Table S3 shows the mean values of each lipid species of all samples of one experiment in % of total lipids. It was not possible to determine the lipid concentrations of the individual samples due to contamination issues of the used standards for the extreme value experiments.

The patterns for growth parameters and lipids are most apparent when the conditions are put into the order "Min", "Me", "Am", and "Fo" (for abbreviations, see chapter 2.1.2). The results of the extreme value experiments reflect those of the DoE setting. OD_{max} (for overall growth curves, see Fig. S4) and the turnover rate maximum decrease, while the ratio diethers/tetraethers is increasing from left to right or from "Min" to "Fo" (Table 4; Fig. 9). The same trend can be seen for GTGT-0a/GDGT-0a and a similar trend for archaeol/macrocyclic archaeol, GDGT-0a/GMGTs-0a, GTGT-0a/GMGTs-0a, and GMGT-0a/0a' (Fig. 10). However, for the last four ratios the condition "Me", not "Min", is expressing the lowest values (see Table 4). With other words, the diether archaeol and the tetraether GTGT-0a exhibit a slightly lower relative abundance at condition "Me" than at condition "Min", but an overall low relative abundance at both conditions (Table 4; Fig. 10).The ratio archaeol/macrocyclic archaeol is clearly highest at condition "Fo" (factor above 6 compared to approx. 1:1 ratio for the other settings, see Table 4 and Fig. 10). This high ratio of archaeol/macrocyclic archaeol goes along with the highest standard deviation. The standard deviations of the ratios GTGT-0a/GDGT-0a and GTGT-0a/GMGTs-0a are also highest at condition "Fo" (see Table 4).

Table 4: Minimum, mean, and maximum values (incl. standard deviation) of the four experimental settings "Min" (all amounts at minimum), "Me" (high CH_3OH), "Am" (high in NH_4Cl), and "Fo" (high in H_2CO) for the parameters OD_{max}, turnover rate max, archaeol/macrocyclic archaeol, diethers/tetraethers, GTGT-0a/GDGT-0a, GDGT-0a/GMGT-0a, GTGT-0a/GMGT-0a, GMGT-0a/0a', and total amino acids [µmol/L]. Table modified from Taubner and Baumann et al. (2019).

	Minimum value	**Mean value**	**Maximum value**
OD_{max}	0.22 ± 0.10 (Fo)	0.73 ± 0.43	1.10 ± 0.05 (Min)
Turnover rate max [h^{-1}]	0.051 ± 0.021 (Fo)	0.079 ± 0.019	0.094 ± 0.005 (Min)
Archaeol/macrocyclic archaeol	0.76 ± 0.20 (Me)	2.23 ± 2.76	6.38 ± 3.96 (Fo)
Diethers/tetraethers	3.68 ± 1.51 (Min)	5.48 ± 2.41	8.83 ± 2.34 (Fo)
GTGT-0a/GDGT-0a	0.03 ± 0.01 (Min)	0.07 ± 0.06	0.16 ± 0.05 (Fo)
GDGT-0a/GMGT-0a	0.83 ± 0.12 (Me)	1.42 ± 0.83	2.67 ± 0.60 (Fo)
GTGT-0a/GMGT-0a	0.02 ± 0.01 (Me)	0.14 ± 0.20	0.44 ±0.17 (Fo)
GMGT-0a/0a'	1.96 ± 0.09 (Me)	2.18 ± 0.40	2.78 ± 0.58 (Fo)
Total amino acids [µmol/L]	47.22 ± 7.93 (Am)	180.70 ± 94.02	268.08 ± 101.83 (Me)

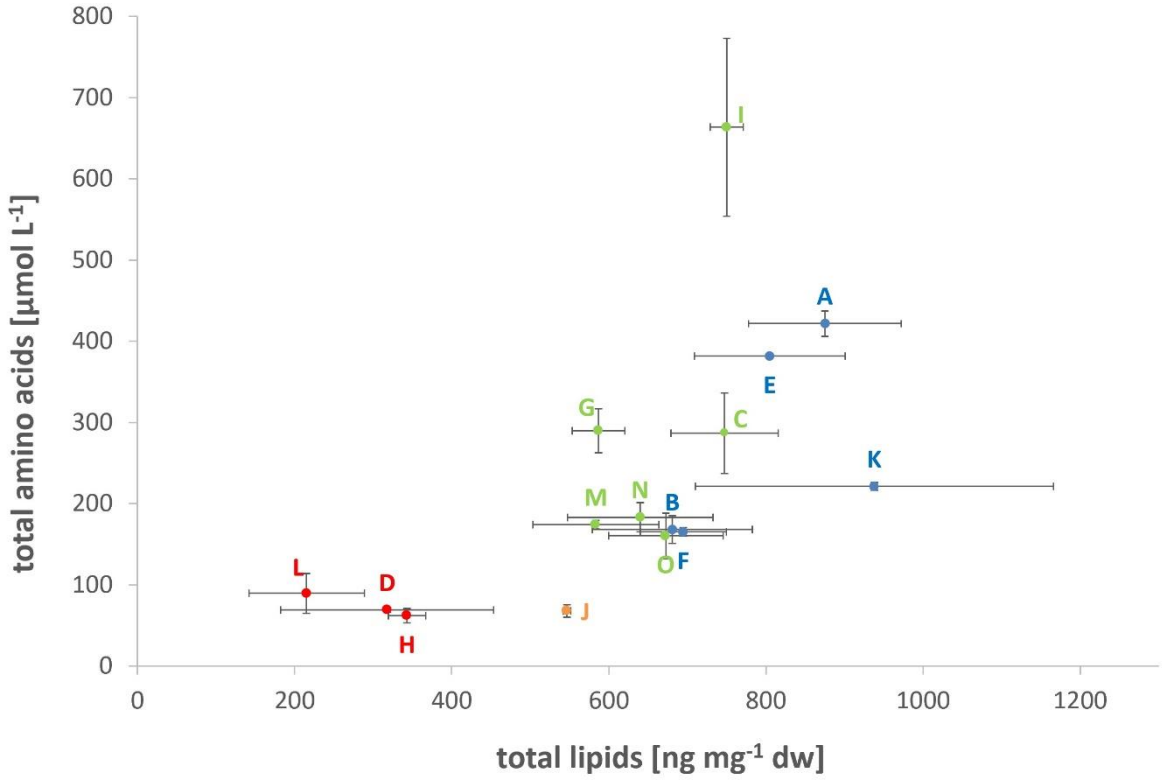

Figure 8: Total lipids [ng/mg dry weight] vs. total amino acids [µmol/L]. The colors are in relation to the grouping observed in the OD_{max} bar chart (Figure 1b) (n = 2 for "E", "F", "J", and "N", all other with n = 3, mean values are shown, error = standard deviation). Figure from Taubner and Baumann et al. (2019).

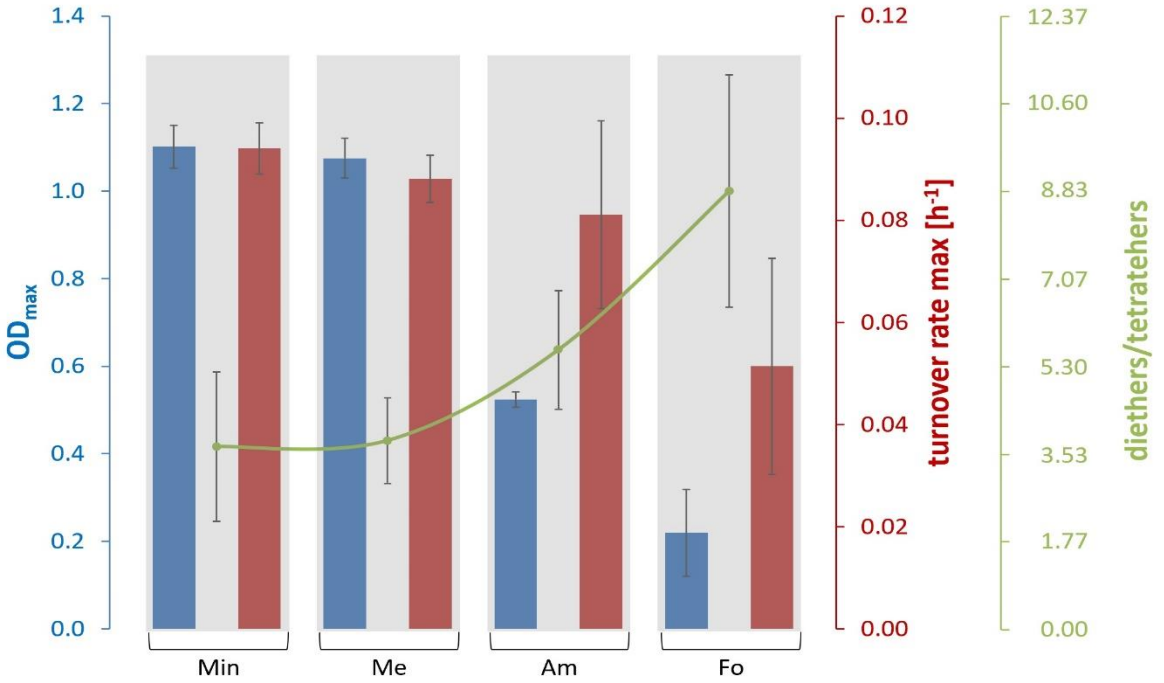

Figure 9: OD_{max}, turnover rate maximum and diether to tetraether ratios for the four experimental settings. These are "Min" (all amounts at minimum), "Me" (high CH_3OH), "Am" (high in NH_4Cl), and "Fo" (high in H_2CO). The reason for the chosen order of the four experimental settings in this figure is explained in the second paragraph of chapter 3.2.2. Figure from Taubner and Baumann et al. (2019).

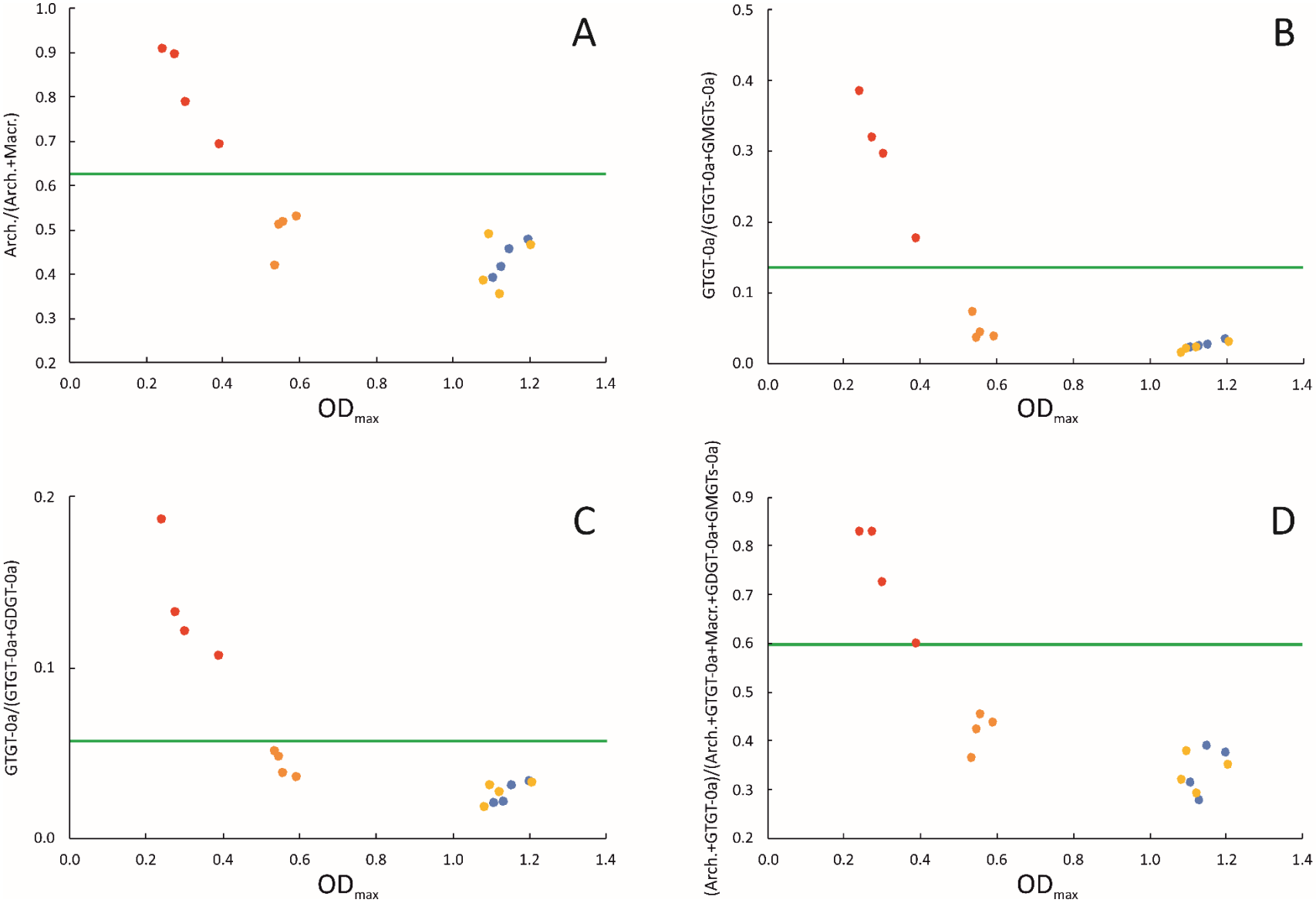
A
Arch./(Arch.+Macr.)
OD$_{max}$
B
GTGT-0a/(GTGT-0a+GMGTs-0a)
OD$_{max}$
C
GTGT-0a/(GTGT-0a+GDGT-0a)
OD$_{max}$
D
(Arch.+GTGT-0a)/(Arch.+GTGT-0a+Macr.+GDGT-0a+GMGTs-0a)
OD$_{max}$

Figure 10

Figure 10: Selected lipid ratios A, B, C, and D plotted against OD_{max} under the extreme value setting. Color code is similar to the one established in Fig. 1: blue = "Min" (all amounts at minimum); yellow = "Me" (high CH_3OH); orange = "Am" (high in NH_4Cl); and red = "Fo" (high in H_2CO). For comparison, the green line shows the lipid ratio at optimum conditions (data from chapter 3.1 and from Baumann and Taubner et al., 2018). "Arch." = archaeol; "Macr." = Macrocyclic archaeol; OD_{max} = OD_{end} in all cases.

As in the DoE setting and in contrast to the growth rate and lipid synthesis, a high amount of NH_4Cl seems to reduce amino acid excretion most substantially (Table 4; Fig. 11). The most prominent excreted amino acids are again Glu and Gly (Fig. S5). The condition "Me" leads to an increase of the total abundance of amino acids. This is especially true for the amino acid Met. The condition "Fo" seems to enhance the excretion of Gln (although with a high standard variation). Interestingly, in some of the samples in the DoE experiments His was detected, whereas no His was found in any of the samples of the extreme value experiments.

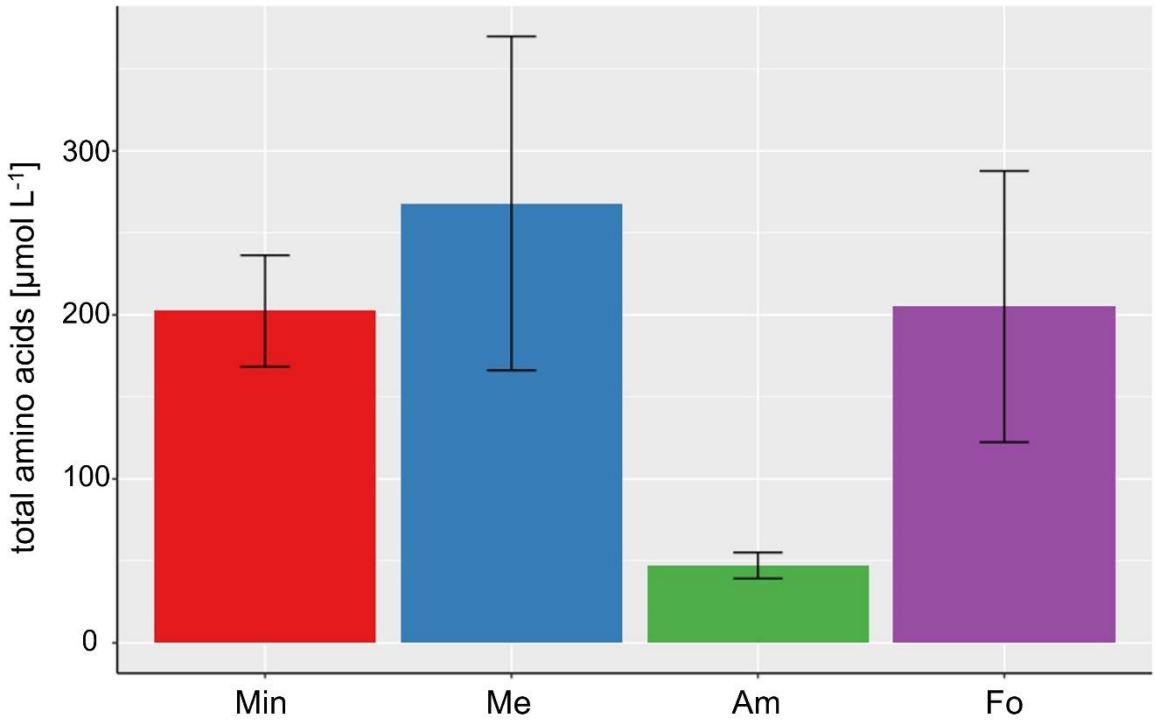

Figure 11: Bar chart of the mean value of the total amino acid concentrations in µmol/L for the four different experimental settings "Min" (all amounts at minimum), "Me" (high CH_3OH), "Am" (high in NH_4Cl), and "Fo" (high in H_2CO) (n = 4 each, error bars present respective standard deviations). As also seen in the statistical analysis, a high concentration of NH_4Cl seems to inhibit the amino acid production most strongly. Figure from Taubner and Baumann et al. (2019).

3.3 Membrane core lipids under varying temperature and nutrient supply

3.3.1 *Methanothermobacter marburgensis*

M. marburgensis has been cultured at three different temperatures, three different volumes of liquid medium, either with or without carbonate in the liquid medium (Table 5). When comparing the mean values of all samples in all experiments, archaeol is the most abundant compound (52.6%), followed by GDGT-0a (22.5%), GDGT-0b (15.0%), and GMGT-0b' (5.1%).The least abundant compounds are GDD-0b (0.02%), GMGT-0b (0.02%), GMD-0b' (<0.01%), and GMD-0a' (<0.01%; Table S4). The mean average content of all lipids is 3949 ng/mg dw, of which diether lipids make up 53% and the tetraether lipids 47% (Table S4). These values are varying with different culture conditions. However, the mean average values of one experiment (composed of quadruplicates) should always be treated with caution, as the standard deviations are often comparably high (Table 6; Table 7; Figs. 12 to 14). The average ratio between standard deviation and mean value for all samples of *M. marburgensis* is 1.75. In the following, relative amounts in % always represent % referred to all lipids measured, unless indicated (e.g. in chapter 3.3.1.3).

3.3.1.1 Cultures at different temperatures

M. marburgensis was cultured at 50°C, 60°C, and its optimum temperature at 65°C (Table 5; Wasserfallen et al., 2000). Additionally, at 65°C, *M. marburgensis* was cultured with different amounts of liquid medium, as well as with and without carbonate in the medium. However, at 50°C and 60°C, *M. marburgensis* was solely cultured at a volume of 50 mL liquid medium including carbonate (Table 5). In the following, only the 50 mL samples with carbonate in the liquid medium for non-OD and OD are compared with each other.

The most apparent pattern is that archaeol is decreasing at 60°C (Fig. 12). The mean proportion of archaeol in % of total lipids is 56.1% at 50°C, 61.9% at 65°C, but just 38.9% at 60°C, with concentrations ranging from ca. 970 ng/mg dw (60°C, non-OD; Table 6) to ca. 2590 ng/mg dw (50°C, non-OD; Table 6, Table S5; Fig. 12). The tetraether lipids GTGT-0a, GDGT-0a, and GDGT-0b behave similarly as archaeol. They show their highest mean concentrations and relative abundances at 50°C and they have their lowest concentrations and in places also relative abundances at 60°C. In contrast, the tetraether lipids GDGT-0c, GMGT-0a, GMGT-0a', GMGT-0b, GMGT-0b', and GMGT-0c' have substantially higher concentrations and relative abundances at 60°C, than at 50°C and 65°C (Table 6, Table S5, Fig. 12). The diethers GDD-0a and GDD-0b have their highest concentrations and relative abundances at 50°C, like GDGT-0a and GDGT-0b. GMD-0b', on the other hand, just occurs at 60°C, similar to the isomers of GMGT-0b (Fig. 12).

To sum it up, archaeol, GTGT-0a, GDGT-0a, GDGT-0b, GDD-0a, and GDD-0b are most abundant at 50°C and least abundant at 60°C. The other lipids; GDGT-0c, GMGT-0a, GMGT-0a', GMGT-0b, GMGT-0b', and GMGT-0c', and GMD-0b' are most abundant at 60°C and with lowest contents at 50°C. There was no clear and consistent variation between non-OD and OD samples. The most apparent difference between non-OD and OD samples occurs at 60°C. At 60°C the concentration of tetraether lipids is much higher in the OD (2200 ng/mg dw) compared to non-OD samples (1070 ng/mg dw; Table 6).

Table 5: Culture conditions of *Methanothermobacter marburgensis*, *Methanocaldococcus villosus*, and *Methanothermococcus okinawensis*. "Carbonate" means, whether or not carbonate was added to the liquid medium (only for culture experiments of *M. marburgensis*). For *M. villosus* and *M. okinawensis*, all cultures had carbonate in the liquid medium. All experiments have been run four times without (non-OD) and four times with measurements of optical density (OD). For OD medium had to be removed. For each of the quadruplicates, "non-OD" as well as "OD", one zero control was conducted.

Strain	**Temperature**	**Liquid medium (volume)**	**Carbonate/Gas exchange times per day**
Methanothermobacter marburgensis	50°C	50 mL	with carbonate
	60°C	50 mL	with carbonate
	65°C	25 mL	without carbonate
			with carbonate
		50 mL	without carbonate
			with carbonate
		75 mL	without carbonate
			with carbonate
Methanocaldococcus villosus	65°C	25 mL	1x
			2x
		50 mL	1x
			2x
		75 mL	1x
			2x
	80°C	25 mL	1x
			2x
		50 mL	1x
			2x
		75 mL	1x
			2x
Methanothermococcus okinawensis	50°C	50 mL	1x
	60°C	50 mL	1x
	65°C	25 mL	1x
			2x
		50 mL	1x
			2x
		75mL	1x
			2x
	70°C	50 mL	1x

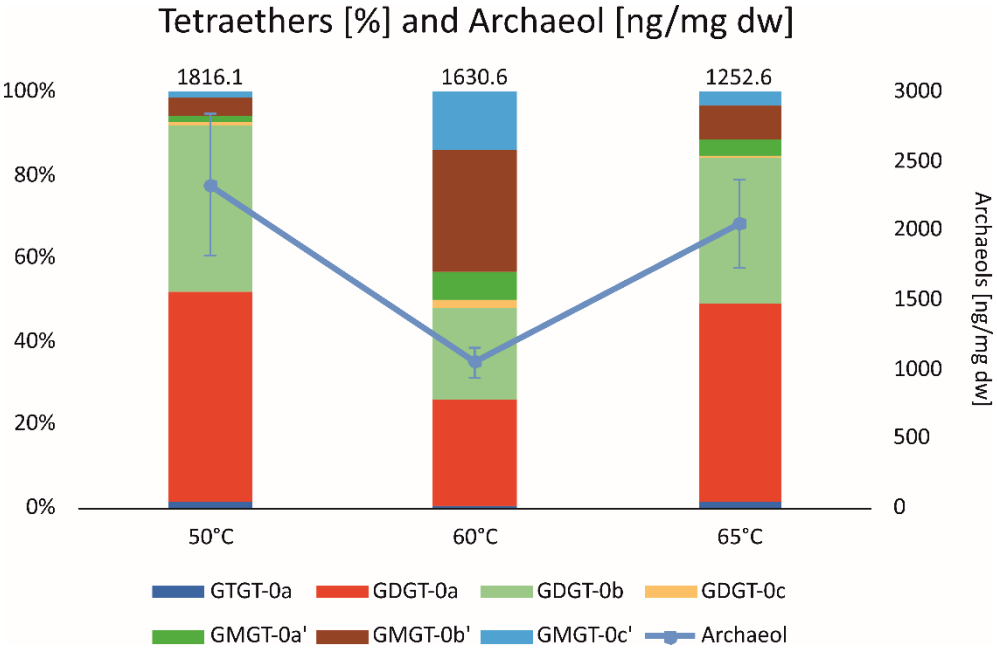

Figure 12: Relative abundance (%) of all tetraether lipids (left) and concentrations of archaeol in nanogram per milligram dry weight (ng/mg dw) (right) of *Methanothermobacter marburgensis* at three different growth temperatures (50 mL, with carbonate). The bars and the blue line represent average values (50°C: n = 7; 60°C: n = 8; 65°C: n = 8). Total concentrations of tetraether lipids in ng/mg dw are above the respective bar. Concentrations of archaeol in ng/mg dw are depicted as blue line with blue error bars. Error = standard deviation. GTGT (glycerol trialkyl glycerol tetraether), GMGT (glycerol monoalkyl glycerol tetraether), and GDGT (glycerol dialkyl glycerol tetraether).

Table 6: Contents of core ether lipids in *Methanothermobacter marburgensis* in nanogram per milligram dry weight of biomass (ng/mg dw) at three different temperatures (50°C/Non-OD: n = 4; 50°C/OD: n = 3; 60°C/Non-OD: n = 4; 60°C/OD: n = 4; 65°C/Non-OD: n = 4; 65°C/OD: n = 4). "Non-OD" = no optical density measurements; "OD" = removal of liquid medium for optical density measurements; "Mean v." = mean value; "SD" = standard deviation. GTGT (glycerol trialkyl glycerol tetraether), GDGT (glycerol dialkyl glycerol tetraether), GMGT (glycerol monoalkyl glycerol tetraether), GDD (glycerol dialkyl diether), and GMD (glycerol monoalkyl diether).

	Temperature; 50 mL with carbonate											
	50°C				**60°C**				**65°C**			
	Non-OD		**OD**		**Non-OD**		**OD**		**Non-OD**		**OD**	
	Mean v.	**SD**	**Mean v.**	**SD**	**Mean v.**	**SD**	**Mean v.**	**SD**	**Mean v.**	**SD**	**Mean v.**	**SD**
Archaeol	2587.4	602.6	2059,2	67.2	970.6	99.8	1112.8	78.3	1891.0	188.7	2190.4	143.9
GTGT-0a	30.1	18.3	21.0	12.1	3.4	0.6	5.8	2.3	13.7	5.6	14.7	4.9
GDGT-0a	1055.2	515.4	787.0	600.3	251.1	14.7	578.1	435.3	554.2	254.4	647.0	328.6
GDGT-0b	865.3	490.0	575.9	372.9	244.8	36.9	476.7	344.9	332.4	158.8	542.5	455.6
GDGT-0c	24.6	15.1	14.0	9.6	21.7	5.3	47.1	29.7	8.7	2.6	13.8	13.6
GMGT-0a	0.4	0.4	0.3	0.3	3.9	0.6	5.1	1.5	1.1	0.4	0.9	0.6
GMGT-0a'	36.3	20.4	24.5	17.8	75.6	2.8	152.7	107.1	40.9	14.4	46.7	17.3
GMGT-0b	0.0	0.0	0.0	0.0	2.2	1.0	3.3	4.3	0.3	0.5	0.9	0.8
GMGT-0b'	93.0	47.9	61.4	43.1	317.6	25.2	635.7	413.7	100.2	56.6	108.1	50.4
GMGT-0c	0.0	0.0	0.0	0.0	0.0	0.0	0.0	0.0	0.0	0.0	0.0	0.0
GMGT-0c'	26.1	12.7	17.6	12.5	152.3	28.9	298.7	138.6	33.7	17.1	48.6	35.2
GDD-0a	1.4	1.0	0.8	0.7	0.0	0.0	0.4	0.4	0.0	0.0	0.0	0.0
GDD-0b	1.0	0.8	0.6	0.5	0.0	0.0	0.0	0.0	0.0	0.0	0.0	0.0
GMD-0a	0.0	0.0	0.0	0.0	0.0	0.0	0.0	0.0	0.0	0.0	0.0	0.0
GMD-0a'	0.0	0.0	0.0	0.0	0.0	0.0	0.0	0.0	0.0	0.0	0.0	0.0
GMD-0b	0.0	0.0	0.0	0.0	0.0	0.0	0.0	0.0	0.0	0.0	0.0	0.0
GMD-0b'	0.0	0.0	0.0	0.0	0.0	0.0	0.2	0.4	0.0	0.0	0.0	0.0
Diethers	2589.8		2060.6		970.6		1113.4		1891.0		2190.4	
Tetraethers	2131.0		1501.7		1072.6		2203.2		1085.2		1423.2	
Sum	4720.8		3562.3		2043.2		3316.6		2976.2		3613.6	

3.3.1.2 Changing liquid medium at one temperature

Here, all cultures at 65°C are compared with each other, which were grown with and without carbonate. The cultures at 50°C and 60°C are excluded, because they were solely cultured at 50 mL with carbonate in the liquid medium. Archaeol, GTGT-0a, GDGT-0a, GDGT-0c, GMGT-0b', and GMGT-0c', are on average most abundant at 25 mL (Table 7; Table S6). GMD-0b' has the same concentration at 25 mL and at 75 mL (Table S6). GDGT-0b, GMGT-0a, GMGT-0a', GMGT-0b, GDD-0a, and GDD-0b are on average most abundant at 75 mL. GMD-0a' just occurs at 50 mL and grown without carbonate. However, in many cases, the difference of the mean values between the different volumes of liquid medium is not as high as the difference between non-OD and OD samples of the same experiment or samples without and with carbonate, but the same volume of liquid medium (Table 7). The comparison of the overall mean values should therefore be treated with caution. Nevertheless, it is rather valid that archaeol is most abundant at 25 mL. Because archaeol is extremely dominant compared to all other membrane lipids produced, it shifts the total lipid concentration in a way that the total lipid concentration is highest at 25 mL (4880 ng/mg dw), medium at 75 mL (4010 ng/mg dw), and lowest at 50 mL (3490 ng/mg dw) (Table S6).

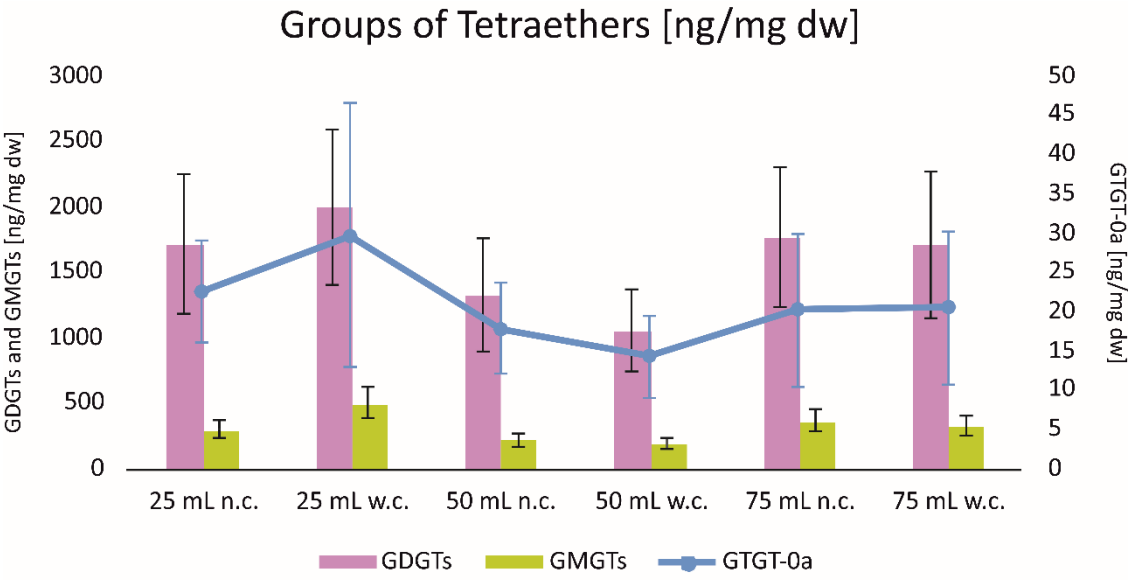

Figure 13: Comparison of the different groups of tetraethers in nanogram per milligram dry weight (ng/mg dw) of *Methanothermobacter marburgensis* at three different volumes of liquid medium with (with carbonate = "w.c.") or without carbonate (no carbonate = "n.c.") in the liquid medium (65°C). The bars and the line represent average values (25 mL n.c.: n = 7; 25 mL w.c.: n = 5; 50 mL n.c.: n = 8; 50 mL w.c.: n = 8; 75 mL n.c.: n = 8; 75 mL w.c.: n = 8). Concentrations of GDGTs and GMGTs are represented by the pink and yellow bars with black error bars. Concentrations of GTGT-0a are depicted as blue line with blue error bars. Error = standard deviation. GTGT (glycerol trialkyl glycerol tetraether), GMGT (glycerol monoalkyl glycerol tetraether), and GDGT (glycerol dialkyl glycerol tetraether).

3.3.1.3 Changing carbonate content

For the same reason as for the liquid medium experiments, the cultures at 50°C and 60°C are excluded. All of the lipids, except for GMD-0a' have their maximum concentrations at either 25 mL or 75 mL of liquid medium, almost independent of the carbonate content (Table 7; Table S4). The condition 25 mL with carbonate is exceptional, because there most GTGT-0a, GDGT-0b, GDGT-0c, GMGT-0b', GMGT-0c', GDD-0b, and GMD-0b' was found. Also, the sum of all GDGTs, GMGTs, and tetraether lipids is highest at the condition 25 mL with carbonate. Archaeol is also very abundant at 25 mL with carbonate, but its concentration and relative abundance is slightly higher at 25 mL without carbonate. Therefore, the sum of diether lipids is highest at 25 mL without carbonate. Similar as archaeol, GDGT-0a has its maximum mean concentration at 25 mL without carbonate, followed by 25 mL with carbonate, and 75 mL without carbonate. At 75 mL without carbonate the highest concentrations can be found of GMGT-0a, GMGT-0a', GDD-0a, and the sum of GDDs (Table 7; Table S4). It seems that at 75 mL without carbonate several lipids with no additional methylation are most abundant, and, in the case of GDGT-0a, very abundant.

The sum of all GDGTs follows the same trend as the sum of all GMGTs (Fig. 13). GTGT-0a shows almost the same trend, it is just slightly different at 75 mL. For all three groups of tetraether lipids, GTGT-0a, GDGTs and GMGTs, the lowest concentrations occur at 50 mL with carbonate and the highest concentrations at 25 mL with carbonate (Fig. 13). The concentration of the sum of diether lipids as well as the sum of tetraether lipids is lower in samples with carbonate at all volumes of liquid medium, except for the tetraethers at 25 mL (43.1% without carbonate; 49.5% with carbonate; Table 7a). GDD-0a and GDD-0b are both less abundant in samples without carbonate compared to samples with carbonate at 25 mL. At 75 mL, both lipids are more abundant in samples without carbonate than in those with carbonate (Table 7c). At 50 mL, they just occur in the samples without carbonate (Table 7b).

When building the mean values of all samples at 65°C without carbonate and all samples at 65°C with carbonate, it turns out that there is no consistent pattern. There are equal amounts of the different lipids more abundant in the cultures without and with carbonate. This does not follow a certain group of lipids, e.g. all GDGTs or all GMGTs are more abundant with carbonate. The sum of all lipids is almost the same in the cultures without (4190 ng/mg dw) and with carbonate (4070 ng/mg dw; Table S4).

However, there seems to be a consistent pattern when comparing the relative amounts of the different degrees of methylation among GDGTs and GMGTs at different carbonate content and volume of liquid medium. Among the GDGTs, GDGT-0a shows an opposing trend to GDGT-0b and the much less abundant GDGT-0c. GDGT-0a is more abundant in samples without carbonate (60%-70% of the GDGTs), compared to those with carbonate (55%-57% of the GDGTs; Fig. 14). The GMGTs show a similar, but slightly different pattern. GMGT-0a and GMGT-0b are negligible as they just occur in minor amounts, and GMGT-0c does not occur at all. So, the focus lies on GMGT-0a', GMGT-0b', and GMGT-0c'. Here, it seems that GMGT-0a' and GMGT-0c' show opposing trends. GMGT-0b' stays more or less the same in relation to the other two. GMGT-0a' is more abundant in samples without carbonate (24%-29% of the GMGTs), than with carbonate (15%-25% of the GMGTs) as it is GDGT-0a. And GMGT-0c' is more abundant in samples with carbonate, than without carbonate, as it is GDGT-0c. So, the GDGTs and the GMGTs behave similarly, with the exception of those compounds with one additional methylation, GDGT-0b and GMGT-0b' (Fig. 14).

3.3.1.4 Non-OD vs. OD

Differences between non-OD and OD samples can be observed and are sometimes substantial, but they do not follow a specific pattern. It appears very random. All of the GDGTs (and hence all of the tetraethers) and all of the GMGTs have in general the same non-OD to OD trends. GTGT-0a has a similar OD-pattern as GDGT-0a, just at 25 mL the trends are opposite. Archaeol and the GDDs have a very different pattern from the tetraethers, and archaeol also has a very different pattern from the GDDs.

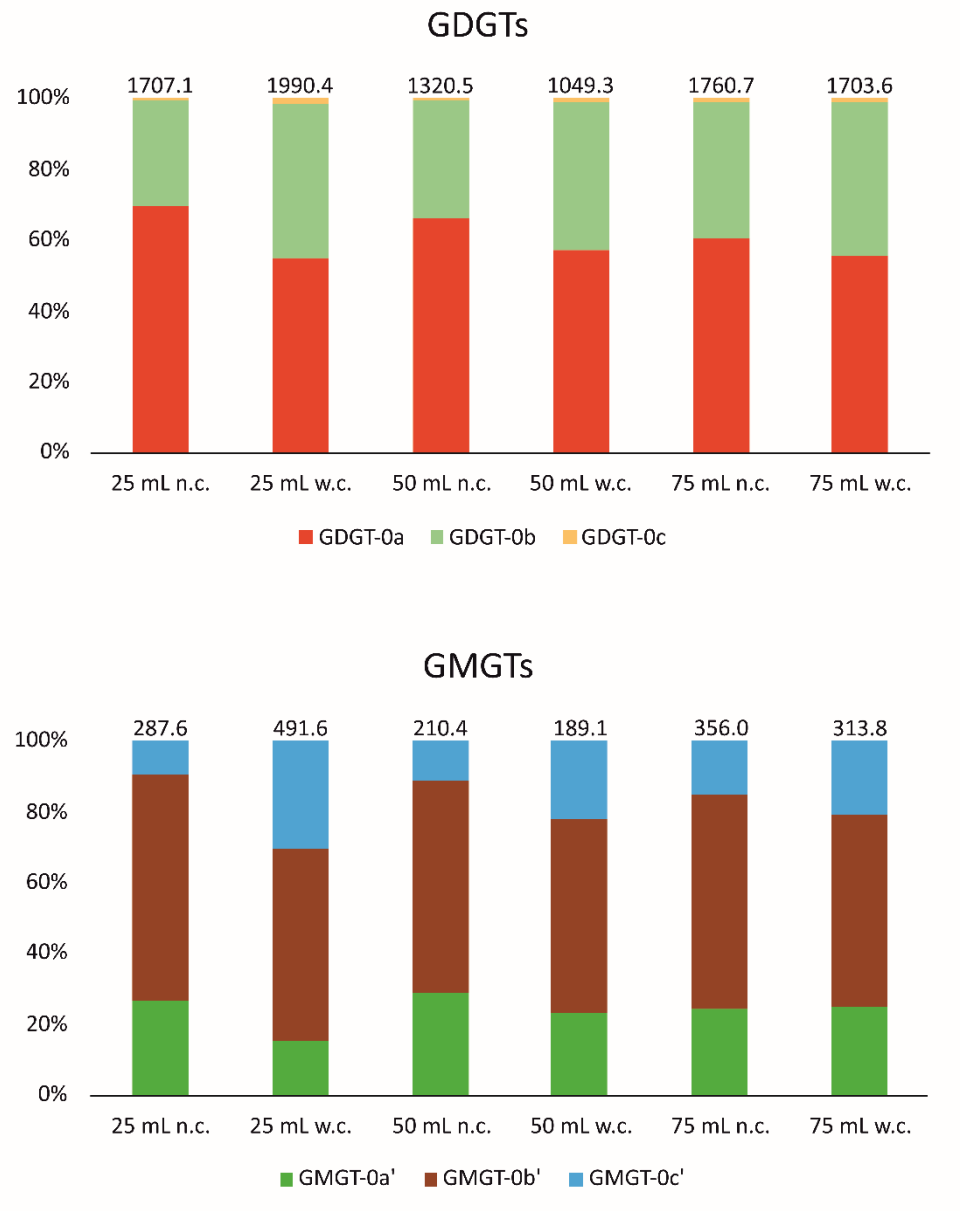

Figure 14: Relative abundance (%) of GDGTs (upper bars) and GMGTs (lower bars) with zero, one, or two additional methylations of *Methanothermobacter marburgensis* at three different volumes of liquid medium with (with carbonate = "w.c.") or without carbonate (no carbonate = "n.c.") in the liquid medium (65°C). The bars represent average values (25 mL n.c.: n = 7; 25 mL w.c.: n = 5; 50 mL n.c.: n = 8; 50 mL w.c.: n = 8; 75 mL n.c.: n = 8; 75 mL w.c.: n = 8). GMGT (glycerol monoalkyl glycerol tetraether), and GDGT (glycerol dialkyl glycerol tetraether).

Table 7a: Contents of core ether lipids in *Methanothermobacter marburgensis* in nanogram per milligram dry weight of biomass (ng/mg dw) at 25 mL of liquid medium with and without carbonate in the liquid medium (25 mL without carbonate/Non-OD: n = 4; 25 mL without carbonate/OD: n = 3; 25 mL without carbonate/Non-OD: n = 3; 25 mL without carbonate/OD: n = 2). "Non-OD" = no optical density measurements; "OD" = removal of liquid medium for optical density measurements; "Mean v." = mean value; "SD" = standard deviation. GTGT (glycerol trialkyl glycerol tetraether), GDGT (glycerol dialkyl glycerol tetraether), GMGT (glycerol monoalkyl glycerol tetraether), GDD (glycerol dialkyl diether), and GMD (glycerol monoalkyl diether).

	25 mL									
	Without carbonate				**With carbonate**				**Mean values**	
	Non-OD		**OD**		**Non-OD**		**OD**			
	Mean v.	**SD**	**Mean v.**	**SD**	**Mean v.**	**SD**	**Mean v.**	**SD**	**Without carb.**	**With carb.**
Archaeol	2473.5	342.9	2845.5	290.8	3024.5	986.8	2106.4	946.8	2659.5	2565.5
GTGT-0a	18.6	5.4	26.3	5.8	40.3	14.1	18.9	13.2	22.5	29.6
GDGT-0a	906.7	315.8	1469.1	293.9	1304.0	244.2	894.9	758.6	1187.9	1099.5
GDGT-0b	448.4	147.4	572.1	72.3	891.5	101.8	827.0	765.6	510.2	859.3
GDGT-0c	7.7	2.6	10.3	1.9	30.6	13.0	32.7	24.3	9.0	31.7
GMGT-0a	1.7	0.6	2.0	0.1	2.0	0.8	1.5	0.4	1.8	1.7
GMGT-0a'	65.7	22.1	89.2	10.4	83.9	14.2	66.3	44.6	77.5	75.1
GMGT-0b	0.2	0.5	0.0	0.0	1.5	2.5	0.0	0.0	0.1	0.7
GMGT-0b'	148.1	58.4	218.7	42.9	279.7	51.1	254.6	192.3	183.4	267.1
GMGT-0c	0.0	0.0	0.0	0.0	0.0	0.0	0.0	0.0	0.0	0.0
GMGT-0c'	22.2	8.1	31.4	8.2	137.8	84.2	160.8	149.1	26.8	149.3
GDD-0a	0.0	0.0	2.5	4.3	2.9	5.0	0.0	0.0	1.2	1.5
GDD-0b	0.0	0.0	0.9	1.5	1.6	2.8	1.0	1.5	0.4	1.3
GMD-0a	0.0	0.0	0.0	0.0	0.0	0.0	0.0	0.0	0.0	0.0
GMD-0a'	0.0	0.0	0.0	0.0	0.0	0.0	0.0	0.0	0.0	0.0
GMD-0b	0.0	0.0	0.0	0.0	0.0	0.0	0.0	0.0	0.0	0.0
GMD-0b'	0.0	0.0	0.0	0.0	0.3	0.6	0.0	0.0	0.0	0.2
Diethers	2473.5		2848.9		3029.3		2107.4		2661.1	2568.5
Tetraethers	1619.3		2419.1		2771.3		2256.7		2019.2	2514.0
Sum	4092.8		5268.0		5800.6		4364.1		4680.3	5082.5

Table 7b: Contents of core ether lipids in *Methanothermobacter marburgensis* in nanogram per milligram dry weight of biomass (ng/mg dw) at 50 mL of liquid medium with and without carbonate in the liquid medium (50 mL without carbonate/Non-OD: n = 4; 50 mL without carbonate/OD: n = 4; 50 mL without carbonate/Non-OD: n = 4; 50 mL without carbonate/OD: n = 4). "Non-OD" = no optical density measurements; "OD" = removal of liquid medium for optical density measurements; "Mean v." = mean value; "SD" = standard deviation. GTGT (glycerol trialkyl glycerol tetraether), GDGT (glycerol dialkyl glycerol tetraether), GMGT (glycerol monoalkyl glycerol tetraether), GDD (glycerol dialkyl diether), and GMD (glycerol monoalkyl diether).

	50 mL									
	Without carbonate				**With carbonate**				**Mean values**	
	Non-OD		**OD**		**Non-OD**		**OD**			
	Mean v.	**SD**	**Mean v.**	**SD**	**Mean v.**	**SD**	**Mean v.**	**SD**	**Without carb.**	**With carb.**
Archaeol	2089.6	548.9	2192.8	212.5	1891.0	188.7	2190.4	143.9	2141.2	2040.7
GTGT-0a	21.7	4.5	13.7	4.1	13.7	5.6	14.7	4.9	17.7	14.2
GDGT-0a	1169.8	149.1	584.3	289.1	554.2	254.4	647.0	328.6	877.1	600.6
GDGT-0b	559.6	148.5	313.7	166.3	332.4	158.8	542.5	455.6	436.6	437.4
GDGT-0c	8.7	0.7	4.9	2.2	8.7	2.6	13.8	13.6	6.8	11.3
GMGT-0a	1.7	0.2	1.3	0.6	1.1	0.4	0.9	0.6	1.5	1.0
GMGT-0a'	75.9	8.0	46.3	19.0	40.9	14.4	46.7	17.3	61.1	43.8
GMGT-0b	0.0	0.0	0.0	0.0	0.3	0.5	0.9	0.8	0.0	0.6
GMGT-0b'	162.8	29.2	87.9	38.8	100.2	56.6	108.1	50.4	125.4	104.2
GMGT-0c	0.0	0.0	0.0	0.0	0.0	0.0	0.0	0.0	0.0	0.0
GMGT-0c'	32.5	7.8	15.5	7.8	33.7	17.1	48.6	35.2	24.0	41.1
GDD-0a	0.4	0.8	2.1	2.5	0.0	0.0	0.0	0.0	1.3	0.0
GDD-0b	0.0	0.0	1.2	1.4	0.0	0.0	0.0	0.0	0.6	0.0
GMD-0a	0.0	0.0	0.0	0.0	0.0	0.0	0.0	0.0	0.0	0.0
GMD-0a'	0.0	0.0	0.1	0.2	0.0	0.0	0.0	0.0	0.1	0.0
GMD-0b	0.0	0.0	0.0	0.0	0.0	0.0	0.0	0.0	0.0	0.0
GMD-0b'	0.0	0.0	0.1	0.2	0.0	0.0	0.0	0.0	0.1	0.0
Diethers	2090.0		2196.3		1891.0		2190.4		2143.3	2040.7
Tetraethers	2032.7		1067.6		1085.2		1423.2		1550.2	1254.2
Sum	4122.7		3263.9		2976.2		3613.6		3693.5	3294.9

Table 7c: Contents of core ether lipids in *Methanothermobacter marburgensis* in nanogram per milligram dry weight of biomass (ng/mg dw) at 75 mL of liquid medium with and without carbonate in the liquid medium (75 mL without carbonate/Non-OD: n = 4; 75 mL without carbonate/OD: n = 4; 75 mL without carbonate/Non-OD: n = 4; 75 mL without carbonate/OD: n = 4). "Non-OD" = no optical density measurements; "OD" = removal of liquid medium for optical density measurements; "Mean v." = mean value; "SD" = standard deviation. GTGT (glycerol trialkyl glycerol tetraether), GDGT (glycerol dialkyl glycerol tetraether), GMGT (glycerol monoalkyl glycerol tetraether), GDD (glycerol dialkyl diether), and GMD (glycerol monoalkyl diether).

	75 mL									
	Without carbonate				**With carbonate**				**Mean values**	
	Non-OD		**OD**		**Non-OD**		**OD**			
	Mean v.	**SD**	**Mean v.**	**SD**	**Mean v.**	**SD**	**Mean v.**	**SD**	**Without carb.**	**With carb.**
Archaeol	1701.0	94.6	2385.9	700.0	1512.3	241.0	2078.2	380.2	2043.5	1795.2
GTGT-0a	18.1	3.4	22.1	14.1	24.6	10.5	16.0	7.7	20.1	20.3
GDGT-0a	872.0	149.9	1257.6	677.7	1189.4	484.8	704.8	349.9	1064.8	947.1
GDGT-0b	750.2	70.2	615.8	336.1	1063.3	498.3	414.2	267.0	683.0	738.7
GDGT-0c	15.5	6.3	10.2	6.0	27.2	11.2	8.4	4.1	12.9	17.8
GMGT-0a	2.1	0.2	1.7	0.7	2.3	0.8	1.3	1.0	1.9	1.8
GMGT-0a'	83.9	21.2	88.1	45.9	102.2	41.2	55.3	22.3	86.0	78.7
GMGT-0b	0.0	0.0	0.2	0.4	1.8	2.5	0.0	0.0	0.1	0.9
GMGT-0b'	228.8	73.1	201.0	112.6	234.5	89.6	105.8	49.2	214.9	170.1
GMGT-0c	0.0	0.0	0.0	0.0	0.0	0.0	0.0	0.0	0.0	0.0
GMGT-0c'	66.1	29.4	44.0	26.1	93.0	30.4	37.0	16.5	55.1	65.0
GDD-0a	2.9	3.5	1.0	2.0	1.1	2.3	1.6	1.8	1.9	1.4
GDD-0b	1.8	2.7	0.8	1.6	0.7	1.4	0.9	1.1	1.3	0.8
GMD-0a	0.0	0.0	0.0	0.0	0.0	0.0	0.0	0.0	0.0	0.0
GMD-0a'	0.0	0.0	0.0	0.0	0.0	0.0	0.0	0.0	0.0	0.0
GMD-0b	0.0	0.0	0.0	0.0	0.0	0.0	0.0	0.0	0.0	0.0
GMD-0b'	0.3	0.5	0.0	0.0	0.0	0.0	0.1	0.1	0.1	0.0
Diethers	1706.0		2387.7		1514.1		2080.8		2046.8	1797.4
Tetraethers	2036.7		2240.7		2738.3		1342.8		2138.8	2040.4
Sum	3742.7		4628.4		4252.4		3423.6		4185.6	3837.8

3.3.2 *Methanocaldococcus villosus*

M. villosus was cultured at 65°C and at 80°C, at 25 mL, 50 mL, and 75 mL, and these with gas exchange either once or twice per day (Table 5). For half of the experiments of *M. villosus*, namely all with the combination 65°C/twice gas exchange and 80°C/once gas exchange, no reliable concentrations in ng/mg dw could be generated for this thesis. This is due to a standard error during lipid extraction. However, the relative amounts of lipids in % of all experiments are reliable. In the following paragraph, the values in % are the mean values of all samples of all experiments.

In *M. villosus*, macrocyclic archaeol is on average more abundant (53%) than archaeol (40%; Table S7). The third most abundant lipid is GDGT-0a (5.6%), followed by GMGT-0a' (1.1%), GTGT-0a (0.5%), GMGT-0a (0.1%), GDD-0a (0.02%), GMD-0a' (<0.01%), and the least abundant GMD-0a (<0.01%; Table S7). Accordingly, the diether lipids are much more abundant (92.6% on average or 87.0% to 96.7%; Tables 8 to 11; Table S7) than the tetraether lipids (7.4% on average or 3.3% to 13.0%; Table 6; Table S7). The total amount of all lipids is on average 3390 ng/mg dw (Table S7). As in *M. marburgensis*, in *M. villosus*, these values fluctuate a lot as a function of culture condition (see below), and between different samples of one experiment (see standard deviations, Tables 8 to 11). The average ratio between standard deviation and mean value for all samples of *M. villosus* is 2.02 and for all reliable samples 1.71.

3.3.2.1 Cultures at different temperatures

M. villosus was cultured at two temperatures, at 65°C and at its optimum growth temperature 80°C (Table 5; Bellack et al., 2011). Here, just the relative amounts in % are compared, as the concentrations available do not show the sole effect of temperature, but are instead always coupled to the gassing frequency (65°C to once daily and 80°C to twice daily). Values in % are displayed in % of all lipids.

Archaeol, GTGT-0a, and GDGT-0a are relatively more abundant at 65°C than at 80°C. In contrast, macrocyclic archaeol, GMGT-0a, GMGT-0a', GDD-0a, GMD-0a, and GMD-0a' are relatively less abundant at 65°C than at 80°C (Fig. 15; Table S8). However, the differences in % are relatively minor. The difference is even negligible when comparing the relative amounts of diethers and tetraethers at 65°C and at 80°C. It seems that the archaeols substitute each other, as well as the tetraethers do (GTGT-0a and GDGT-0a vs. the GMGTs).

Nevertheless, this rather simple pattern becomes more complex, when also considering the volume of liquid medium, the gassing frequency or the OD measurements. At 25 mL of liquid medium the pattern is like in the overall comparison. However, this is different at 50 mL and at 75 mL (Table S8). At 50 mL archaeol has almost the same relative amount at both temperatures, but is slightly higher at 80°C. The GMGTs are more abundant at 65°C than at 80°C. At 75 mL GDGT-0a is more abundant at 80°C. When comparing the different gassing frequency it turns out that gassing once per day gives the same pattern as the overall comparison and the comparison at 25 mL. In contrast, gassing twice per day leads to different patterns. The differences become smaller and almost disappear in the case of the archaeols. GDGT-0a becomes more abundant at 80°C, and GMGT-0a becomes slightly more abundant at 65°C. The comparison between non-OD and OD samples reveals no considerable differences. At non-OD, GDGT-0a is slightly more abundant at 80°C, and at OD, GMGT-0a is slightly more abundant at 65°C. Beside that, non-OD as well as OD samples follow the overall pattern.

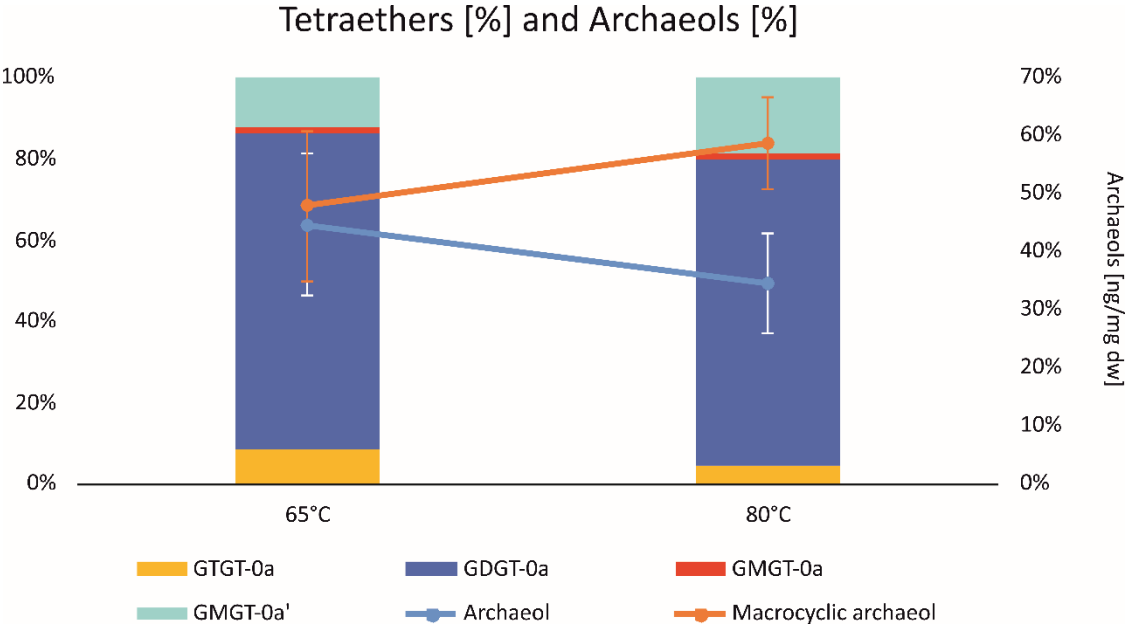

Figure 15: Relative abundance (%) of tetraether lipids (left; in % of total tetraethers), archaeol, and macrocyclic archaeol (right; in % of total lipids) of *Methanocaldococcus villosus* at two different growth temperatures (50 mL; gas exchange once per day at 65°C, and gas exchange twice per day at 80°C). The bars and the lines represent average values (65°C: n = 21; 80°C: n = 20). Relative abundances of archaeol and macrocyclic archaeol are depicted as blue (archaeol; with white error bars) and orange (macrocyclic archaeol; with orange error bars) lines. Error = standard deviation. GTGT (glycerol trialkyl glycerol tetraether), GMGT (glycerol monoalkyl glycerol tetraether), and GDGT (glycerol dialkyl glycerol tetraether).

3.3.2.2 Changing liquid medium at one temperature

When comparing the mean values of all experiments at 25 mL, 50 mL, and at 75 mL, the concentrations of the reliable results of the lipids in % of total lipids are quite similar at all three conditions (Table S7). The highest concentration of total lipids can be found at 50 mL, because the concentrations of archaeol and macrocyclic archaeol are highest at this condition. Hence, 50 mL is also the condition with the highest concentration of diether lipids. 75 mL is the condition with the highest concentration of tetraether lipids, because the concentrations of GTGT-0a and GDGT-0a are highest there. Interestingly, the highest concentration of GDGT-0a at 75 mL coincides with the highest concentration of GDD-0a. The lowest concentration of total lipids is 2920 ng/mg dw at 25 mL. The lowest concentration of archaeol is 1400 ng/mg dw and of macrocyclic archaeol it is 1280 ng/mg dw, both also found at 25 mL. All lipids have their minimum concentration at 25 mL, except for GMGT-0a', which has its minimum at 50 mL. Nevertheless, the difference between the lowest and the highest concentration of GMGT-0a' is minor (Table S7).

There is also only a minor difference in the relative proportions of the mean values of all experiments at 25 mL, 50 mL, and 75 mL (Fig. 16; Table S7). Archaeol, GTGT-0a, GDGT-0a, and GMGT-0a' have their highest relative amounts at 25 mL and their lowest at 50 mL. In contrast, macrocyclic archaeol and GMD-0a have their highest relative amounts at 50 mL and their lowest at 25 mL. GMGT-0a, GDD-0a, and GMD-0a' have their highest relative amounts at 75 mL and their lowest relative abundance at 25 mL (Table S7). However, this order is different, if temperature, gassing frequency, or OD measurements are taken into consideration (Tables S8 to S10). The trends are all different when comparing the relative ratios at different

volumes of liquid medium at 65°C vs. 80°C (Table S8 and see above), at once vs. twice daily gassing (Table S9 and see below), and in non-OD vs. OD samples (Table S10 and see below). Nevertheless, the difference in % between the different conditions is never substantial. This gives an overall vague pattern. The two groups established above partly also appear here, but with various exceptions such as GMGT-0a'.

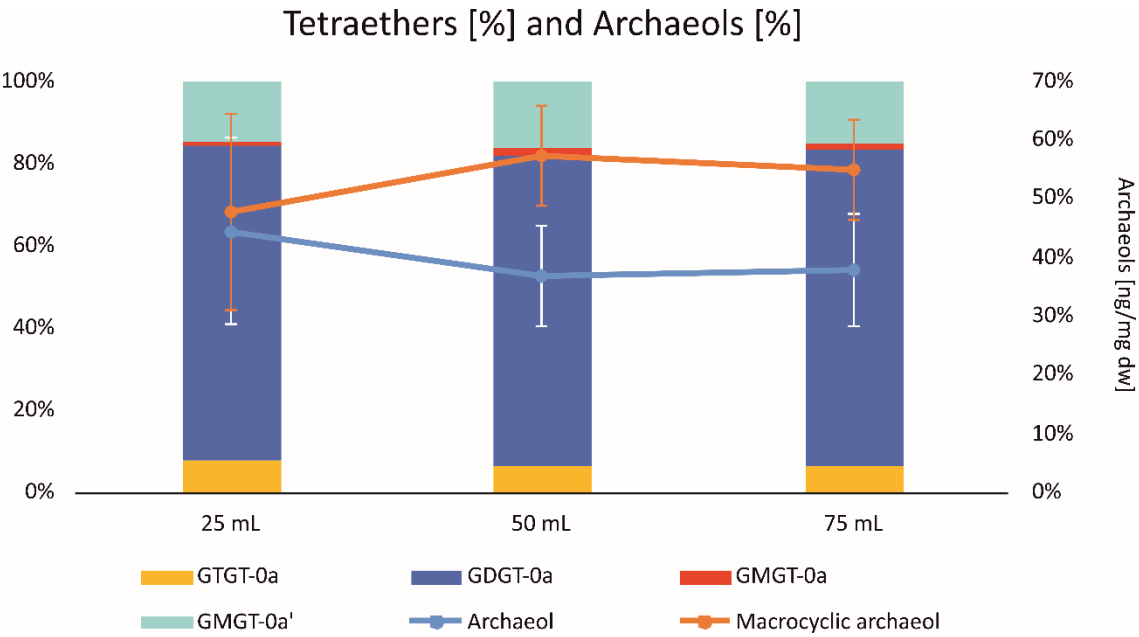

Figure 16: Relative abundance (%) of tetraether lipids (left; in % of total tetraethers), archaeol, and macrocyclic archaeol (right; in % of total lipids) of *Methanocaldococcus villosus* at three different volumes of liquid medium (gas exchange once per day at 65°C; gas exchange twice per day at 80°C). The bars and the lines represent average values (25 mL: n = 13; 50 mL: n = 14; 75 mL: n = 14). Relative abundances of archaeol and macrocyclic archaeol are depicted as blue (archaeol; with white error bars) and orange (macrocyclic archaeol, with orange error bars) line. Error = standard deviation. GTGT (glycerol trialkyl glycerol tetraether), GMGT (glycerol monoalkyl glycerol tetraether), and GDGT (glycerol dialkyl glycerol tetraether).

3.3.2.3 Gassing frequency

For the same reason as for the temperature comparisons, just relative amounts in % are compared with each other here. Gassing once per day is coupled to 65°C and gassing twice per day is coupled to 80°C for those samples, from which concentrations are available. In the comparison of all samples with once gassing per day and all samples with twice gassing per day all lipids, except for archaeol (1x: 41.5%; 2x: 37.4%) are more abundant at twice gassing per day than at once. However, the differences between gassing once and twice per day are minor (Table S9). When comparing gassing once and twice at different volumes of liquid media, trends are most similar to the overall comparison at 75 mL. At 25 mL, the archaeols switch their predominance. Whereas archaeol is more abundant when gassing twice (46.7%), macrocyclic archaeol is more abundant at gassing once (50.4%). At 50 mL, archaeol, GTGT-0a, and GDGT-0a are more abundant when gassing once, whereas the remaining lipids are more abundant when gassing twice (Table S9). When comparing the difference between gassing once or twice, first at non-OD and second at OD samples, the differences between the two cases are negligible (Tables 8 to 11).

3.3.2.4 Non-OD vs. OD

Regarding the concentrations of half of the samples and compare the overall values in ng/mg dw at non-OD and OD, the differences are rather small (Tables 8 to 11). A specific grouping of lipids is not visible. The two archaeols, GTGT-0a, GDGT-0a, and GMD-0a are more abundant at OD, the remaining lipids, the GMGTs, GDD-0a, and GMD-0a' are more abundant at non-OD. The total amount of lipids and the total amounts of diether and tetraether lipids are hence higher at OD than at non-OD. This is different for samples cultured at 50 mL. There, all lipids except for GMGT-0a, GDD-0a, and GMD-0a are more abundant at non-OD than at OD. At 75 mL nearly the opposite was observed; all lipids except for GDD-0a are more abundant at OD. At 25 mL, the trends are again different, but more similar to the overall pattern than 50 mL and 75 mL.

Much of this part has already been described above. The differences between non-OD and OD samples in % are minor (Tables 8 to 11; Table S10). When comparing non-OD and OD samples at different volumes of liquid medium the differences in % are somewhat larger and the patterns of 50 mL and 75 mL are very similar. Archaeol, GDD-0a, and GMD-0a' are more abundant at non-OD than at OD. The other lipids are more abundant at OD than at non-OD. At 25 mL, archaeol, GTGT-0a, and GDGT-0a (group 1) are more abundant at OD. The other lipids are more abundant at non-OD.

Table 8a: Contents of core ether lipids in *Methanocaldococcus villosus* in nanogram per milligram dry weight of biomass (ng/mg dw) at three different volumes of liquid medium at 65°C and gas exchange once per day (25 mL/Non-OD: n = 3; 25 mL/OD: n = 4; 50 mL/Non-OD: n = 3; 50 mL/OD: n = 4; 75 mL/Non-OD: n = 3; 75 mL/OD: n = 4). "Macr. arch." = macrocyclic archaeol; "Non-OD" = no optical density measurements; "OD" = removal of liquid medium for optical density measurements; "Mean v." = mean value; "SD" = standard deviation. GTGT (glycerol trialkyl glycerol tetraether), GDGT (glycerol dialkyl glycerol tetraether), GMGT (glycerol monoalkyl glycerol tetraether), GDD (glycerol dialkyl diether), and GMD (glycerol monoalkyl diether).

	65°C; 1x daily gas exchange											
	25 mL				**50 mL**				**75 mL**			
	Non-OD		**OD**		**Non-OD**		**OD**		**Non-OD**		**OD**	
	Mean v.	**SD**	**Mean v.**	**SD**	**Mean v.**	**SD**	**Mean v.**	**SD**	**Mean v.**	**SD**	**Mean v.**	**SD**
Archaeol	1375.2	742.3	1219.8	492.2	2147.3	229.7	1771.4	269.3	2183.1	328.5	2219.2	487.8
Macr. arch.	831.1	614.8	709.7	351.4	2219.2	428.7	1987.3	437.8	1705.5	192.0	1895.8	215.9
GTGT-0a	16.3	10.0	27.1	15.2	30.5	20.1	25.8	11.5	15.8	1.2	26.7	10.7
GDGT-0a	120.4	84.7	224.2	153.3	294.5	238.5	236.6	124.3	113.5	9.5	267.5	176.6
GMGT-0a	1.5	1.6	1.4	1.8	4.6	3.0	5.5	2.6	1.8	0.4	3.3	2.5
GMGT-0a'	15.2	9.9	21.9	13.6	46.0	37.1	39.5	16.1	17.3	3.8	32.0	18.8
GDD-0a	0.0	0.0	0.0	0.0	0.0	0.0	0.0	0.0	0.9	0.6	0.4	0.7
GMD-0a	0.0	0.0	0.0	0.0	0.0	0.0	0.0	0.0	0.0	0.0	0.0	0.0
GMD-0a'	0.0	0.0	0.0	0.0	0.0	0.0	0.0	0.0	0.0	0.0	0.0	0.0
Diethers	2206.3		1929.5		4366.5		3758.7		3889.5		4115.4	
Tetraethers	153.4		274.6		375.6		307.4		148.4		329.5	
Sum	2359.7		2204.1		4742.1		4066.1		4037.9		4444.9	

Table 8b: Contents of core ether lipids in *Methanocaldococcus villosus* in % at three different volumes of liquid medium at 65°C and gas exchange once per day (25 mL/Non-OD: n = 3; 25 mL/OD: n = 4; 50 mL/Non-OD: n = 3; 50 mL/OD: n = 4; 75 mL/Non-OD: n = 3; 75 mL/OD: n = 4). "Macr. arch." = macrocyclic archaeol; "Non-OD" = no optical density measurements; "OD" = removal of liquid medium for optical density measurements; "Mean v." = mean value; "SD" = standard deviation. GTGT (glycerol trialkyl glycerol tetraether), GDGT (glycerol dialkyl glycerol tetraether), GMGT (glycerol monoalkyl glycerol tetraether), GDD (glycerol dialkyl diether), and GMD (glycerol monoalkyl diether).

	65°C; 1x daily gas exchange											
	25 mL				**50 mL**				**75 mL**			
	Non-OD		**OD**		**Non-OD**		**OD**		**Non-OD**		**OD**	
	Mean v.	**SD**	**Mean v.**	**SD**	**Mean v.**	**SD**	**Mean v.**	**SD**	**Mean v.**	**SD**	**Mean v.**	**SD**
Archaeol	58.3%	7.6%	55.3%	6.8%	45.3%	4.1%	43.6%	4.1%	54.1%	2.7%	49.9%	4.1%
Macr. arch.	35.2%	9.3%	32.2%	3.3%	46.8%	8.7%	48.9%	1.9%	42.2%	2.6%	42.7%	3.7%
GTGT-0a	0.7%	0.4%	1.2%	0.5%	0.6%	0.4%	0.6%	0.2%	0.4%	0.02%	0.6%	0.1%
GDGT-0a	5.1%	1.9%	10.2%	5.4%	6.2%	4.5%	5.8%	2.3%	2.8%	0.2%	6.0%	2.8%
GMGT-0a	0.06%	0.03%	0.07%	0.08%	0.1%	0.06%	0.14%	0.05%	0.04%	0.01%	0.07%	0.04%
GMGT-0a'	0.6%	0.1%	1.0%	0.4%	1.0%	0.7%	1.0%	0.3%	0.4%	0.0%	0.7%	0.3%
GDD-0a	0.0%	0.0%	0.0%	0.0%	0.0%	0.0%	0.0%	0.0%	0.02%	<0.01%	<0.01%	0.01%
GMD-0a	0.0%	0.0%	0.0%	0.0%	0.0%	0.0%	0.0%	0.0%	0.0%	0.0%	0.0%	0.0%
GMD-0a'	0.0%	0.0%	0.0%	0.0%	0.0%	0.0%	0.0%	0.0%	0.0%	0.0%	0.0%	0.0%
Diethers	93.5%		87.5%		92.1%		92.5%		96.3%		92.6%	
Tetraethers	6.5%		12.5%		7.9%		7.5%		3.7%		7.4%	
Sum	100.0%		100.0%		100.0%		100.0%		100.0%		100.0%	

Table 9: Contents of core ether lipids in *Methanocaldococcus villosus* in % at three different volumes of liquid medium at 65°C and gas exchange twice per day (25 mL/Non-OD: n = 4; 25 mL/OD: n = 4; 50 mL/Non-OD: n = 4; 50 mL/OD: n = 4; 75 mL/Non-OD: n = 4; 75 mL/OD: n = 4). "Macr. arch." = macrocyclic archaeol; "Non-OD" = no optical density measurements; "OD" = removal of liquid medium for optical density measurements; "Mean v." = mean value; "SD" = standard deviation. GTGT (glycerol trialkyl glycerol tetraether), GDGT (glycerol dialkyl glycerol tetraether), GMGT (glycerol monoalkyl glycerol tetraether), GDD (glycerol dialkyl diether), and GMD (glycerol monoalkyl diether).

	65°C; 2x daily gas exchange											
	25 mL				**50 mL**				**75 mL**			
	Non-OD		**OD**		**Non-OD**		**OD**		**Non-OD**		**OD**	
	Mean v.	**SD**	**Mean v.**	**SD**	**Mean v.**	**SD**	**Mean v.**	**SD**	**Mean v.**	**SD**	**Mean v.**	**SD**
Archaeol	47.1%	2.5%	56.3%	1.8%	34.9%	5.6%	21.4%	5.5%	38.5%	2.8%	30.2%	6.7%
Macr. arch.	43.2%	4.0%	33.4%	4.7%	59.1%	1.9%	71.4%	5.1%	55.8%	5.2%	62.6%	7.2%
GTGT-0a	0.9%	0.2%	1.0%	0.3%	0.4%	0.2%	0.4%	0.1%	0.4%	0.3%	0.5%	0.1%
GDGT-0a	7.6%	1.6%	8.4%	2.6%	4.5%	3.4%	5.2%	0.6%	4.2%	1.8%	5.3%	1.0%
GMGT-0a	0.1%	0.02%	0.04%	0.01%	0.1%	0.1%	0.2%	0.1%	0.1%	0.04%	0.2%	0.03%
GMGT-0a'	1.1%	0.2%	0.8%	0.1%	1.0%	1.0%	1.4%	0.5%	0.9%	0.4%	1.1%	0.2%
GDD-0a	<0.01%	<0.01%	0.0%	0.0%	0.02%	0.03%	<0.01%	0.01%	0.02%	0.03%	0.03%	0.02%
GMD-0a	0.0%	0.0%	0.0%	0.0%	0.0%	0.0%	0.0%	0.0%	0.0%	0.0%	0.0%	0.0%
GMD-0a'	0.0%	0.0%	0.0%	0.0%	0.0%	0.0%	<0.01%	<0.01%	<0.01%	<0.01%	<0.01%	<0.01%
Diethers	90.3%		89.7%		94.0%		92.8%		94.3%		92.9%	
Tetraethers	9.7%		10.3%		6.0%		7.2%		5.7%		7.1%	
Sum	100.0%		100.0%		100.0%		100.0%		100.0%		100.0%	

Table 10: Contents of core ether lipids in *Methanocaldococcus villosus* in % at three different volumes of liquid medium at 80°C and gas exchange once per day (25 mL/Non-OD: n = 4; 25 mL/OD: n = 4; 50 mL/Non-OD: n = 3; 50 mL/OD: n = 3; 75 mL/Non-OD: n = 4; 75 mL/OD: n = 4). "Macr. arch." = macrocyclic archaeol; "Non-OD" = no optical density measurements; "OD" = removal of liquid medium for optical density measurements; "Mean v." = mean value; "SD" = standard deviation. GTGT (glycerol trialkyl glycerol tetraether), GDGT (glycerol dialkyl glycerol tetraether), GMGT (glycerol monoalkyl glycerol tetraether), GDD (glycerol dialkyl diether), and GMD (glycerol monoalkyl diether).

	80°C; 1x daily gas exchange											
	25 mL				**50 mL**				**75 mL**			
	Non-OD		**OD**		**Non-OD**		**OD**		**Non-OD**		**OD**	
	Mean v.	**SD**	**Mean v.**	**SD**	**Mean v.**	**SD**	**Mean v.**	**SD**	**Mean v.**	**SD**	**Mean v.**	**SD**
Archaeol	25.5%	7.4%	27.7%	4.6%	38.7%	0.9%	33.7%	1.4%	30.9%	2.5%	35.5%	1.9%
Macr. arch.	68.1%	6.9%	66.0%	5.1%	57.9%	1.0%	60.5%	0.6%	62.1%	2.7%	58.1%	3.3%
GTGT-0a	0.2%	0.0%	0.2%	0.1%	0.2%	0.0%	0.3%	0.0%	0.3%	0.1%	0.4%	0.1%
GDGT-0a	4.8%	0.8%	4.4%	0.5%	2.6%	0.4%	4.3%	0.9%	5.3%	1.4%	4.8%	1.7%
GMGT-0a	0.1%	0.03%	0.1%	0.02%	0.1%	0.02%	0.1%	0.01%	0.1%	0.03%	0.1%	0.03%
GMGT-0a'	1.4%	0.2%	1.4%	0.1%	0.5%	0.2%	1.0%	0.2%	1.1%	0.4%	1.1%	0.3%
GDD-0a	<0.01%	<0.01%	0.0%	0.0%	0.01%	0.03%	0.0%	0.0%	0.04%	0.04%	<0.01%	0.02%
GMD-0a	0.0%	0.0%	0.0%	0.0%	0.0%	0.0%	0.0%	0.0%	0.0%	0.0%	0.0%	0.0%
GMD-0a'	<0.01%	<0.01%	0.0%	0.0%	<0.01%	0.01%	0.0%	0.0%	0.01%	0.02%	<0.01%	<0.01%
Diethers	93.5%		93.8%		96.6%		94.2%		93.1%		93.6%	
Tetraethers	6.5%		6.2%		3.4%		5.8%		6.9%		6.4%	
Sum	100.0%		100.0%		100.0%		100.0%		100.0%		100.0%	

Table 11a: Contents of core ether lipids in *Methanocaldococcus villosus* in nanogram per milligram dry weight of biomass (ng/mg dw) at three different volumes of liquid medium at 80°C and gas exchange twice per day (25 mL/Non-OD: n = 4; 25 mL/OD: n = 2; 50 mL/Non-OD: n = 3; 50 mL/OD: n = 4; 75 mL/Non-OD: n = 4; 75 mL/OD: n = 3). "Macr. arch." = macrocyclic archaeol; "Non-OD" = no optical density measurements; "OD" = removal of liquid medium for optical density measurements; "Mean v." = mean value; "SD" = standard deviation. GTGT (glycerol trialkyl glycerol tetraether), GDGT (glycerol dialkyl glycerol tetraether), GMGT (glycerol monoalkyl glycerol tetraether), GDD (glycerol dialkyl diether), and GMD (glycerol monoalkyl diether).

	80°C; 2x daily gas exchange											
	25 mL				**50 mL**				**75 mL**			
	Non-OD		**OD**		**Non-OD**		**OD**		**Non-OD**		**OD**	
	Mean v.	**SD**	**Mean v.**	**SD**	**Mean v.**	**SD**	**Mean v.**	**SD**	**Mean v.**	**SD**	**Mean v.**	**SD**
Archaeol	1090.9	734.1	1917.3	75.4	1446.6	344.2	995.8	152.9	684.7	220.9	928.2	239.1
Macr. arch.	1924.8	999.9	1660.3	38.4	1879.1	139.2	1724.2	84.7	1206.5	101.5	1805.9	461.5
GTGT-0a	11.4	6.2	16.9	1.7	9.6	1.9	7.9	0.6	10.2	4.5	21.6	8.7
GDGT-0a	176.9	128.2	174.0	14.4	149.6	25.8	136.0	18.6	185.9	86.2	316.0	122.0
GMGT-0a	7.7	11.6	2.1	0.3	2.8	0.2	3.2	1.2	2.6	0.6	5.5	1.4
GMGT-0a'	79.5	103.8	37.8	3.0	33.4	1.1	32.0	4.8	37.9	16.3	65.3	22.4
GDD-0a	0.2	0.4	0.0	0.0	0.3	0.5	0.5	0.6	2.3	0.6	2.1	0.4
GMD-0a	0.0	0.0	0.0	0.0	0.0	0.0	0.1	0.2	0.0	0.0	0.0	0.0
GMD-0a'	0.2	0.3	0.0	0.0	0.1	0.2	0.1	0.1	0.6	0.5	0.7	0.1
Diethers	3016.1		3577.6		3326.1		2720.7		1894.1		2736.9	
Tetraethers	275.5		230.8		195.4		179.1		236.6		408.4	
Sum	3291.6		3808.4		3521.5		2899.8		2130.7		3145.3	

Table 11b: Contents of core ether lipids in *Methanocaldococcus villosus* in % at three different volumes of liquid medium at 80°C and gas exchange twice per day (25 mL/Non-OD: n = 4; 25 mL/OD: n = 2; 50 mL/Non-OD: n = 3; 50 mL/OD: n = 4; 75 mL/Non-OD: n = 4; 75 mL/OD: n = 3). "Macr. arch." = macrocyclic archaeol; "Non-OD" = no optical density measurements; "OD" = removal of liquid medium for optical density measurements; "Mean v." = mean value; "SD" = standard deviation. GTGT (glycerol trialkyl glycerol tetraether), GDGT (glycerol dialkyl glycerol tetraether), GMGT (glycerol monoalkyl glycerol tetraether), GDD (glycerol dialkyl diether), and GMD (glycerol monoalkyl diether).

	80°C; 2x daily gas exchange											
	25 mL				**50 mL**				**75 mL**			
	Non-OD		**OD**		**Non-OD**		**OD**		**Non-OD**		**OD**	
	Mean v.	**SD**	**Mean v.**	**SD**	**Mean v.**	**SD**	**Mean v.**	**SD**	**Mean v.**	**SD**	**Mean v.**	**SD**
Archaeol	33.1%	19.7%	50.3%	1.3%	41.1%	4.3%	34.3%	4.3%	32.1%	5.6%	29.5%	5.1%
Macr. arch.	58.5%	16.2%	43.6%	1.6%	53.4%	4.0%	59.5%	4.0%	56.6%	4.4%	57.4%	5.6%
GTGT-0a	0.3%	0.1%	0.4%	0.0%	0.3%	0.1%	0.3%	0.0%	0.5%	0.2%	0.7%	0.4%
GDGT-0a	5.4%	3.0%	4.6%	0.3%	4.2%	0.5%	4.7%	0.6%	8.7%	4.4%	10.0%	5.8%
GMGT-0a	0.2%	0.3%	0.1%	0.01%	0.1%	0.01%	0.1%	0.04%	0.1%	0.03%	0.2%	0.1%
GMGT-0a'	2.4%	3.0%	1.0%	0.1%	0.9%	0.1%	1.1%	0.1%	1.8%	0.8%	2.1%	1.0%
GDD-0a	<0.01%	0.01%	0.0%	0.0%	<0.01%	0.01%	0.02%	0.02%	0.1%	0.03%	0.1%	0.01%
GMD-0a	0.0%	0.0%	0.0%	0.0%	0.0%	0.0%	<0.01%	<0.01%	0.0%	0.0%	0.0%	0.0%
GMD-0a'	<0.01%	<0.01%	0.0%	0.0%	<0.01%	<0.01%	<0.01%	<0.01%	0.03%	0.02%	0.02%	<0.01%
Diethers	91.6%		93.9%		94.5%		93.8%		88.9%		87.0%	
Tetraethers	8.4%		6.1%		5.5%		6.2%		11.1%		13.0%	
Sum	100.0%		100.0%		100.0%		100.0%		100.0%		100.0%	

3.3.3 *Methanothermococcus okinawensis*

Similar to the cultures described in chapter 3.1, the by far two most abundant lipids are archaeol and macrocyclic archaeol. Archaeol is on average more abundant (54%) than macrocyclic archaeol (36.5%). GDGT-0a is the most abundant tetraether lipid (5.5%). Further, GMGT-0a is more abundant (2.4%) than GMGT-0a' (1.1%), and GTGT-0a is the least abundant tetraether (0.3%). GDD-0a (0.2%), GMD-0a (0.03%) and GMD-0a' (<0.01%) are the least abundant lipids. The diether lipids are much more abundant (90.8%) than the tetraether lipids (9.2%). This gives a mean total lipid concentration of 1520 ng/mg dw. The standard deviations between different samples of one experiment of *M. okinawensis* lie in a similar range as those of *M. marburgensis* and *M. villosus* (Tables 6 to 11; Figs. 17 to 19). The average ratio between standard deviation and mean value is 1.84.

3.3.3.1 Cultures at different temperatures

In contrast to *M. marburgensis*, which was cultured at three different temperatures, and *M. villosus*, which was cultured at two temperatures, *M. okinawensis* was cultured at four different temperatures, 50°C, 60°C, 65°C, and 70°C (Table 5). Its temperature optimum lies between 60°C and 65°C (Takai et al., 2002). At 65°C, *M. okinawensis* was additionally cultured under varying liquid medium volumes and varying gassing frequencies (Table 5). However, as for the other two temperatures the experiments were just conducted at 50 mL and a gassing frequency of once per day, also just the 65°C samples cultured at 50 mL and gassing once per day shall be included into this temperature comparison. All concentrations in ng/mg dw can be found in Tables 12 to 14 (Fig. 17; Table S11). GMD-0a' was not detected in any of the mentioned samples.

Archaeol and GTGT-0a are clearly most abundant at 50°C. Archaeol is least abundant at 60°C. GTGT-0a has its lowest concentration at 70°C, and is relative to all other lipids least abundant at 60°C, the same as for archaeol. GDGT-0a has its highest concentration at 60°C and its highest relative abundance at 70°C. It is least abundant at 50°C. Macrocyclic archaeol, GMGT-0a, GMGT-0a', GDD-0a, and GMD-0a have their highest concentrations at 60°C. All of them except for macrocyclic archaeol have their lowest concentration at 50°C. Macrocyclic archaeol has its lowest concentration at 70°C. However, relatively, it is also least abundant at 50°C as the GMGTs and GDDs. The highest relative abundance of macrocyclic archaeol at 60°C coincides with its highest concentration. The GMGTs are relatively most abundant at 70°C and least abundant at 50°C. Diether, as well as tetraether lipids have their highest concentrations at 60°C. However, the diether lipids have their highest relative abundance at 50°C due to the high relative abundance of archaeol there. They have their lowest relative abundance at 70°C.

As all other experiments, these temperature experiments were conducted with and without OD measurements. Whether there was liquid medium removed for OD measurements or not did not have a remarkable impact on the lipid concentrations or ratios (Tables 12 to 14). There are fluctuations between non-OD and OD samples, but these seem to be random and do not change the above-mentioned trends.

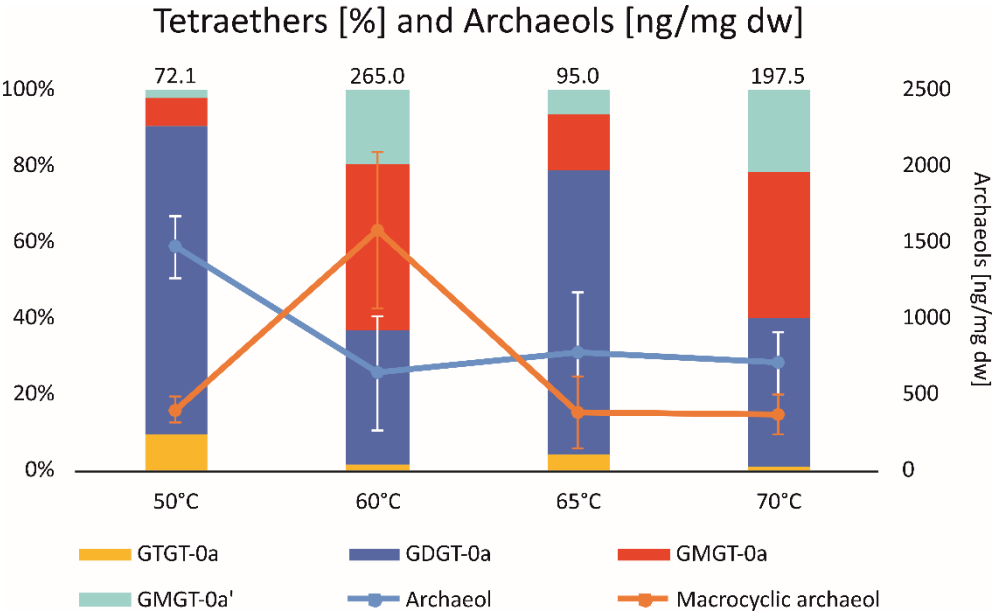

Figure 17: Relative abundance (%) of tetraether lipids (left) and concentrations of archaeol and macrocyclic archaeol (right) in nanogram per milligram dry weight (ng/mg dw) of *Methanothermococcus okinawensis* at four different growth temperatures (50 mL; gas exchange once per day). The bars and the lines represent average values (50°C: n = 8; 60°C: n = 8; 65°C: n = 8; 70°C: n = 8). Total concentrations of tetraether lipids in ng/mg dw are written above the respective bar. Concentrations of archaeol in ng/mg dw are depicted as blue line (with white error bars) and of macrocyclic archaeol as orange line (with orange error bars). Error = standard deviation. GTGT (glycerol trialkyl glycerol tetraether), GMGT (glycerol monoalkyl glycerol tetraether), and GDGT (glycerol dialkyl glycerol tetraether).

3.3.3.2 Changing liquid medium at one temperature

Experiments with changing liquid medium are available with changing gassing frequency, with and without OD measurements, at 65°C only (Table 5). A comparison of the mean values of all samples cultured at 25 mL, 50 mL (65°C only), and 75 mL shows rather clear patterns (Fig. 18; Table S12). Archaeol and GTGT-0a have their highest abundance at 25 mL, and their lowest abundance at 75 mL. GDGT-0a has its highest abundance at 50 mL and its lowest abundance at 25 mL. The remaining lipids have their highest abundances at 75 mL, and their lowest abundances at 25 mL. The diether lipids are in terms of concentration most abundant at 50 mL and relatively at 25 mL. The tetraether lipids are in both aspects most abundant at 75 mL. The highest concentration of total lipids can be found at 50 mL (1370 ng/mg dw; Table S12). The differences in the sum of diethers, tetraethers and total lipids are quite small. However, the values of diethers, tetraethers and total lipids have limited significance, as they are the sum of the complex behavior of the single lipids.

Whether liquid medium was removed for OD measurements had no consistent effect. It is similar as in the temperature comparisons. There are differences between non-OD and OD samples, especially when looking at the concentrations (Table S13). Nevertheless, these differences do not follow a consistent pattern and appear again random. The differences in % of each lipid between non-OD and OD samples are minor (Tables 12 and 13). However, when comparing gassing once or twice per day at the different volumes, it becomes apparent that at one time gassing per day the patterns described above are partly stronger, partly weaker compared to gassing twice per day (Fig. 19; Table S14). Sometimes, the trends are even

different between these two conditions. This is the case for macrocylic archaeol (twice), GTGT-0a (twice), GDGT-0a (once), and GMGT-0a (twice).

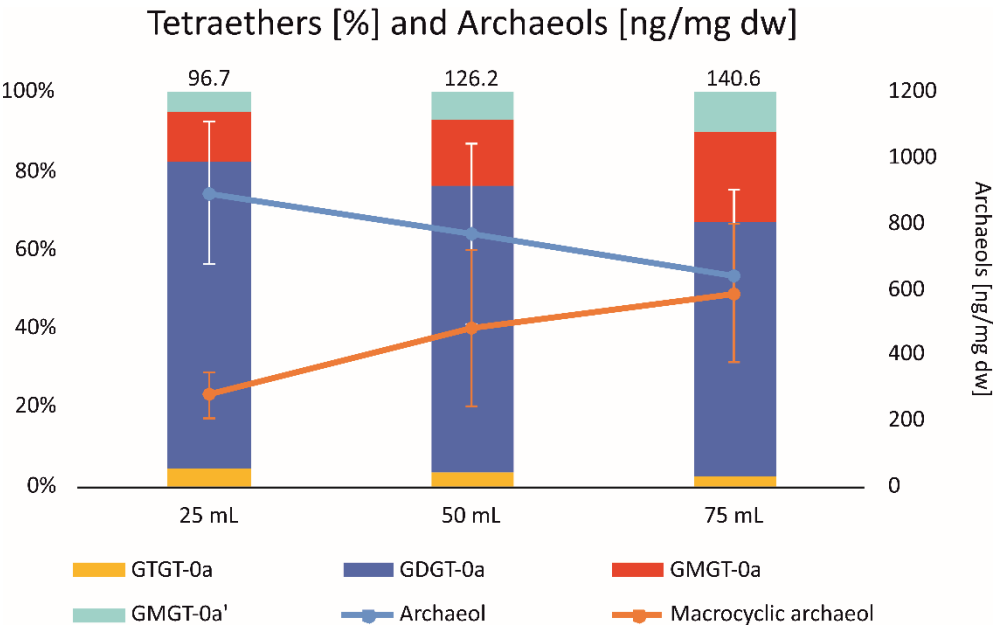

Figure 18: Relative abundance (%) of tetraether lipids (left) and concentrations of archaeol and macrocyclic archaeol (right) in nanogram per milligram dry weight (ng/mg dw) of *Methanothermococcus okinawensis* at three different volumes of liquid medium (65°C; gas exchange once or twice per day). The bars and the lines represent average values (25 mL: n = 16; 50 mL: n = 16; 75 mL: n = 16). Total concentrations of tetraether lipids in ng/mg dw are written above the respective bar. Concentrations of archaeol in ng/mg dw are depicted as blue line (with white error bars) and of macrocyclic archaeol as orange line (with orange error bars). Error = standard deviation. GTGT (glycerol trialkyl glycerol tetraether), GMGT (glycerol monoalkyl glycerol tetraether), and GDGT (glycerol dialkyl glycerol tetraether).

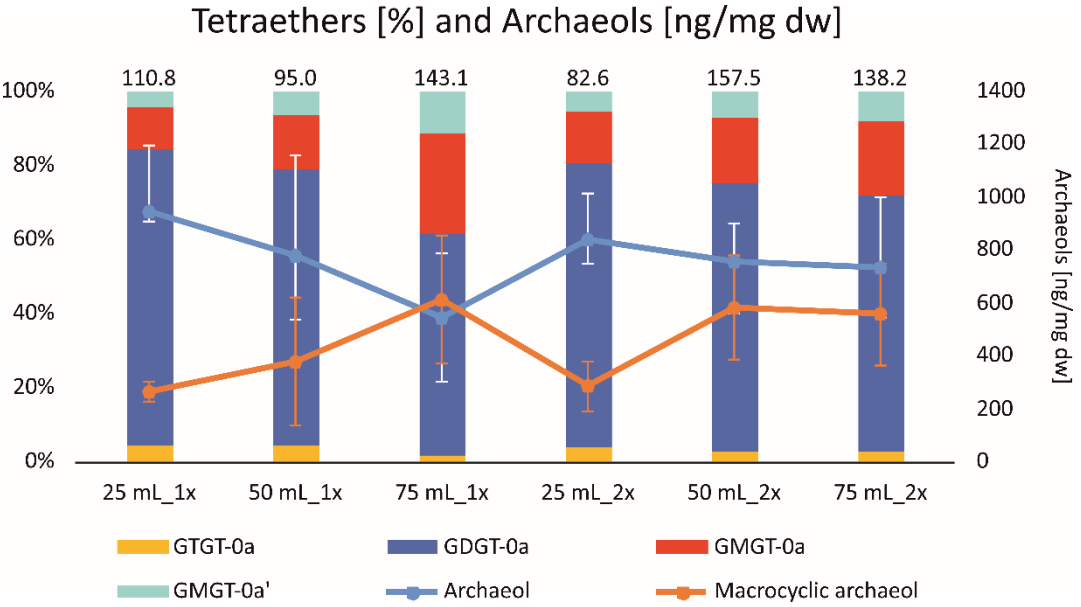

Figure 19: Relative abundance (%) of tetraether lipids (left) and concentrations of archaeol and macrocyclic archaeol (right) in nanogram per milligram dry weight (ng/mg dw) of *Methanothermococcus okinawensis* at three different volumes of liquid medium (65°C; gas exchange once or twice per day). The bars and the lines represent average values (25 mL_1x: n = 8; 50 mL_1x: n = 8; 75 mL_1x: n = 8; 25 mL_2x: n = 8; 50 mL_2x: n = 8; 75 mL_2x: n = 8). Total concentrations of tetraether lipids in ng/mg dw are written above the respective bar. Concentrations of archaeol in ng/mg dw are depicted as blue line (with white error bars) and of macrocyclic archaeol as orange line (with orange error bars). Error = standard deviation. GTGT (glycerol trialkyl glycerol tetraether), GMGT (glycerol monoalkyl glycerol tetraether), and GDGT (glycerol dialkyl glycerol tetraether).

3.3.3.3 Gassing frequency

The difference between all samples cultured with gassing once per day (at 65°C) and all samples cultured with gassing twice per day is very low, in concentration as well as % (Table S15). The concentration of the most abundant lipids archaeol, macrocyclic archaeol, GDGT-0a, and GMGT-0a is slightly higher at a gas exchange twice per day. The concentration of the lipids with a general low abundance, GTGT-0a, GMGT-0a', and the GDDs is slightly higher at gassing once per day. Therefore, the total lipid concentration is higher at a gas exchange twice (1377 ng/mg dw) than once per day (1287 ng/mg dw; Table S15). The total concentrations of diethers and tetraethers are both also higher at gassing twice than once. The differences in % are negligible. The groups of lipids are not visible in this comparison. However, the gassing frequency has indeed an effect, when comparing the difference at each volume of liquid medium separately, as described above.

3.3.3.4 Non-OD vs. OD

The difference between all samples without and all samples with OD measurements is negligible in terms of concentration, as well as %.

Table 12: Contents of core ether lipids in *Methanothermococcus okinawensis* in nanogram per milligram dry weight of biomass (ng/mg dw) at 65°C and gas exchange once per day (25 mL/Non-OD: n = 4; 25 mL/OD: n = 4; 50 mL/Non-OD: n = 4; 50 mL/OD: n = 4; 75 mL/Non-OD: n = 4; 75 mL/OD: n = 4). "Macr. arch." = macrocyclic archaeol; "Non-OD" = no optical density measurements; "OD" = removal of liquid medium for optical density measurements; "Mean v." = mean value; "SD" = standard deviation. GTGT (glycerol trialkyl glycerol tetraether), GDGT (glycerol dialkyl glycerol tetraether), GMGT (glycerol monoalkyl glycerol tetraether), GDD (glycerol dialkyl diether), and GMD (glycerol monoalkyl diether).

	65°C; 1x daily gas exchange											
	25 mL				**50 mL**				**75 mL**			
	Non-OD		**OD**		**Non-OD**		**OD**		**Non-OD**		**OD**	
	Mean v.	**SD**	**Mean v.**	**SD**	**Mean v.**	**SD**	**Mean v.**	**SD**	**Mean v.**	**SD**	**Mean v.**	**SD**
Archaeol	1008.0	358.1	871.8	98.0	665.0	290.1	881.1	474.4	544.9	202.9	539.1	311.6
Macr. arch.	266.6	56.6	265.7	5.5	308.6	145.3	440.8	320.3	684.3	198.3	535.4	280.5
GTGT-0a	5.1	2.0	5.4	2.0	4.2	2.4	3.9	0.5	3.0	2.6	2.7	1.7
GDGT-0a	81.2	29.5	94.6	40.8	70.8	51.4	71.1	15.1	84.0	65.0	87.3	62.7
GMGT-0a	11.7	3.7	13.6	5.4	12.7	7.0	14.8	3.5	38.3	28.5	38.5	28.7
GMGT-0a'	4.8	1.3	5.3	1.6	6.1	3.3	6.3	1.8	18.3	12.7	14.1	9.2
GDD-0a	0.0	0.0	0.9	0.6	1.1	0.2	1.6	0.6	4.1	1.9	4.0	3.4
GMD-0a	0.0	0.0	0.0	0.0	0.0	0.0	0.0	0.0	0.9	0.7	0.6	0.4
GMD-0a'	0.0	0.0	0.0	0.0	0.0	0.0	0.0	0.0	0.1	0.2	0.0	0.0
Diethers	1274.6		1138.4		974.7		1323.5		1234.3		1079.1	
Tetraethers	102.8		118.9		93.8		96.1		143.6		142.6	
Sum	1377.4		1257.3		1068.5		1419.6		1377.9		1221.7	

Table 13: Contents of core ether lipids in *Methanothermococcus okinawensis* in nanogram per milligram dry weight of biomass (ng/mg dw) at 65°C and gas exchange twice per day (25 mL/Non-OD: n = 4; 25 mL/OD: n = 4; 50 mL/Non-OD: n = 4; 50 mL/OD: n = 4; 75 mL/Non-OD: n = 4; 75 mL/OD: n = 4). "Macr. arch." = macrocyclic archaeol; "Non-OD" = no optical density measurements; "OD" = removal of liquid medium for optical density measurements; "Mean v." = mean value; "SD" = standard deviation. GTGT (glycerol trialkyl glycerol tetraether), GDGT (glycerol dialkyl glycerol tetraether), GMGT (glycerol monoalkyl glycerol tetraether), GDD (glycerol dialkyl diether), and GMD (glycerol monoalkyl diether).

	65°C; 2x daily gas exchange											
	25 mL				**50 mL**				**75 mL**			
	Non-OD		**OD**		**Non-OD**		**OD**		**Non-OD**		**OD**	
	Mean v.	**SD**	**Mean v.**	**SD**	**Mean v.**	**SD**	**Mean v.**	**SD**	**Mean v.**	**SD**	**Mean v.**	**SD**
Archaeol	879.5	163.3	796.6	198.2	673.3	76.3	840.0	140.6	577.0	303.4	892.5	38.7
Macr. arch.	297.8	124.4	267.6	69.5	466.4	33.4	693.7	236.1	539.6	287.9	571.1	57.8
GTGT-0a	3.5	2.3	3.1	3.1	2.8	1.1	5.9	3.8	3.7	3.9	4.0	1.9
GDGT-0a	62.3	46.1	64.2	76.1	73.7	39.1	153.4	116.6	114.0	96.2	77.5	36.4
GMGT-0a	12.1	8.3	10.9	10.1	19.4	10.0	38.2	26.2	35.6	29.8	18.8	8.8
GMGT-0a'	4.9	3.4	4.2	3.9	7.9	4.1	13.7	8.1	15.1	12.3	7.8	3.5
GDD-0a	0.0	0.0	0.1	0.2	1.9	0.7	2.2	1.5	2.6	2.5	1.8	0.5
GMD-0a	0.0	0.0	0.1	0.2	0.0	0.0	0.2	0.3	0.4	0.3	0.1	0.1
GMD-0a'	0.0	0.0	0.0	0.0	0.0	0.0	0.0	0.0	0.0	0.0	0.0	0.0
Diethers	1177.3		1064.4		1141.6		1536.1		1119.6		1465.5	
Tetraethers	82.8		82.4		103.8		211.2		168.4		108.1	
Sum	1260.1		1146.8		1245.4		1747.3		1288.0		1573.6	

Table 14: Contents of core ether lipids in *Methanothermococcus okinawensis* in nanogram per milligram dry weight of biomass (ng/mg dw) at three different temperatures, 50 mL of liquid medium, and gas exchange once per day (50°C/Non-OD: n = 4; 50°C/OD: n = 4; 60°C/Non-OD: n = 4; 60°C/OD: n = 4; 70°C/Non-OD: n = 4; 70°C/OD: n = 4). "Macr. arch." = macrocyclic archaeol; "Non-OD" = no optical density measurements; "OD" = removal of liquid medium for optical density measurements; "Mean v." = mean value; "SD" = standard deviation. GTGT (glycerol trialkyl glycerol tetraether), GDGT (glycerol dialkyl glycerol tetraether), GMGT (glycerol monoalkyl glycerol tetraether), GDD (glycerol dialkyl diether), and GMD (glycerol monoalkyl diether).

	50 mL; 1x daily gas exchange; different temperatures											
	50°C				**60°C**				**70°C**			
	Non-OD		**OD**		**Non-OD**		**OD**		**Non-OD**		**OD**	
	Mean v.	**SD**	**Mean v.**	**SD**	**Mean v.**	**SD**	**Mean v.**	**SD**	**Mean v.**	**SD**	**Mean v.**	**SD**
Archaeol	1513.7	272.8	1408.6	115.3	810.6	479.0	453.4	123.8	624.4	184.4	770.0	212.4
Macr. arch.	430.6	102.0	352.3	40.6	1672.0	752.7	1469.8	155.8	337.7	159.3	375.2	118.4
GTGT-0a	5.8	1.6	7.8	3.8	4.5	2.3	2.9	1.8	2.1	0.5	2.7	1.2
GDGT-0a	46.4	10.1	70.0	39.0	109.9	49.8	76.2	46.7	82.8	46.8	69.8	23.3
GMGT-0a	5.3	1.9	5.8	2.2	112.9	61.3	119.7	68.5	82.6	44.4	68.8	20.4
GMGT-0a'	1.4	0.8	1.6	0.7	49.3	24.1	54.5	27.6	44.1	23.0	42.3	10.3
GDD-0a	0.0	0.0	0.2	0.4	8.3	4.3	11.3	5.6	2.4	1.5	2.0	0.2
GMD-0a	0.0	0.0	0.0	0.0	2.6	1.5	1.8	1.3	1.2	0.6	0.8	0.3
GMD-0a'	0.0	0.0	0.0	0.0	0.0	0.0	0.0	0.0	0.0	0.0	0.0	0.0
Diethers	1944.3		1761.1		2493.5		1936.3		965.7		1148.0	
Tetraethers	58.9		85.2		276.6		253.3		211.6		183.6	
Sum	2003.2		1846.3		2770.1		2189.6		1177.3		1331.6	

4. Discussion

4.1 The relevance of the membrane lipid inventories of *M. villosus* and *M. okinawensis* for the geological record and the biomarker concept

M. villosus and *M. okinawensis* are closely related based on 16S rRNA and 16S rDNA sequences and DNA-DNA hybridization analysis. The lipids of close relatives of these strains were described previously. *M. jannaschii*, belonging to the same genus as *M. villosus*, is one of the best-studied archaea to date. It was isolated from the base of a white smoker chimney on the East Pacific Rise (Jones et al., 1983) and its lipids were first described by Comita and Gagosian (1983). Lipid-culture experiments were so far conducted under varying temperatures (Sprott et al., 1991) and varying pressures (Kaneshiro and Clark, 1995). The only other species from the genus *Methanothermococcus* beside *M. okinawensis* is *M. thermolithotrophicus*, which was isolated from geothermally heated sea sediments close to Naples, Italy, and first described by Huber et al. (1982). Similar to *M. okinawensis*, its optimum growth temperature is 65°C. The lipids of *M. thermolithotrophicus* comprise GDGT-0 to -2, several isomers of OH-GDGT-0 and 2OH-GDGT-0 and GDD-0 (Liu et al., 2012b,c). However, there are hints that *M. thermolithotrophicus* is not the closest known relative of *M. okinawensis*. Based on 16S rRNA gene sequences, *Methanococcus aeolicus* is suggested to be the closest relative of *M. okinawensis*, despite the fact that it has a lower growth temperature (mesophilic or slightly above 46°C; Keswani et al., 1996; Takai et al., 2002; Kendall et al., 2006). The type and reference strains of *M. aeolicus* were isolated from sediment from the Nankai Trough near the coast of Japan and from shallow marine sediment from the Lipari Islands near Sicily, Italy (Kendall et al., 2006). The lipids of *M. aeolicus* were described by Koga et al. (1998).

M. villosus and *M. okinawensis* exhibit the same inventory of core lipids, but have different IPL compositions. *M. villosus* produces dominantly diglycosidic head groups, whereas monoglycosidic head groups are most prominent in *M. okinawensis* (Table 2; Fig. 6). Minor amounts of phosphoglycosidic lipids have been detected in *M. okinawensis*, which were not found in *M. villosus*. This work did not find the same diversity of head groups for *M. villosus* as reported for *M. jannaschii*. Beside mono- and diglycolipids *M. jannaschii* additionally contains phospholipids, aminolipids, phosphoglycolipids, aminophospholipids, and even an aminophosphoglycolipid (Ferrante et al., 1990; Koga et al., 1993; Koga et al., 1998; Sturt et al., 2004). *M. thermolithotrophicus* exhibits mono-, di-, and triglycolipids, phospholipids, and aminophospholipids (Koga et al., 1993; Koga et al., 1998; Sturt et al., 2004; Liu et al., 2012a). It was also in contrast to previous data that *M. villosus* yielded no GMGT-0a with phosphoglycosidic head groups and *M. okinawensis* yielded just minor amounts of GMGT-0a with phosphoglycosidic head groups, whereas Schouten et al. (2008a) found that GMGTs occur mainly with phosphoglycosidic head groups. However, it cannot be excluded that these differences in observed head groups are at least in part due to different culture conditions. Culture experiments showed that glycolipids are favored over the more permeable phospholipids under heat stress, low pH, and nutrient limitation (Yoshinaga et al., 2015; Sollich et al., 2017). Their high optimum growth temperatures could eventually be an explanation for the low abundance of GMGTs with phosphoglycosidic head groups in *M. okinawensis*, grown at 65°C, and in the complete lack of them in *M. villosus*, grown at 80°C. Possibly, these (hyper)thermophilic strains have adopted to "permanent heat stress" by preferably synthesizing glycolipids instead of phospholipids. Although, the taxonomic specificity of the present results is limited, IPLs can indeed have taxonomic significance (e.g. Sturt et al., 2004; Gibson et al., 2013) and might be used to distinguish between certain orders of methanogens. There are various examples of methanogenic orders with already known IPL composition (Koga et al.,

1998). Methanococcales reveal glycolipids with glucose *N*-acetylglucosamine, and phospholipids with ethanolamine and serine (Koga et al., 1998). In Methanobacteriales phospholipids with *myo*-inositol and serine, and some with ethanolamine have been detected. One group of the Methanobacteriales exhibits glycolipids with glucose *N*-acetylglucosamine; and glycolipids with galactose and phospholipids with aminopentanetetrols and glycerol occur in the order Methanomicrobiales. In Methanopyrales glycolipids with galactose and with mannose have been found (Koga et al., 1998). Some members of the order Methanosarcinales produce glycolipids with galactose and mannose, others produce phospholipids with serine, and almost all of them have phospholipids with *myo*-inositol, ethanolamine, and glycerol. All of the methanogenic orders mentioned above have glycolipids with glucose as their sugar (Koga et al., 1998). It is therefore not mentioned explicitly in each of these orders. The present results are in accord with these data.

IPL analysis was solely conducted for the compound inventory, but not for precise quantification. In contrast, much effort was made to quantify core lipids. Hence, several consistent differences in the relative abundances of core lipids between *M. villosus* and *M. okinawensis* could be identified. Under the applied culture conditions, *M. villosus* contains predominantly macrocyclic archaeol, whereas *M. okinawensis* contains predominantly archaeol. Moreover, the two strains could easily be distinguished based on the GMGT-0a/GMGT-0a' ratio. The ratio was 0.1 in *M. villosus* and 2.5 in *M. okinawensis*. Based on these differences, these strains can easily be distinguished from each other as axenic cultures. The more intriguing question is, however, whether these two strains can be distinguished from other groups of Archaea. A major, but very common, obstacle to this is that most of the core lipids of *M. villosus* and *M. okinawensis* are ubiquitously distributed among the Archaea and have thus only little taxonomic specificity. GDGT-0a for instance is often considered as typical for methanogens. Yet, it has already been reported from euryarchaea, crenarchaea, and thaumarchaea (De Rosa et al., 1977; Langworthy, 1977; Schouten et al., 2013). Archaeol has been described from these groups too and is even more widespread than GDGT-0a (e.g. De Rosa and Gambacorta, 1988; Koga et al., 1998; Schouten et al, 2013). GTGT-0a was originally described from the crenarchaeon *Sulfolobus solfataricus* (De Rosa et al. 1983), but was detected in a diverse array of archaea since then (e.g. De Rosa and Gambacorta, 1988; Schouten et al., 2008a, c, 2013; Knappy et al., 2011, 2015; Jaeschke et al., 2014). Among them are for instance the thaumarchaeon "Candidatus *Nitrosopumilus maritimus*" (Schouten et al., 2008b) and various methanogenic Euryarchaeota (Bauersachs et al., 2015). Archaeol, GTGT-0a, and GDGT-0a are thus not specific for methanogenic archaea. GMGT-0a, on the other hand, has been considered to be more specific several years ago. It was originally reported from two different axenic cultures of the order Methanobacteriales, namely *Methanothermus fervidus* (Morii et al., 1998) and *M. thermautotrophicus* (Knappy, 2010; Knappy et al., 2015). However, GMGTs were detected in cultures of non-methanogenic archaea as well and even in archaea, which do not belong to the euryarchaea. Some representatives of the order Thermococcales (also euryarchaea, Sugai et al., 2004) and the thermoacidophilic euryarchaeon *Candidatus Aciduliprofundum boonei* revealed GMGTs with up to four cyclopentane rings (Schouten et al., 2008a). Such GMGTs were later on also found in the crenarchaeon *Ignisphaera aggregans*, which belongs to the Desulfurococcales (Knappy et al., 2011). GMGTs were not only found in cultures, but also in various environmental samples including geothermally heated marine settings. There, GMGT synthesis was assumed to be an adaptation to high temperatures (Jaeschke et al., 2012, 2014; Liu et al., 2012a; Gibson et al., 2013; Bauersachs and Schwark, 2016; Sollich et al., 2017). Nevertheless, GMGTs turned out to also occur in mesophilic marine and lacustrine sediments (Schouten et al., 2008c) and in peat soils (Naafs et al., 2018). The occurrences in non-hydrothermal settings seem to be a function of latitude, with increased abundances in tropical areas. However, this alone is no proof that GMGTs are generally more

abundant at higher temperatures. The temperature difference between tropical soils, mesophilic sediments, and hydrothermal vent systems is so big that it is hard to generalize the observed patterns.To sum it up, GMGTs have so far been found in axenic cultures of methanogenic and non-methanogenic (hyper)thermophilic euryarchaea, in one crenarchaeon, as well as in various geothermally heated and temperate environments. The findings here represent the first identification of GMGTs in members of the order Methanococcales, and the first identification of a second isomer of GMGT-0 overall. These two isomers of GMGT-0a are most likely no regioisomers with parallel and antiparallel configuration of the glycerol units, because there were also two isomers of GMD-0a observed in other samples of *M. villosus* and *M. okinawensis* (see chapter 3.3), which have just one glycerol unit. Hence, it is more likely that the location of the covalent bond between the two isoprenoid chains is different. The performed MS/MS measurements did not allow identification of the exact position of the covalent bond. For this, nuclear magnetic resonance (NMR) analysis would be needed to unequivocally determine the nature of the structural difference of the two isomers.

This is the first report of macrocyclic archaeol in the genus *Methanothermococcus* and the first report in *M .villosus*. Nevertheless, the latter finding was not surprising, as this component has already been reported from members of the genus *Methanocaldococcus* (Comita and Gagosian, 1983; Comita et al., 1984; Sprott et al., 1991). Both, *M. villosus* and *M. okinawensis*, yielded high amounts of macrocyclic archaeol. It is the most abundant lipid in *M. villosus* (55%) and the second most abundant lipid in *M. okinawensis* (35%). Hence, if high amounts of macrocyclic archaeol are found in environmental samples, this may be an indicator for methanogens of the order Methanococcales. Of course, it has to be taken into consideration that, as always in environmental samples, other archaea are present as well, which may dilute the signal. Macrocyclic archaeol was first found in isolates of the closest known relative of *M. villosus, M. jannaschii* (Comita and Gagosian, 1983; Comita et al., 1984; Sprott et al., 1991). Besides *M. jannaschii*, macrocyclic archaeol was later on found in the Guaymas CS-1 hydrothermal vent isolate, a close relative of *M. villosus* and *M. okinawensis* based on its DNA base composition (G+C; Jones et al., 1989); and in the haloalkaliphilic, methylotrophic methanogen *Methanosalsum natronophilum*, isolated from a hypersaline soda lake in the Kulunda Steppe, Siberia (Sorokin et al., 2015). In the Guaymas isolate CS-1 macrocyclic archaeol accounted for 15% of the total polar lipids (Jones et al., 1989), while it made up no more than 7% in the more distantly related *M. natronophilum* (Sorokin et al., 2015). Surprisingly, macrocyclic archaeol has not been found in pure cultures of the close relative of *M. okinawensis, M. thermolithotrophicus* (Liu et al., 2012b,c). Apart from cultures, this compound has been detected in recent environmental samples, namely in a methane-derived carbonate crust from a mud volcano from the northeastern Black Sea (Stadnitskaia et al., 2003) and in sulfidic hydrothermal vent deposits from the Turtle pits hydrothermal field on the Mid-Atlantic Ridge (Blumenberg et al., 2007, 2012). Macrocyclic archaeol has also been found in samples from the geological record, including a Miocene methane-seep limestone from northern Italy (Birgel and Peckmann, 2008), and tubular concretions from a subsurface plumbing network of an Early Eocene methane-seep system in northeastern Bulgaria (De Boever et al., 2009). The source organisms of these occurrences of macrocyclic archaeol might have been methanogenic archaea in the case of Turtle pits (Blumenberg et al., 2007, 2012), but in the case of the other locations it might have been methanotrophic archaea instead. The latter is a plausible assumption, since many methanotrophic archaea are closely related to methanogenic archaea. In fact, phylogenetically, some members of methanotrophs and methanogens are more closely related than the entirety of the methanotrophs and the entirety of the methanogens among each other (Hinrichs et al, 1999; Blumenberg et al., 2004; Schrenk et al., 2004; Niemann and Elvert, 2008; Rossel et al., 2008; Timmers et al., 2017). In the environmental samples described above not only macrocyclic archaeol without cyclopentane

moieties, but also macrocyclic archaeol with one or two cyclopentane moieties has been reported (Stadnitskaia et al., 2003; Birgel and Peckmann, 2008; De Boever et al., 2009). In short, macrocyclic archaeol has so far been described from pure cultures of hyperthermophilic and non-thermophilic methanogens from hydrothermal and non-hydrothermal settings, where either methanogens or methanotrophs constitute the most likely source organisms.

For these reasons, a most likely higher specificity and higher relative abundance, macrocyclic archaeol may be a better indicator for methanogens than GMGT-0a. Two isomers of GMGT-0a have not been reported from other (hyper)thermophilic archaea to date, so, they might be diagnostic for the two studied strains. However, in this work two isomers of GMGT-0a have also been detected in *M. marburgensis*, and not only two isomers of GMGT-0a, but also GMGTs with additional methylations (GMGT-0b and -0c). As *M. marburgensis* is rather distanctly related to *M. villosus* and *M. okinawensis*, compared to other methanogens, this could mean that two isomers of GMGT-0 (and GMD-0) are common and just have not been detected so far. Hence, further studies are required, with cultures and on environmental samples, searching for isomers of GMGTs. For now, with the limitation of the current data in mind, the presence of two isomers of GMGT-0a in environmental samples might be taken as a marker for archaea belonging to the Methanococcales, Methanobacteriales, or for thermophilic methanogens in general. The combination of high amounts of macrocyclic archaeol with two isomers of GMGT-0a may even be diagnostic for members of the genera *Methanocaldococcus* and *Methanothermococcus*.

Isoprenoid GDD-0a and GMD-0a are only minor constituents of the encountered core lipid inventories. Nevertheless, they may serve as good biomarkers as well. Previously, isoprenoid GDDs have been found in a culture of *M. thermolithotrophicus* (Liu et al., 2012b), various modern marine sediments (Liu et al., 2012b), and in sediments of a Jurassic manganese-ore deposit (Bauersachs and Schwark, 2016). GDDs usually occur together with GDGTs and biphytane diols with a similar ring distribution (Liu et al., 2012c, 2016; Bauersachs and Schwark, 2016). This finding implies that GDDs derive from the same source like the other two compound classes. Hence, they could be either a product of sample preparation, represent biosynthetic intermediates, or diagenetic or enzymatic degradation products of GDGTs (Liu et al., 2012b, 2016, Bauersachs and Schwark, 2016). The occurence of GMD-0a in the present samples seems to be typical for (hyper)thermophilic archaea, as this compound has so far only been reported from marine hydrothermal environments (Bauersachs and Schwark, 2016). However, if GMGTs and GMDs derive from the same source, it needs to be stressed that GMGTs have also been described from temperate environments, as mentioned above (Schouten et al., 2008c, Naafs et al., 2018). GDDs have been found as intact polar lipids (Meador et al., 2014), but in the current work *M. villosus* and *M. okinawensis* did not yield such compounds, most likely due to the small amounts, in which they occurred. In summary, GDD-0a and GMD-0a should not yet be considered as possible biomarkers for *M. villosus* or *M. okinawensis*, since it cannot be excluded that the compounds found here are artifacts of sample preparation.

4.2 Implications for the search for life on Enceladus and other ocean worlds with hydrothermal activity

4.2.1 Effect of varying concentrations of inhibitors on the lipid inventory of *M. okinawensis*

M. okinawensis was also cultivated at conditions mimicking those potentially occurring on Enceladus, with H_2 and CO_2 present, but also with CH_3OH, NH_4Cl and H_2CO in amounts, which are thought to reflect those on Enceladus (Taubner and Baumann et al., 2019). The three latter components are known to inhibit growth and activity of methanogenic archaea, and of the strains tested in a previous study, solely *M. okinawensis* was able to grow under the harsh conditions expected to prevail on Enceladus (Taubner et al., 2018). In this thesis, changes in the composition of membrane core lipids and free amino acids were analyzed under varying concentrations of the three potential inhibitors for the first time. Previously, lipid production in Archaea was studied at varying temperatures, pressures, pH values, and salinities (e.g. Yoshinaga et al., 2015; Siliakus et al., 2017). The first of such lipid-culture-experiments were conducted with *M. jannaschii*, at various temperatures (Sprott et al., 1991) and at varying pressures (Kaneshiro and Clark, 1995). Later on, the lipids of the methylotrophic, psychrophilic *Methanococcoides burtonii* grown under changing temperatures were studied (Nichols et al., 2004). The core lipids of *M. thermautotrophicus* were analysed under changing ambient temperatures (Knappy, 2010; Knappy et al., 2015), at different growth stages (Kramer and Sauer, 1991). Its IPL composition was determined at different growth stages (Morii and Koga, 1993) and at varying H_2 and micronutrient (potassium and phosphate) availability (Yoshinaga et al., 2015). There were also lipid-culture studies conducted with *M. marburgensis*, grown with the addition of detergents (polysorbate or Tween®-20 or -80, which can lyse mammalian cells; Gräther, 1994). Addition of detergents led to an increased production of GDGT-0 with one additional methyl group in one of the biphytanyl chains. To the best of the author's knowledge, the thesis of Gräther (1994) is the only other study apart from the present one, which investigated core lipids of a methanogen grown in the presence of inhibitors.

The membrane core lipid patterns of *M. okinawensis* exposed to DoE and to the extreme concentrations of the three inhibitors revealed clear and partially unexpected trends. The lipid content of the DoE design space cultures generally followed the population growth curves as determined by OD measurements (Table 3). Hence, there is a positive correlation between OD_{max} and lipid content. H_2CO had the largest influence on this ratio, followed by NH_4Cl. Both, OD_{max} and lipid content were lowest at the highest concentrations of H_2CO and were highest at its lowest concentrations. Unlike the lipids, the amount of excreted amino acids was mainly a function of the concentration of NH_4Cl. The reason for the varying ratio of lipid/biomass, and why it correlates with growth, is unknown. The lipid/biomass ratio could for instance change when cells change their size. In this case, a high lipid content would mean a higher surface-to-volume ratio and consequently, smaller cells. Cells would become smaller when they grow quicker and divide faster in the current experiments. Perhaps, producing less and bigger cells is a stress response caused by substrate limitation. Any further assumptions on that issue cannot be made, as the cell sizes of the cultures were not determined. An intracellular accumulation of lipids could be another cause for changes in lipid contents. As shown for a strain of unicellular microalgae, a bigger population size correlates with a higher lipid content (De-Bashan et al., 2002). The study with the microalgae additionally found that an increase in cell size, which lowers the surface-to-volume ratio, leads to a lower lipid content per cell. Of course, it needs to be kept in mind that microalgae are photosynthetic eukaryotes, not methanogenic archaea. Therefore, any conclusions from this comparison should be drawn with caution. Nevertheless, it could be that these basic functions are similar or alike for all cellular, terrestrial organisms.

In the DoE design space as well as the extreme value experiments, it seems that those lipids likely making the cell membranes less rigid and more permeable (archaeol and GTGT-0a) substitute membrane-spanning, membrane-stabilizing lipids (macrocyclic archaeol, GDGT-0a, GMGT-0a, and GMGT-0a') at enhanced concentrations of inhibitors. In archaeol, the ends of the alkyl chains are loose, while in macrocyclic archaeol they are connected via a covalent C-C bond. It is similar for GDGT-0a and even more for the GMGTs in comparison with GTGT-0a. GTGT-0a has two loose ends of phytane chains in its center, which GDGT-0a has not. In the GMGTs, there is an additional covalent C-C bond, which links both biphytane chains together, and thus provides even more structural stability. Apart from these theoretical considerations, there are empirical studies, which indeed showed a higher content of macrocyclic archaeol and GMGTs at higher temperatures (Sprott et al., 1991; Naafs et al., 2018) and a higher content of GDGT-0a at a lower pH (McCartney et al., 2014; for reviews on that topic, see Van de Vossenberg et al., 1998; and Siliakus et al., 2017). Assuming the degree of intoxication is increasing with increasing amounts of H_2CO and NH_4Cl, these relationships seem to be counterintuitive for the present work. It would imply that *M. okinawensis* makes its membrane more permeable in the presence of – what is commonly seen as – inhibitor for cell growth.

The inhibiting effect of NH_4Cl and H_2CO on cell growth has been demonstrated before, among others for *M. thermautotrophicus* (Lu and Hegemann, 1998; Kato et al., 2008). Hence, another explanation for the observations of the current experiment may be that H_2CO and NH_4Cl made the cells more permeable by injuring them. One study tested the effect of artificial antimicrobial peptides mimicking those of the human intestinal immune system on the methanogens *Methanobrevibacter smithii*, *M. stadtmanae*, and *Methanosarcina mazei* (Bang et al., 2012). The peptides indeed did some damage to the pseudomurein walls, the proteinaceous surface layers, and the membranes of the cells. When *M. thermautotrophicus* was exposed to different environmental stimuli, including 500 mmol/L NH_4Cl (Kato et al., 2008; in the present thesis, a maximum amount of 263 mmol/L was used), changes in gene regulation could be identified. The environmental stimuli led to an upregulation of several genes related to cell wall modification. Another study demonstrated that *M. thermautotrophicus* makes its cells less permeable under nutrient limitation in order to maintain a sufficiently high concentration of the respective nutrient within the cell (Yoshinaga et al., 2015). This represents an example, where a methanogen optimized its membrane to challenging environmental conditions. In contrast, the changes in lipid composition of *M. okinawensis* in the current experiments do not indicate that the organism adapts by producing more resistant lipids (i.e., GDGT-0a, GMGTs, and macrocyclic archaeol). It rather seems that the presence of the inhibitors had a negative impact on the production of those lipids in *M. okinawensis*, which are considered to build a more rigid membrane.

To assess this effect in more detail, it would be helpful to identify the biosynthesis routes of ether lipids in *M. okinawensis*. *M. okinawensis* might require more steps to build macrocyclic archaeol, GDGT-0a, and the GMGTs than it does to synthesize archaeol and GTGT-0a. Consequently, archaeol could be the precursor of macrocyclic archaeol or tetraethers and GTGT-0a could be a precursor in GDGT-0a and the GMGTs synthesis. Since the early 1980s, many studies addressed the question, how tetraethers are built and whether diethers are their precursors or not (for review, see Koga et al., 1993; Koga and Morii, 2007; Caforio and Driessen, 2017). The outcomes of these studies are partly contradictory. Kushwaha et al. (1981) analyzed the polar lipids of *Methanospirillum hungatei* and concluded that tetraether polar lipids are synthesized from fully saturated diether lipids, which already have the respective polar head groups attached. Morii and Koga (1994) came to the same conclusion when testing

the lipids of *M. thermautotrophicus*, as well as Kon et al. (2002) and Nemoto et al. (2003) with their inhibition study with the thermoacidophilic archaeon *Thermoplasma acidophilum*. In contrast, Poulter et al. (1988), who did labelling experiments with *M. hungatei*, suggested that diethers are not the immediate precursors of tetraethers. Instead, the authors suggested that tetraethers are formed from unsaturated C_{20} hydrocarbon moieties. Later on, Eguchi et al. (2000) conducted labelling experiments with *M. jannaschii* and *M. thermautotrophicus*, and came to similar conclusions, namely that the formation of the C-C bond between two C_{20} hydrocarbon moieties preceded the saturation of the double bonds. Villanueva et al. (2014) suggested a biosynthetic pathway for tetraethers, which first step is more or less the same as in the assumptions of Poulter et al. (1988) and Eguchi et al. (2000). They propose that the first unsaturated biphythane becomes attached to the first glycerol via an ether bond. Then, the second, unsaturated biphytane also forms an ether bond at the same glycerol. After that, the second glycerol becomes ether-attached at the other ends of the two still unsaturated biphytanes. Then, the saturation of the biphytane chains follows (the tetraether core lipid is now formed), and finally the attachment of the polar head groups at the two glycerol moieties (Villanueva et al., 2014). Caforio and Driessen (2017) reviewed this and, in light of the previous studies, rather argued for a tail-to-tail condensation of two unsaturated diether lipids. However, they also state that the enzymatic mechanisms still remain to be elucidated. For the current findings from *M. okinawensis*, it would make more sense, if the first theory of Kushwaha et al. (1981), Morii and Koga (1994), Kon et al. (2002) and Nemoto et al. (2003) holds true. That way, one could argue that macrocyclic archaeol is formed from archaeol by adding an additional C-C bond; or that GDGT-0a and the GMGTs are formed from either archaeol or GTGT-0a through additional C-C condensations. Nevertheless, it has not been tested here and ultimate conclusions cannot be drawn.

4.2.2 Amino acids and lipids as biomarkers for potential extraterrestrial methanogenic life

Amino acids and (precursors of) lipids might be widely distributed throughout space. Various amino and fatty acids were detected in carbonaceous meteorites such as the Murchison meteorite including the proteinogenic amino acids Ser and Thr (Koga and Naraoka, 2017). Simple fatty acids are the most abundant organic components in carbon-rich meteorites (Huang et al., 2005). They were found in several carbonaceous chondrites like the Murchison meteorite (e.g. Huang et al., 2005) or the Tagish Lake meteorite (e.g. Hilts et al., 2014). The estimated amount of interplanetary dust particles hitting the early Earth approx. 4.0 Gyr ago was about 108 kg per year (Chyba and Sagan, 1992). There were also observations of amino acids in interstellar space. The first one happened in 2003, when Gly was detected (Kuan et al., 2003). Thereafter, it was also found in samples of the comets Wild 2 (Elsila et al., 2009) and 67P/Churyumov-Gerasimenko (Altwegg et al., 2016). In several experiments performed to simulate the interstellar medium, a large variety of amino acids was synthesized (Zaia et al., 2008). Taken this together, extraterrestrial organics likely influenced and triggered the origin of life on Earth.

In the present work, a total of 18 amino acids excreted by *M. okinawensis* was detected (Asp, Glu, Asn, Ser, Gln, His, Gly, Thr, Arg, Ala, Tyr, Val, Met, Trp, Phe, Ile, Leu, and Lys). The relative abundance of amino acids determined in the current or similar future studies can be compared with those found in the Murray and Murchison meteorites (Cronin and Moore, 1971; Huang et al., 2005; Koga and Naraoka, 2017). In addition, to distinguish between biotically and abiotically produced amino acids, either the relative abundance compared to Gly could be used or the enantiomeric excess, if applicable in the case of Enceladus. Biosynthetic processes can

lead to a higher abundance of complex amino acids to optimize protein function and stability. Hence, another approach could be to determine the relative abundance of the detected amino acids to Gly or other prebiotic amino acids (Guzman et al., 2018). Alternatively, groups in the side chains of amino acids, which are characterized by the highest similarities to terrestrial life, could be used as biomarkers (Georgiou, 2018).

Compared to amino acids, lipids are more durable and known to be stable over millions to even billions of years when isolated from oxygen (e.g., Summons et al., 1988). For this reason, they are commonly used to study and reconstruct terrestrial ecosystems over geological time scales (Summons et al., 2008). As described above, lipid biomarkers of possibly methanogenic or methanotrophic archaea have been successfully extracted from various different hydrothermal vent precipitates, such as carbonate chimneys (Bradley et al., 2009), massive sulphides (Blumenberg et al., 2007; 2012), vent chimneys made of amorphous silica and barite (Jaeschke et al., 2014); and also in hydromagnesite-containing serpentinization spring precipitates (Zwicker et al., 2018). Also in old rocks, pristine lipid biomarkers have been successfully assigned to their source. Isoprenoid hydrocarbons of methanotrophic archaea have even been reported from authigenic limestones from the late Pennsylvanian (ca. 300 Ma) in southern Namibia (Birgel et al., 2008) and lipids of methanogenic and halophilic archaea in mid-Neoproterozoic (~820 Ma old) evaporites from central Australia (Schinteie and Brocks, 2017). Biological precursors of geolipids as well as simple lipids (such as fatty acids and short-chain isoprenoids) could potentially act as biomarkers in astrobiology (Summons et al., 2008). More specific information may be obtained by the analysis of the hydrocarbon chain properties of membrane lipids (Georgiou and Deamer, 2014). The lipid biomarker approach may therefore become a useful tool for future space missions in the search for signs of life in extraterrestrial worlds.

Next generation ground based and orbital telescopes could aim to detect biomarkers by using infrared spectroscopy and polarimetry (Judge, 2017). The latter observation would be possible when Enceladus crosses the bright disk of Saturn, which will happen again in 2022 (Judge, 2017). However, analysing the transmission spectra of Europa's plumes would be easier than the observation of Enceladus' plume due to its larger physical scale and shorter distance. Apart from observing Enceladus from Earth or from its orbit, it is one of the major goals for the next decades to send a space probe to Enceladus. There are various promising concepts for future missions to Enceladus, such as *Enceladus Life Finder* (ELF) or *Journey to Enceladus and Titan* (JET), both proposed for NASA's Discovery Mission funding. *Enceladus Life Signatures and Habitability* (ELSAH) was proposed for NASA's New Frontiers program (Taubner, 2018). These missions would perform multi-flybys over the South Polar Terrain of Enceladus. For Europa, the missions Europa Clipper (NASA) and JUICE (Jupiter Icy Moons Explorer, ESA) are planned. Scientists all over the world from different fields are contributing with their research to construction and calibration of the instruments for the future missions to these intriguing ice worlds (Taubner et al., 2020). The current work may as well contribute to this effort.

4.3 Membrane core lipid patterns under changing temperature and nutrient supply

4.3.1 The effect of changing culture conditions on lipid patterns of *Methanothermobacter marburgensis*

The core lipid inventory of *M. marburgensis* has been described for the first time by Gräther (1994). However, most of the detected lipids have been already described much earlier from a close relative of *M. marburgensis*, *M. thermautotrophicus* (Makula and Singer, 1978; Tornabene et al., 1979; Tornabene and Langworthy, 1979). Makula and Singer (1978) detected 26% of a diether lipid and 74% of tetraether lipids in *M. thermautotrophicus* after acid hydrolysis of the phospholipid fraction. GDDs have been detected in *M. thermautotrophicus* (Knappy and Keely, 2012), but GMDs have not been described from the genus *Methanothermobacter* so far.

In *M. marburgensis*, archaeol, GTGT-0a, GDGT-0a, GDGT-0b, GDD-0a, and GDD-0b are most abundant at 50°C and least abundant at 60°C. In contrast, GDGT-0c, GMGT-0a, GMGT-0a', GMGT-0b, GMGT-0b', and GMGT-0c', and GMD-0b' are most abundant at 60°C and least abundant at 50°C. As a comparison, the lipids of *M. thermautotrophicus* cultured at 45°C, 60°C and 70°C have been reported (Knappy et al., 2015). In the current thesis, *M. marburgensis* was cultured at 50°C, 60°C, and 65°C. With 65°C-70°C *M. thermautotrophicus* has a slightly higher temperature optimum than *M. marburgensis*, which has 65°C as optimum temperature (Wasserfallen et al., 2000). Knappy et al. (2015) did not report the archaeol content. Nevertheless, they give a detailed description of the varying relative amounts of GTGT-0a, GDGT-0a, -0b, and -0c, and GMGT-0a, -0b, and -0c in % of total tetraether lipids (Knappy et al., 2015). In the study of Knappy et al. (2015) GTGT-0a is more abundant at 60°C (1.4% of total tetraethers) than at 45°C (1.0% of total tetraethers). It is least abundant at 70°C (0.2% of total tetraethers). This is in contrast to the present results, where GTGT-0a is most abundant at 50°C (0.6% of total lipids) and least abundant at 60°C (0.2% of total lipids; Table 6; Table S5). Like GTGT-0a, GDGT-0a and GDGT-0b in this work are most abundant at 50°C and least abundant at 60°C. The same holds true for GDGT-0b in Knappy et al. (2015), but not for GDGT-0a, which is most abundant at 70°C and least abundant at 45°C there. Also, GDGT-0c does not behave similarly here, where it is most abundant at 60°C (1.3% of total lipids; Table S5) and in Knappy et al. (2015), where it solely occurs at 45°C (0.3% of total tetraethers). GMGT-0a and GMGT-0b are both most abundant at 60°C and GMGT-0c occurs just at 45°C in Knappy et al. (2015). This is more or less in accord with the results of the current study. Because Knappy et al. (2015) did not distinguish between two isomers of GMGT-0a, -0b, and -0c, they are compared with GMGT-0a', -0b', and -0c' of the present thesis here, which are the much more abundant isomers. Regarding the degree of methylation Knappy et al. (2015) observed a much higher percentage of methylated lipids at 45°C than at 60°C and 70°C, for both, GDGTs and GMGTs. This is not in accord with the present results, where the highest degree of methylation was found at 60°C, for both GDGTs and GMGTs (Fig. 20). In great contrast to Knappy et. (2015), which reported a clearly higher content of non-methylated GDGT-0 and GMGT-0 relative to those with additional methylations, in the present work an almost equal amount of GDGT-0a and GDGT-0b and a predominance of GMGT-0b' over GMGT-0a' and GMGT-0c' at all temperatures was observed. Although, also in Knappy et al. (2015) the GMGTs had a higher proportion of methylated homologs than the GDGTs at all three temperatures. Moreover, the addition of a stress-inducing detergent (Tween 80) to cultures of *M. marburgensis* increased the production of GDGT-0b (Gräther, 1994). One could argue that *M. thermautotrophicus* and *M. marburgensis* show a different degree of methylation of

their tetraether lipids. However, another study reported a predominance of mono-, di-, and even trimethylated GDGT-0 as intact polar lipid and core lipid in *M. thermautotrophicus* grown at 65°C (see Supplementary Table 1 in Yoshinaga et al., 2015). For instance, 2G-GDGT-0 with one additional methylation was more abundant than 2G-GDGT-0 without an additional methylation at almost all conditions (one exception: late exponential phase in hydrogen-limited experiments). Monomethylated core GDGT-0 and G-GDGT-0 were more abundant than nonmethylated core GDGT-0 at late exponential phase, and were more abundant than nonmethylated G-GDGT-0 at all growth stages in the potassium- and phosphate-limited experiments (Yoshinaga et al., 2015). It is unclear, what exactly triggers the expression of varying lipid patterns at different temperatures in *M. marburgensis*. However, it should at least be considered as a possible factor that temperature affects the solubility of CO_2 in the liquid medium and hence, its availability and the pH of the medium.

To conclude, the development of methylations is not in accord with results of lipid-temperature experiments from *M. thermautotrophicus* and also not the development of GTGT-0a. Nevertheless, in Knappy et al. (2015) and in the present thesis the GMGTs are most abundant at 60°C and least abundant at the lower temperature (45°C in *M. thermautotrophicus*, 50°C in *M. marburgensis*) in both organisms (Fig. 21). In contrast to the study of Knappy et al. (2015), here and in Yoshinaga et al. (2015) tetraethers with additional methylations dominate at certain conditions and in some lipid species over their counterparts without them. These conditions are growth at 60°C for GDGTs and GMGTs in this thesis; and potassium and phosphate limitation for G-GDGT-0 in Yoshinaga et al. (2015). However, it has to be considered that these are different growth temperatures and that *M. marburgensis* and *M. thermautotrophicus* have different optimum temperatures.

The study of Yoshinaga et al. (2015) with *M. thermautotrophicus* is the only study the author knows about so far that analyzed archaeal lipids under varying hydrogen and micronutrient availability (limitation of potassium and phosphate). This is comparable with the changing volume of liquid medium in this work, because also the changing ratio of liquid medium to head space has an effect on the availability of hydrogen. As the total volume of the serum bottles remains constant, 25 mL of liquid medium means that the ratio of macronutrients in the head space relative to the micronutrients in the liquid medium is highest, whereas at 75 mL this ratio is lowest. The amount of macronutrients is the limiting factor, hence, conditions should be most ideal at 25 mL, followed by 50 mL and 75 mL. The growth temperature in both studies is the same, namely 65°C (for 50°C and 60°C there is no comparison of different volumes of liquid medium; see also Table 5). In the current study, the proportion of the different tetraethers and archaeol shifts in relation to the amount of liquid medium. Archaeol, GTGT-0a, GDGT-0a, GDGT-0c, GMGT-0b', and GMGT-0c' are most abundant at 25 mL. GDGT-0b, GMGT-0a, GMGT-0a', GMGT-0b, GDD-0a, and GDD-0b are most abundant at 75 mL. GMD-0b' has the same concentration at 25 mL and at 75 mL, and GMD-0a' is exceptional, because it just occurs at 50 mL without carbonate. However, as stated above, the difference in concentration beween the different volumes of liquid medium is not substantial. The only exception is archaeol, which is having its highest contents at 25 mL (Table 7; Table S6). The high abundance of the least rigid membrane core lipids at 25 mL, archaeol and GTGT-0a is not surprising, since these conditions are considered as most favourable for *M. marburgensis*. In contrast, the high abundance of some GMGTs at 75 mL can be explained by the opposite effect, as GMGTs are considered as the most rigid lipids here and 75 mL the least favorable amount of liquid medium. However, other GMGTs are most abundant at 25 mL and many lipids are least abundant at 50 mL, which is in great contrast and cannot be explained so far (Fig. 21).

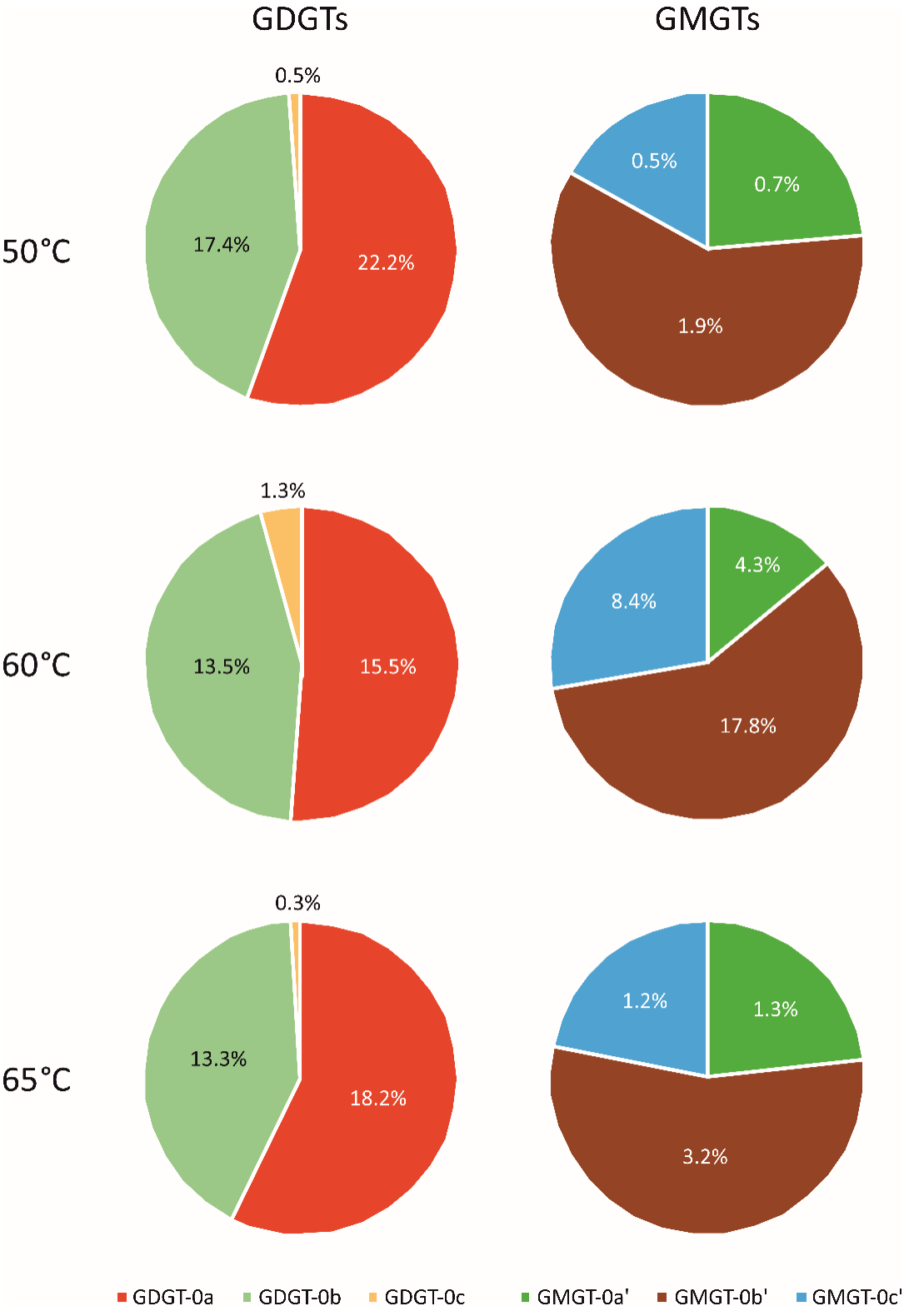

Figure 20: Relative abundance (%) of lipid species with zero, one, or two additional methylations in GDGTs and GMGTs of *Methanothermobacter marburgensis* at three different growth temperatures. The pie charts represent average values (50°C: n = 7; 60°C: n = 8; 65°C: n = 8). GMGT (glycerol monoalkyl glycerol tetraether), and GDGT (glycerol dialkyl glycerol tetraether).

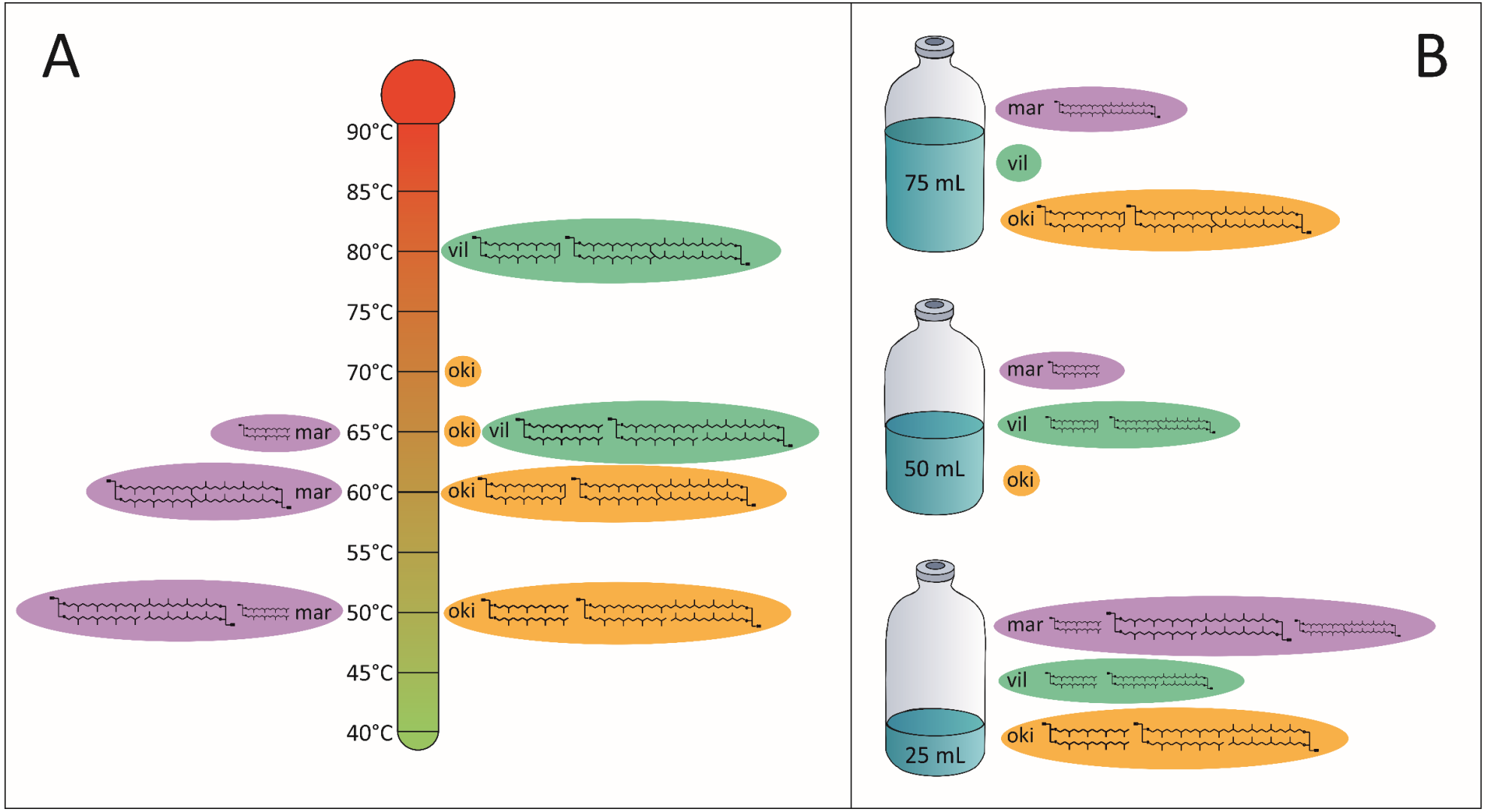
A
90°C
85°C
80°C
75°C
70°C
65°C
60°C
55°C
50°C
45°C
40°C
vil
oki
oki
vil
mar
mar
oki
mar
oki
B
75 mL
mar
vil
oki
50 mL
mar
vil
oki
25 mL
mar
vil
oki

Figure 21

Figure 21: Schematic comparison of the lipid patterns of *Methanothermobacter marburgensis* ("mar", purple), *Methanocaldococcus villosus* ("vil", green), and *Methanothermococcus okinawensis* ("oki", yellow) **A**) in response to different temperatures (represented by the thermometer symbol) and **B**) volumes of liquid medium (25 mL, 50 mL, and 75 mL; represented by bottle symbols). This figure refers to mean values of all experiments conducted at a specific temperature or volume of liquid medium. Lipids depicted in this image as schematic structural formula are: archaeol, macrocyclic archaeol, GTGT-0a, and the two GMGT isomers summarized as one symbol (for explanation of the structural formula see Fig. 2). The dominance of a certain lipid in a certain organism is represented by its structural formula symbol in combination with the abbreviations and the background color of the respective strain. Depending on where this symbol combination is arranged, either close to a certain temperature on the thermometer symbol or a certain volume of liquid medium at its bottle symbol represents its dominance in the organisms at this respective culture condition. For instance, macrocyclic archaeol and the GMGTs have their highest abundance (relative and in concentrations) in *M. okinawensis* at 60°C and at 75 mL. The lipid symbols have two sizes. A full-size lipid symbol represents a clear trend, whereas half-size lipid symbols represent a dominance at a certain condition, which is either not so clear or where a lipid is relatively most abundant at one condition, but in terms of concentrations most abundant at another condition. In *M. villosus*, for instance, the relative predominance of a lipid is not clear at varying volumes of liquid medium. In contrast, in *M. marburgensis* the GMGTs have their highest concentration at 25 mL, but are relative to all other lipids most abundant at 75 mL. Symbols of organisms occur at every temperature and at every volume of liquid medium, where this organism was cultured. If no lipid is displayed, none of the lipids depicted in this figure has its highest absolute or relative abundance at this culture condition. Temperature optima are: *M. marburgensis*: 65°C; *M. villosus*: 80°C; *M. okinawensis*: 60-65°C.

In contrast to *M. villosus* and *M. okinawensis*, *M. marburgensis* was also grown without carbonate in the liquid medium (see also below). Changing carbonate content alone has a less apparent effect than a varying liquid medium content. It has to be compared with changing liquid medium. All of the tetraether lipids, except for GDGT-0a, GMGT-0a, and GMGT-0a' have their highest concentrations at the condition 25 mL with carbonate. GDGT-0a and archaeol have their highest mean concentration at 25 mL without carbonate. GMGT-0a, GMGT-0a', and GDD-0a have their maximum concentration at 75 mL without carbonate. As mentioned above, the latter condition seems to favor those lipids without an additional methylation in their carbon chain. Among the GDGTs and among the GMGTs, those without an additional methylation (GDGT-0a and GMGT-0a') are more abundant in samples without carbonate. In contrast, GDGT-0b, GDGT-0c, and GMGT-0c' are relatively more abundant in samples with carbonate. The amount of GMGT-0b' relative to the other GMGTs barely changes (Fig. 14). These are intriguing observations, because carbonate in the liquid medium serves as a buffer, which is relevant, because CO_2 from the head space will lower the pH of the liquid medium more substantially, if not buffered. Carbonate in the liquid medium serves also as an additional source of carbon for *M. marburgensis*. CO_2 first has to dissolve in the liquid medium, before it is available for the organism. CO_3^{2-} is most likely more quickly available compared to CO_2. This could be more relevant at higher growth temperatures, when also the growth rate increases. However, in this work, carbonate vs. no-carbonate addition was applied just for 65°C. Tetraether lipids with additional methyl groups in their hydrocarbon chain are most abundant when the ratio of head space to liquid medium is highest, so at 25 mL, and when there is an additional and probably more quickly available carbon source, namely carbonate in the liquid medium. The condition 25 mL with carbonate is therefore the condition with the highest relative abundance of GDGT-0b, GDGT-0c, and GMGT-0c' (Fig. 14). The GMGTs without an additional methylation are most abundant at the complete opposite condition: at low head space to liquid medium ratio (75 mL) and no additional carbon source in the liquid medium (without carbonate in the liquid medium; Fig. 14). Having just this information, the most favorable conditions for *M. marburgensis* are not straightforward to determine. Nevertheless, due to its

function as a buffer ion and an additional carbon source, the addition of carbonate to the liquid medium is most likely beneficial for growth of *M. marburgensis*.

M. marburgensis revealed most methylations at 60°C, and not at its optimum temperature of 65°C. However, 60°C is close to 65°C and the standard deviations of the concentrations are high. Knappy et al. (2015) reported less methylations close to the temperature optimum of *M. thermautotrophicus* compared to the lower temperature of 45°C. The temperature comparison alone is not sufficient for determining, whether a higher degree of methylation makes the membrane more or less permeable, or better adapted to lower or higher temperatures. Hence, it is also difficult to draw conclusions about the effect of volume of liquid medium and the carbonate content of the liquid medium on *M. marburgensis*.

Studies, which compare the lipid compositions of *M. thermautotrophicus* under changing nutrient supply and different growth stages did not compare the same lipids as in the current thesis. In the study of Yoshinaga et al. (2015), just archaeol and GDGT-0 (including methylated and non-methylated homologs) were compared with each other, although not only the core, but also the intact polar lipids. They did not find a considerable change in the ratio of archaeol to GDGT-0, or diethers to tetraethers, but rather a shift in headgroup composition. This study is one out of three studies, which examined the diether-to-tetraether ratio of *M. thermautotrophicus* at different growth stages. All three studies came to very contradictory results. Kramer and Sauer (1991) found that with increasing age of the cell culture, diethers clearly increased relative to the tetraethers. In contrast, Morii and Koga (1993) observed an apparent decrease of diethers relative to tetraethers. Morii and Koga (1993) and Yoshinaga et al. (2015) explain these striking discrepancies with the different methods employed for lipid extraction and analysis. Using HPLC-MS for quantification, Yoshinaga et al. (2015) observed a higher proportion of diethers relative to tetraethers at all growth stages and treatments (ca. 87%). In the current work, this is not the case at every condition. Archaeol makes up less than 50% of total lipids at 60°C and at 75 mL (Tables S5 and S6). Unfortunately, this study did not mention GTGT-0, any kind of GMGT, and it did not compare the degree of methylation of the GDGTs.

To the best of the author's knowledge, there is no study so far, which compares the lipid yield when medium was removed or not removed for OD measurements. However, if this has an effect, it should be comparable with the effect of the changing volume of liquid medium. In other words, OD measurements should shift the lipid yield towards the values observed at a volume of 50 mL or 25 mL of liquid medium. At a starting liquid medium of 25 mL, this effect should be strongest, because there is relatively more liquid medium removed from 25 mL samples. This is not reflected by the lipid patterns of the present experiments. In fact, the differences between non-OD and OD samples appear to be not meaningful.

Molecular dynamics simulations compared the physicochemical properties of five theoretical polar (phosphatidylcholine head groups) tetraether lipids with the same alkyl chain length (C_{32}) and glycerol backbone stereochemistry as archaeal GDGTs have (Chugunov et al., 2014). Among the outcomes of this simulation study was that the methyl branches and cyclopentane moieties in archaeal GDGTs lead to less dense packing, less rigid, more flexible, "liquid-crystalline" membranes compared to the more gel-like phase of the straight alkyl chains without methyl branches or cyclopentane moieties. The study further shows that methyl branches and cyclopentane moieties have similar, but not exactly the same effects on membranes' properties. At the site of the cyclopentane moieties the hydrophobic lipid cores have a more dense packing, which makes the resulting cytoplasmic membrane even more flexible and even less permeable for solvents than methyl branches alone (Chugunov et al., 2014). Although this study did not

address the effect of additional methyl branches in the alkyl chains of GDGT-0, GTGT-0 or GMGT-0, it shows the principal effect of methyl branches on the physicochemical properties of archaeal tetraether lipids. More evidence that cyclopentane moieties enhance the packing tightness of a membrane comes from a previous molecular modeling study (Gabriel and Chong, 2000); as well as from culture studies with (hyper)thermophilic archaea, which increased the number of cyclopentane moieties in their alkyl chains with increasing growth temperature (e.g. De Rosa et al., 1980; Uda et al., 2001; 2004; Shimada et al., 2008).

However, while Bacteria extensively adjust their membrane lipid composition in response to varying temperature, pressure, and pH, Archaea change their membrane lipid composition in a much lesser extent (Koga, 2012; Siliakus et al., 2017). This does not contradict the finding of a correlation between temperature and number of cyclopentane moieties. In fact, unlike Bacteria the archaeal membrane maintains its liquid crystalline phase over the entire biological temperature range (Koga, 2012; Siliakus et al., 2017). The high degree of methyl branching of the archaeal alkyl chains guarantees fluidity and permeability, and at the same time enough rigidity to withstand temperatures beyond 100°C. Psychrophilic archaea often reveal the same membrane lipids as hyperthermophilic archaea (Koga, 2012; Siliakus et al., 2017). Nevertheless, Bacteria outcompete Archaea at very low temperatures and very high pH values, while Archaea are better adapted to extremely high temperatures and extremely low pH values (Siliakus et al., 2017). This could be, at least in part, explained by the higher number of methyl branches in the archaeal hydrocarbon chains, which makes Archaea more efficient in rigidifying their membrane (Siliakus et al., 2017).

All of these considerations do not refer to the occurrence of GDGTs or GMGTs with additional methyl groups in their hydrocarbon chains, but they try to explain the basic function of methyl groups in archaeal di- and tetraethers. As stated above, apart from the present study, the study of Knappy et al. (2015) is the only study the author knows about so far that reports different degrees of methylation as a response to varying culture conditions. Although the results of these two studies are in this regard contradictory, both studies show that a member of the genus *Methanothermobacter* changes the degree of methylation with changing temperature. The present work additionally reveals that *M. marburgensis* is changing the amount of methyl groups also in response to a varying nutrient supply.

4.3.2 Lipid substitutions in *Methanocaldococcus villosus* and *Methanothermococcus okinawensis* – a comparison

As described above and in Baumann and Taubner et al. (2018), *M. villosus* and *M. okinawensis* exhibit the same membrane core lipid inventory. In contrast to *M. marburgensis*, the tetraether lipids of *M. villosus* and *M. okinawensis* occur in much smaller amounts and together account for less than 10% of the total lipid inventory in *M. villosus* and up to 15% in *M. okinawensis*. Nevertheless, unlike *M. marburgensis* with its abundant and partly methylated tetraether lipids, both strains comprise not only archaeol, but also macrocyclic archaeol as a diether lipid. Macrocyclic archaeol is found with varying contents, depending on the strain and the growth conditions. As described in Baumann and Taubner et al. (2018), on average, *M. villosus* has more macrocyclic archaeol than archaeol and for *M. okinawensis* it is the opposite. However, at 60°C *M. okinawensis* also produces more macrocyclic archaeol than archaeol (Fig. 17). Additionally, the ratio of GMGT-0a/GMGT-0a' is reversed in *M. villosus* and *M. okinawensis* (Baumann and Taubner et al., 2018). The ratio is below 1 in *M. villosus* and above 1 in *M. okinawensis*. It seems that at certain growth conditions some of the membrane core lipids of

M. villosus and *M. okinawensis* are favored at the expense of others. These are mostly the same lipids or similar patterns in both strains.

In *M. villosus* these substitutions are in most cases not as clear as in *M. okinawensis*. The differences between various culture conditions are almost negligible. However, if any modification can be described, it seems that temperature has the strongest effect in *M. villosus*. When summarizing all results at 65°C and 80°C and comparing them with each other, then archaeol, GTGT-0a, and GDGT-0a are slightly more abundant at 65°C and the rest of the lipids are slightly more abundant at 80°C (Fig. 21). This is true for the relative distribution of lipids, but also the total abundance. The combinations 65°C and 25 mL lead to a high relative proportion of archaeol, GTGT-0a, and GDGT-0a, but the combination 80°C and 50 mL leads to a high proportion of archaeol and the combination 80°C and 75 mL leads to a high proportion of GDGT-0a. This is similar to *M. marburgensis*, where the least rigid lipids such as archaeol, GTGT-0a, GDGT-0a, and GDGT-0b or GDGT-0c are also most abundant at the lower temperature of 50°C and 25 mL of liquid medium. In *M. okinawensis* the trends are much more obvious than in *M. villosus*, although somewhat different. While *M. villosus* was cultured at two different temperatures, the optimum temperature and 15°C below, *M. okinawensis* was cultured at four temperatures, at the lower and the upper boundary of the optimum temperature (60-65°C; Takai et al., 2002), 10°C below the lower boundary and 5°C above the upper boundary (Table 5). This makes the temperature comparison between the two strains incomplete. However, at least for the optimum and the lower temperature, some conclusions can be drawn. In *M. villosus* as well as in *M. okinawensis* archaeol, GTGT-0a, and GDGT-0a are most abundant at the lowest temperature chosen for the current experiments, which is also the temperature below the optimum for both strains (Fig. 21). The other lipids are most abundant at the temperature optimum of 80°C in *M. villosus* and at its lower boundary at 60°C in *M. okinawensis* (Fig. 21). Interestingly, *M. okinawensis* shows at 65°C and at 70°C a lipid distribution, which lies in-between the lipid patterns at 50°C and at 60°C. However, this is in line with observations from *M. marburgensis*, where the lipid patterns at 65°C lie in-between the lipid patterns at 50°C and at 60°C. Hence, it seems that those core lipids, which are supposed to make the membrane more rigid and less permeable, are most abundant at the temperature optimum and least abundant at the lower temperature in both organisms (Fig. 21). Lipid-culture experiments with *M. jannaschii* cultured in the range from 47°C to 78°C (optimum near 85°C, Jones et al., 1983) revealed a clear increase of macrocyclic archaeol and GDGT-0a at the expense of archaeol with increasing temperature (Sprott et al., 1991). Unfortunately, this experiment was conducted below the proposed optimum temperature of *M. jannaschii*, and the behavior of GDGT-0a is different from the current experiments. It is relatively more abundant at the lower temperature in *M. villosus*, but at the highest temperature in *M. okinawensis*. However, the overall trend of having more rigid and less permeable core lipids at higher temperatures can be confirmed with the current data.

Because higher pressures have, at least theoretically, a similar effect on membrane lipids as lower temperatures, the second lipid-culture study involving *M. jannaschii* shall be compared with the results of the present thesis (Kaneshiro and Clark, 1995; Siliakus et al., 2017). Therefore, the content of archaeol should increase, while the content of macrocyclic archaeol and tetraethers should decrease at increased pressures. This was different in the lipid-culture experiment with *M. jannaschii*, where macrocyclic archaeol became more abundant relative to archaeol and GDGT-0a at higher growth pressures (Kaneshiro and Clark, 1995). Methanogenesis and growth rate were higher and the membrane fluidity was reduced at elevated pressures. These developments and the decrease of GDGT-0a were expected, but the decrease of archaeol and the increase of macrocyclic archaeol were not. The authors suggest a special role for macrocyclic archaeol in *M. jannaschii* at higher temperatures and pressures.

Nevertheless, a high pressure does not seem to affect *M. jannaschii* negatively. In fact, also another study showed that it grows faster at elevated pressures and temperatures (Miller et al., 1988). Therefore, a high proportion of macrocyclic archaeol could mean that *M. jannaschii* is thriving at such conditions. For the current work it is beneficial to take notice of the sometimes unexpected behavior of members of the order Methanococcales and that macrocylic archaeol is an essential part of the cell membrane of *M. jannaschii*, *M. villosus* and *M. okinawensis* at elevated temperatures and most likely also at elevated pressures. Lipid-pressure experiments with *M. villosus* and *M. okinawensis* are definitely worth to be conducted in the near future.

At 25 mL *M. villosus* and *M. okinawensis* should theoretically have the best growth conditions, because, as described above, at 25 mL of liquid medium, the organisms have the highest relative amount of the growth-limiting macronutrients. The change in the volume of the liquid medium leads to different patterns in *M. villosus* and *M. okinawensis*. Ignoring the other parameters, in *M. villosus* archaeol, GTGT-0a, and GDGT-0a are relative to the other lipids most abundant at 25 mL and least abundant at 50 mL (Fig. 21). In contrast, macrocyclic archaeol is relative to the other lipids most abundant at 50 mL and least abundant at 25 mL. The comparison of all samples with gas exchange once or twice per day reveals that archaeol is the only lipid, which is relatively more abundant at gasssing once per day. The other lipids are relatively more abundant at a gas exchange twice per day, but the differences are overall minor. Whether or not liquid medium was removed for OD measurements did not have a considerable effect on the relative lipid amounts or the concentrations in *M. villosus*.

M. okinawensis shows clearer patterns under changing culture conditions. The abundance of archaeol and GTGT-0a is decreasing progressively from 25 mL to 75 mL, while the abundance of macrocyclic archaeol and the GMGTs is increasing from 25 mL to 75 mL (Fig. 18; Fig. 21). However, also in *M. villosus*, archaeol, GTGT-0a, and GDGT-0a are most abundant at 25 mL, where macrocyclic archaeol is least abundant. GDGT-0a is most abundant at 50 mL and least abundant at 25 mL, which is the complete opposite of the behavior of GDGT-0a in *M. villosus*. These patterns can become stronger or weaker in response to a different gas exchange frequency. However, the overall difference in lipid patterns between once and twice gas exchange per day is minor; and so is the difference between OD and non-OD samples. Assuming that the relative error is more substantial for less abundant compounds, the fact that the more abundant lipids (archaeols, GDGT-0a, and GMGT-0a) reveal higher concentrations at a gas exchange twice per day in *M. okinawensis* could let someone assume that the organism grew better at this higher gas exchange frequency. This seems plausible, if it is assumed that at a gas exchange twice per day, in contrast to once per day, *M. okinawensis* received more macronutrients over the entire growth period. However, the concentrations are already normalized by biomass so they should stay constant. Possible causes for concentration shifts are discussed in chapter 4.2.1 and in Taubner and Baumann et al. (2019).

The temperature experiments reveal a higher relative abundance of the supposedly more stable or rigid lipids at the optimum temperature in both strains. In this regard, the comparison of different volumes of liquid medium is contradictory to the temperature experiments, because at the supposedly most beneficial volume of 25 mL of liquid medium, archaeol and GTGT-0a, the least rigid lipids, are most abundant. Nevertheless, if one assumes that 50 mL, the suggested standard condition, is the most optimal condition, then at least for *M. villosus*, it would mean that the production of macrocyclic archaeol and GMGTs is higher at ideal conditions. This cannot be concluded for *M. okinawensis*, because those lipids, which are most abundant at 60°C, are clearly least abundant at 25 mL and most abundant at 75 mL (Fig. 21). However, as mentioned above, the lipid distribution of *M. okinawensis* grown at 65°C and at 70°C is intermediate between those at 50°C and at 60°C. This makes an interpretation even more

difficult. An experiment with *M. villosus* grown above its temperature optimum could be helpful in this respect. From the results here, one cannot draw conclusions about which lipid proportions are optimal either for *M. villosus* or *M. okinawensis*. It can be assumed that apparently the lipid proportions are affected by varying temperatures and nutrient supply, and that they are affected differently in *M. villosus* and *M. okinawensis*. Low temperatures and a high ratio of macronutrients versus micronutrients lead to a high proportion of archaeol and GTGT-0a relative to macrocylic archaeol and the GMGTs in both organisms. Possibly, the organisms actively make the membrane more flexible and permeable at lower temperatures, which was expected and is confirmed by literature many times (e.g. De Rosa et al., 1980; Sprott et al., 1991; Shimada et al., 2008; Siliakus et al., 2017). Maybe, the same membrane shall also be very permeable at a high supply of macronutrients. There is also the possibility that these methanogens do not actively control their lipid composition, but are rather not capable of synthesizing those lipids, which would be ideal for present conditions. For instance, maybe *M. villosus* and *M. okinawensis* are not able to synthesize a higher proportion of macrocyclic archaeol and GMGTs at 25 mL. Hints that this is the case during intoxication can be found for *M. okinawensis* in chapter 3.2 and in Taubner and Baumann et al. (2019).

5. Conclusions and final remarks

The present dissertation has an interdisciplinary approach, strongly rooted in the bio- and geosciences. The aim of this work was to contribute valuable data to the biomarker concept for geobiology and astrobiology. Methanogenic archaea, or shortly methanogens, are promising study objects in this regard, because their metabolism and overall way of living is believed to be very basic and ancient, if not belonging to the first forms of life on Earth. It thus makes sense to study potential biosignatures of methanogens to expand the set of tools we have for research on first and early life, recent life in extreme environments, and the search for extraterrestrial life on other planets and moons.

There were very few studies on the lipid inventory and how it changes at changing conditions of the order Methanococcales, prior to this thesis. Exceptions are *Methanothermococcus thermolithotrophicus*, *Methanococcus aeolicus*, and the very well-studied *Methanocaldococcus jannaschii*. This thesis describes for the first time the lipid inventory of *Methanocaldococcus villosus* and *Methanothermococcus okinawensis*. It also describes how their membrane core lipids and the membrane core lipids of *Methanothermobacter marburgensis* change under varying temperature and nutrient supply. In the case of *M. okinawensis*, the membrane core lipids as well as excreted amino acids were additionally analyzed in response to multivariate concentrations of certain inhibitors. The lipids of *Methanothermobacter marburgensis* were known prior to this thesis, but were so far not analyzed under the conditions tested here. *Methanothermobacter marburgensis* was originally isolated from mesophilic sewage sludge (Wasserfallen et al., 2000), while *Methanocaldococcus villosus* and *Methanothermococcus okinawensis* derive from submarine hydrothermal vents (Takai et al., 2002; Bellack et al., 2011).

M. villosus and *M. okinawensis* have the same membrane core lipids and very similar intact polar lipids. Yet, the relative proportions are different in the two strains, allowing for a distinction of the two methanogens by means of lipid biomarkers. While *M. villosus* contains solely glycolipids as intact polar lipids, *M. okinawensis* has as well minor phosphoglycolipids in its extracts. Membrane lipids with additional methylations, as found in *M. marburgensis*, or cyclopentane ring-containing tetraether lipids have not been identifed, neither in *M. villosus*, nor in *M. okinawensis*. This is in accord with previous studies of membrane lipids of the order Methanococcales. As typical for (hyper)thermophilic archaea, *M. villosus* and *M. okinawensis* produce abundant archaeol, GDGT-0a, GTGT-0a, and GMGT-0a. However, to the best of the author's knowledge, GTGT-0a and GMGT-0a have not been reported from the order Methanococcales to date, and two isomers of GMGT-0a not in any other archaeal culture. Very likely the most specific of the detected lipids occurs also in high abundance in both strains: macrocyclic archaeol. This lipid has been reported from only few archaeal cultures so far and may consequently be of moderate source specificity for methanogens. Yet, it has also been considered as a biomarker of methanotrophs. Additionally, small quantities of isoprenoid GDD-0a and GMD-0a were detected in the core lipid extracts. GDD-0a may be a degradation product of GDGT-0a, and GMD-0a may be a degradation product of GMGT-0a. If that is correct, GMD-0a may, as GMGT-0a, be a biomarker for marine, (hyper)thermophilic, archaea. Briefly, the lipid biomarker inventory of *M. villosus* and *M. okinawensis* is very similar to the inventory of other methanogenic archaea. The most specific pattern is the high abundance of macrocyclic archaeol combined with the presence of the two structural isomers of GMGT-0a. When found in the environment, this pattern may serve as a signature of *M. villosus* and *M. okinawensis*.

Although the inventory of lipids and amino acids remained unchanged, the relative proportions of the core lipids and also the excreted amino acids of *M. okinawensis* changed, when exposed to varying concentrations of the inhibitors ammonium chloride (NH_4Cl), formaldehyde (H_2CO), and methanol (CH_3OH). NH_4Cl, H_2CO, and CH_3OH were identified in the plumes at Enceladus' south pole. Enceladus is one of the icy moons of the planet Saturn and, albeit most likely not inhabited yet (Deamer and Damer, 2017), may provide a habitable environment for life to develop, especially for methanogenic life forms. However, organisms that may thrive on Enceladus would have to face extreme environmental conditions such as varying temperature, high pH, high pressure, and various substances, such as the above-mentioned inhibitors, that might perhaps inhibit the formation and prosperity of life. *M. okinawensis* turned out to easily survive when exposed to multivariate concentrations of NH_4Cl, H_2CO, and CH_3OH and, as a function of their varying concentrations, exhibits different patterns in its lipid and amino acid synthesis. CH_3OH showed no appreciable influence in the tested concentration range (0.224 to 5.207 mmol/L) on neither growth nor lipid or amino acid production rates. However, the other two inhibitors had a strong impact on either growth and lipid production or amino acid excretion. High concentrations of H_2CO (tested concentration range 0.33 to 7.656 mmol/L) had a noteworthy diminishing effect on the growth and lipid production of *M. okinawensis*, especially in combination with higher concentrations of NH_4Cl. In contrast, high concentrations of NH_4Cl (tested concentration range 0.027 to 0.263 mol/L), even when combined with lower concentrations of H_2CO, mainly suppressed amino acid excretion.

Not only the response to different inhibitors was tested, but also the varying temperature and nutrient supply. Lipid-culture studies with varying nutrient supply were very scarce for methanogens, but also for Archaea in general. The current thesis thus also aimed to assign certain lipid patterns to specific environmental parameters and to find lipid patterns, which reflect not only optimum temperatures, but also optimum nutrient supply and combinations of both. As the optimum temperatures of the three methanogens *M. marburgensis*, *M. villosus*, and *M. okinawensis* are known from former experiments, here, the lipid patterns at these temperatures were compared with the lipid patterns at varying volume and carbonate content of liquid medium and at different gas exchange frequencies. Because of the different culture conditions of these three strains, it is not straightforward to compare their lipid patterns in response to varying temperatures and nutrient availability. The three strains were cultured at two (*M. villosus*), three (*M. marburgensis*), and four (*M. okinawensis*) different temperatures; *M. marburgensis* partly without carbonate in the liquid medium, and *M. villosus* and *M. okinawensis* at a varying frequency of gas exchange. Additionally, *M. marburgensis* has a different lipid inventory than the other two, more closely related, strains.

Nevertheless, even under these comparably different starting conditions there were several patterns observable, which are shared by all three organisms. These are a high abundance of macrocyclic archaeol (not for *M. marburgensis*), certain GDGTs and GMGTs at or slightly below the optimum temperature and a high abundance of archaeol and GTGT-0a at the lowest culture temperature (about 15°C below the optimum) and at 25 mL (Fig. 21). This partly reproduces results of previous lipid-culture studies (Sprott et al., 1991; Knappy et al., 2015). Surprisingly, *M. villosus*, not *M. marburgensis* is outstanding in the sense that it reveals the weakest response of lipid patterns at changing culture conditions of all three strains. However, in *M. villosus*, as in the other two strains, temperature turned out to have the strongest effect on lipid patterns. In *M. marburgensis*, also the volume of liquid medium in combination with its carbonate content turned out to have a potent influence on the expression of certain lipids. *M. okinawensis* showed the clearest lipid patterns in response to varying volume of liquid medium. The frequency of gas exchange and whether liquid medium was removed for OD measurements had an inconsistent or a negligible effect on the lipid patterns.

It is difficult to define the ideal lipid pattern of each organism. Looking at the temperature experiments one would assume that a high relative abundance of the supposedly more rigid lipids, such as macrocyclic archaeol, GDGTs, GMGTs or a higher degree of methylation of the same would be ideal. However, assuming that 25 mL are better than 50 mL or 75 mL of liquid medium for these organisms (because it provides relatively more macronutrients), then a higher content of archaeol and GTGT-0a seems to be the optimal lipid composition. There might be no ideal lipid composition for any of these organisms, just an ideal lipid composition for a certain condition. A more flexible and permeable cell membrane can be beneficial at temperatures below optimum as well as at a high supply of macronutrients. Interestingly, *M. marburgensis* and *M. okinawensis* both do not reveal the most extreme of the observed lipid patterns at the highest temperatures, but at the intermediate temperature, which cannot be explained at the moment. Alternatively, the observed patterns could as well reflect not adaptation, but rather an inability to express those lipids in comparably high amounts as under optimized conditions. To answer these questions it would be beneficial to have more lipid-temperature studies at several temperatures, including also temperatures higher than the optimum; with methanogens from the same genera (and maybe also *M. aeolicus,* most likely the closest relative of *M. okinawensis* available as pure culture), where all core lipids, and perhaps also the intact polar lipids are evaluated. At each of these temperatures, there should be different groups with varying nutrient supply, as it was conducted here just for *M. villosus*. Considering the possible function of carbonate as a buffer ion and an additional source of carbon, it seems likely that growth rate increases more quickly with rising temperatures in those samples with carbonate in the liquid medium. There are molecular dynamics simulations for the principal effect of isoprenoid vs. non-isoprenoid alkyl chains (Chugunov et al., 2014) and for the effect of cyclopentane moieties in the alkyl chains (Gabriel and Chong, 2000). For the strains studied here it would be also beneficial to have molecular dynamics simulations for GDGTs and GMGTs with different numbers of additional methyl groups in their carbon chains. Lipid-pressure experiments with *M. marburgensis*, *M. villosus* and *M. okinawensis*, similar to the one conducted by Kaneshiro and Clark (1995) with *M. jannaschii*, could as well complement the findings of this work.

In short, this dissertation covers a range of basic research on (hyper)thermophilic methanogens. First, it provides the first description of the intact polar and core lipids of *M. villosus* and *M. okinawensis*. Second, it shows how the core lipids and amino acid excretions patterns of *M. okinawensis* change at multivariate concentrations of potential inhibitors detected in the Enceladian plume. Third, and finally, it describes the change in core lipid patterns of *M. marburgensis*, *M. villosus*, and *M. okinawensis*, when exposed to changing temperature and nutrient supply.

The outcomes of this thesis could help to detect remnants of (hyper)thermophilic methanogens in recent and fossil environmental samples, may help to understand possible differences of lipid patterns at various sites, and may perhaps also help to calibrate or adapt instruments for future space missions on their search for extraterrestrial life using biomarkers such as lipids or amino acids. As described above, there are still a lot of questions to answer and more experiments and simulations to be conducted, with these three strains and with others. Nevertheless, the present work provides several intriguing and useful findings, which contribute to the toolbox of geobiology and astrobiology.

6. References

Altwegg, K.; Balsiger, H.; Bar-Nun, A.; Berthelier, J.-J.; Bieler, A.; Bochsler, P.; Briois, C.; Calmonte, U.; Combi, M.R.; Cottin, H.; De Keyser, J.; Dhooge, F.; Fiethe, B.; Fuselier, S.A.; Gasc, S.; Gombosi, T.I.; Hansen, K.C.; Haessig, M.; Jäckel, A.; Kopp, E.; Korth, A.; Le Roy, L.; Mall, U.; Marty, B.; Mousis, O.; Owen, T.; Rème, H.; Rubin, M.; Sémon, T.; Tzou, C.-Y.; Waite, J.H.; Wurz, P.; **2016**. Prebiotic chemicals – amino acid and phosphorus – in the coma of comet 67P/Churyumov-Gerasimenko. *Science Advances* 2, 1–5.

Ambrogelly, A.; Palioura, S.; Söll, D., **2007**. Natural expansion of the genetic code. *Nature Chemical Biology* 3, 29–35.

Bang, C.; Schilhabel, A.; Weidenbach, K.; Kopp, A.; Goldmann, T.; Gutsmann, T.; Schmitz, R.A.; **2012**. Effects of antimicrobial peptides on methanogenic archaea. *Antimicrobial Agents and Chemotherapy* 56, 4123–4130.

Baross, J.A.; Lilley, M.D.; Gordon, L.I.; **1982**. Is the CH_4, H_2 and CO venting from submarine hydrothermal systems produced by thermophilic bacteria? *Nature* 298, 366–368.

Bauersachs, T.; Weidenbach, K.; Schmitz, R.A.; Schwark, L.; **2015**. Distribution of glycerol ether lipids in halophilic, methanogenic and hyperthermophilic archaea. *Organic Geochemistry* 83-84, 101–108.

Bauersachs, T.; Schwark, L.; **2016**. Glycerol monoalkanediol diethers: a novel series of archaeal lipids detected in hydrothermal environments. *Rapid Communications in Mass Spectrometry* 30, 54–60.

Baumann, L.M.F.; Taubner, R.-S.; Bauersachs, T.; Steiner, M.; Schleper, C.; Peckmann, J.; Rittmann, S.K.-M.R.; Birgel, D., **2018**. Intact polar lipid and core lipid inventory of the hydrothermal vent methanogens *Methanocaldococcus villosus* and *Methanothermococcus okinawensis*. *Organic Geochemistry* 126, 33–42.

Becker, K.W.; Elling, F.J.; Yoshinaga, M.Y.; Söllinger, A.; Urich, T.; Hinrichs, K.-U.; **2016**. Unusual butane- and pentanetriol-based tetraether lipids in *Methanomassiliicoccus luminyensis*, a representative of the seventh order of methanogens. *Applied and Environmental Microbiology* 82, 4505–4516.

Bellack, A.; Huber, H.; Rachel, R.; Wanner, G.; Wirth, R.; **2011**. *Methanocaldococcus villosus* sp. nov., a heavily flagellated archaeon that adheres to surfaces and forms cell–cell contacts. *International Journal of Systematic and Evolutionary Microbiology* 61, 1239–1245.

Birgel, D.; Peckmann, J., **2008**. Aerobic methanotrophy at ancient marine methane seeps: A synthesis. *Organic Geochemistry* 39, 1659–1667.

Birgel, D.; Himmler, T.; Freiwald, A.; Peckmann, J.; **2008**. A new constraint on the antiquity of anaerobic oxidation of methane: Late Pennsylvanian seep limestones from southern Namibia. *Geology* 36, 543–546.

Blumenberg, M.; Seifert, R.; Reitner, J.; Pape, T.; Michaelis, W.; **2004**. Membrane lipid patterns typify distinct anaerobic methanotrophic consortia. *Proceedings of the National Academy of Sciences of the United States of America* 101, 11111–11116.

Blumenberg, M.; Seifert, R.; Petersen, S.; Michaelis, W.; **2007**. Biosignatures present in a hydrothermal massive sulfide from the Mid-Atlantic Ridge. *Geobiology* 5, 435–450.

Blumenberg, M.; Seifert, R.; Buschmann, B.; Kiel, S.; Thiel, V.; **2012**. Biomarkers reveal diverse microbial communities in black smoker sulfides from Turtle Pits (Mid-Atlantic Ridge, Recent) and Yaman Kasy (Russia, Silurian). *Geomicrobiology Journal* 29, 66–75.

Borrel, G.; Adam, P.S.; Gribaldo, S.; **2016**. Methanogenesis and the Wood-Ljungdahl Pathway: an ancient, versatile, and fragile association. *Genome Biology and Evolution* 8, 1706–1711.

Bottke, W.F.; Norman, M.D.; **2017**. The Late Heavy Bombardment. *Annual Review of Earth and Planetary Sciences* 45, 619–647.

Bradley, A.S.; Hayes, J.M.; Summons, R.E.; **2009**. Extraordinary ^{13}C enrichment of diether lipids at the Lost City Hydrothermal Field indicates a carbon-limited ecosystem. *Geochimica et Cosmochimica Acta* 73, 102–118.

Brochier-Armanet, C.; Forterre, P.; Gribaldo, S.; **2011**. Phylogeny and evolution of the Archaea: One hundred genomes later. *Current Opinion in Microbiology* 14, 274–281.

Caforio, A.; Driessen, A.J.M.; **2017**. Archaeal phospholipids: Structural properties and biosynthesis. *Biochimica et Biophysica Acta – Molecluar and Cell Biology of Lipids* 1862, 1325–1339.

Cario, A.; Grossi, V.; Schaeffer, P.; Oger, P.M.; **2015**. Membrane homeoviscous adaptation in the piezo-hyperthermophilic archaeon *Thermococcus barophilus*. *Frontiers in Microbiology* 6, 1152: 1–12.

Charlou, J.L.; Donval, J.P.; Fouquet, Y.; Jean-Baptiste, P.; Holm, N.; **2002**. Geochemistry of high H_2 and CH_4 vent fluids issuing from ultramafic rocks at the Rainbow hydrothermal field (36°14'N, MAR). *Chemical Geology* 191, 345–359.

Cheung, A.C.; Rank, D.M.; Townes, C.H.; Thornton, D.D.; Welch, W.J.; **1968**. Detection of NH_3 molecules in the interstellar medium by their microwave emission. *Physical Review Letters* 21, 1701–1705.

Chugunov, A.O.; Volynsky, P.E.; Krylov, N.A.; Boldyrev, I.A.; Efremov, R.G.; **2014**. Liquid but durable: Molecular dynamics simulations explain the unique properties of archaeal-like membranes. *Scientific Reports* 4, 7462: 1–8.

Chyba, C.; Sagan, C.; **1992**. Endogenous production, exogenous delivery and impact-shock synthesis of organic molecules: an inventory for the origins of life. *Nature* 355, 125–132.

Clifford, E.L.; Hansell, D.A.; Varela, M.M.; Nieto-Cid, M.; Herndl, G.J.; Sintes, E.; **2017**. Crustacean zooplankton release copious amounts of dissolved organic matter as taurine in the ocean. *Limnology and Oceanography* 62, 2745–2758.

Comita P.B.; Gagosian, R.B.; **1983**. Membrane lipid from deep-sea hydrothermal vent methanogen: a new macrocyclic glycerol diether. *Science* 222, 1329–1331.

Comita, P.B.; Gagosian, R.B.; Pang, H.; Costello, C.E.; **1984**. Structural elucidation of a unique macrocyclic membrane lipid from a new, extremely thermophilic, deep-sea hydrothermal vent archaebacterium, *Methanococcus jannaschii*. *The Journal of Biological Chemistry* 259, 15234–15241.

Cooper, G.; Kimmich, N.; Belisle, W.; Sarinana, J.; Brabham, K.; Garrel, L.; **2001**. Carbonaceous meteorites as a source of sugar-related organic compounds for the early Earth. *Nature* 414, 879–883.

Corliss, J.B.; Dymond, J.; Gordon, L.I.; Edmond, J.M.; Von Herzen, R.P.; Ballard, R.D.; Green, K.; Williams, D.; Bainbridge, A.; Crane, K.; Van Andel, T.H.; **1979**. Submarine thermal springs on the Galápagos Rift. *Science* 203, 1073–1083.

Cronin, J.R.; Moore, C.B.; **1971**. Amino acid analyses of the Murchison, Murray, and Allende Carbonaceous Chondrites. *Science* 172, 1327–1329.

Dasuri, K.; Ebenezer, P.J.; Uranga, R.; Gavilán, E.; Zhang, L.; Fernandez-Kim, S.O.K.; Bruce-Keller, A.J.; Keller, J.N.; **2011**. Amino acid analog toxicity in primary rat neuronal and astrocyte cultures: Implications for protein misfolding and TDP-43 regulation. *Journal of Neuroscience Research* 89, 1471–1477.

Dawson, K.S.; Freeman, K.H.; Macalady, J.L.; **2012**. Molecular characterization of core lipids from halophilic archaea grown under different salinity conditions. *Organic Geochemistry* 48, 1–8.

Deamer, D.; Damer, B.; **2017**. Can Life begin on Enceladus? A perspective from hydrothermal chemistry. *Astrobiology* 17, 834–839.

De-Bashan, L.E.; Bashan, Y.; Moreno, M.; Lebsky, V.K.; Bustillos, J.J.; **2002**. Increased pigment and lipid content, lipid variety, and cell and population size of the microalgae *Chlorella spp.* when co-immobilized in alginate beads with the microalgae-growth-promoting bacterium *Azospirillum brasilense*. *Canadian Journal of Microbiology* 48, 514–521.

De Boever, E.; Birgel, D.; Thiel, V.; Muchez, P.; Peckmann, J.; Dimitrov, L.; Swennen, R.; **2009**. The formation of giant tubular concretions triggered by anaerobic oxidation of methane as revealed by archaeal molecular fossils (Lower Eocene, Varna, Bulgaria). *Palaeogeography, Palaeoclimatology, Palaeoecology* 280, 23–36.

Deienno, R.; Morbidelli, A.; Gomes, R.S.; Nesvorný, D.; **2017**. Constraining the giant planets' initial configuration from their evolution: Implications for the timing of the planetary instability. *The Astronomical Journal* 153, 153: 1–13.

De Rosa, M.; De Rosa, S.; Gambacorta, A.; Minale, L.; Bu'Lock, J.D.; **1977**. Chemical structure of the ether lipids of thermophilic acidophilic bacteria of the *Caldariella* group. *Phytochemistry* 16, 1961–1965.

De Rosa, M.; Esposito, E.; Gambacorta, A.; Nicolaus, B.; Bu'Lock, J.D.; **1980**. Effects of temperature on ether lipid composition of *Caldariella acidophila*. *Phytochemistry* 19, 827–831.

De Rosa, M.; Gambacorta, A.; Nicolaus, B.; Chappe, B.; Albrecht, P.; **1983**. Isoprenoid ethers; backbone of complex lipids of the archaebacterium *Sulfolobus solfataricus*. *Biochimica et Biophysica Acta* 753, 249–256.

De Rosa, M.; Gambacorta, A.; **1988**. The lipids of archaebacteria. *Progress in Lipid Research* 27, 153–175.

Dorn, E.D; Nealson, K.H; Adami, C.; **2011**. Monomer abundance distribution patterns as a universal biosignature: Examples from terrestrial and digital life. *Journal of Molecular Evolution* 72, 283–295.

Dridi, B.; Fardeau, M.-L.; Ollivier, B.; Raoult, D.; Drancourt, M.; **2012**. *Methanomassiliicoccus luminyensis* gen. nov., sp. nov., a methanogenic archaeon isolated from human faeces. *International Journal of Systematic and Evolutionary Microbiology* 62, 1902–1907.

Eguchi, T.; Takyo, H.; Morita, M.; Kakinuma, K.; Koga, Y.; **2000**. Unusual double-bond migration as a plausible key reaction in the biosynthesis of the isoprenoidal membrane lipids of methanogenic archaea. *Chemical Communications*, 1545–1546.

Ehrenfreund, P.; Charnley, S.B.; **2000**. Organic molecules in the interstellar medium, comets, and meteorites: A voyage from dark clouds to the Early Earth. *Annual Review of Astronomy and Astrophysics* 38, 427–483.

Elsila, J.E.; Glavin, D.P.; Dworkin, J.P.; **2009**. Cometary glycine detected in samples returned by Stardust. *Meteoritics & Planetary Science* 44, 1323–1330.

Ferrante, G.; Ekiel, I.; Sprott, G.D.; **1986**. Structural characterization of the lipids of *Methanococcus voltae*, including a novel *N*-acteylglucosamine 1-phosphate diether. *The Journal of Biological Chemistry* 261, 17062–17066.

Ferrante, G.; Richards, J.C.; Sprott, G.D.; **1990**. Structures of polar lipids from the thermophilic, deep-sea archaebacterium *Methanococcus jannaschii*. *Biochemistry and Cell Biology* 68, 274–283.

Fricke, H.; Giere, O.; Stetter, K.; Alfredsson, G.A.; Kristjansson, J.K.; Stoffers, P.; Svavarsson, J.; **1989**. Hydrothermal vent communities at shallow subpolar Mid-Atlantic ridge. *Marine Biology* 102, 425–429.

Gabriel, J.L.; Chong, P.L.G.; **2000**. Molecular modeling of archaebacterial bipolar tetraether lipid membranes. *Chemistry and Physics of Lipids* 105, 193–200.

Georgiou, C.D.; Deamer, D.W.; **2014**. Lipids as universal biomarkers of extraterrestrial life. *Astrobiology* 14, 541–549.

Georgiou, C.D; **2018**. Functional properties of amino acid side chains as biomarkers of extraterrestrial life. *Astrobiology* 18, 1479–1496.

Gibb, E.L.; Whittet, D.C.B.; Chiar, J.E.; **2001**. Searching for ammonia in grain mantles toward massive young stellar objects. *The Astrophysical Journal* 558, 702–716.

Gibb, E.L.; Whittet, D.C.B.; Boogert, A.C.A.; Tielens, A.G.G.M.; **2004**. Interstellar ice: The

infrared space observatory legacy. *The Astrophysical Journal Supplement Series* 151, 35–73.

Gibson, R.A.; Van der Meer M.T.J.; Hopmans, E.C.; Reysenbach, A.-L.; Schouten, S.; Sinninghe Damsté, J.S.; **2013**. Comparison of intact polar lipid with microbial community composition of vent deposits of the Rainbow and Lucky Strike hydrothermal fields. *Geobiology* 11, 72–85.

Gräther, O.W.; **1994**. Zur Struktur und Biosynthese der Tetraetherlipide der Archea. P.h.D. thesis, ETH Zürich.

Guzman, M.; Lorenz, R.; Hurley, D.; Farrell, W.; Spencer, J.; Hansen, C.; Hurford, T.; Ibea, J.; Carlson, P.; McKay, C.P.; **2018**. Collecting amino acids in the Enceladus plume. *International Journal of Astrobiology*, 1–13.

Hilts, R.W.; Herd, C.D.K.; Simkus, D.N.; Slater, G.F.; **2014**. Soluble organic compounds in the Tagish Lake meteorite. *Meteoritics & Planetary Science* 49, 526–549.

Hinrichs, K.-U.; Hayes, J.M.; Sylva, S.P.; Brewer, P.G.; DeLong, E.F.; **1999**. Methane-consuming archaebacteria in marine sediments. *Nature* 398, 802–805.

Ho, P.T.P.; Townes, C.H.; **1983**. Interstellar ammonia. *Annual Review of Astronomy and Astrophysics* 21, 239–270.

Hopmans, E.C.; Schouten, S.; Pancost, R.D.; Van der Meer, M.T.J.; Sinninghe Damsté, J.S.; **2000**. Analysis of intact tetraether lipids in archaeal cell material and sediments by high performance liquid chromatography/atmospheric pressure chemical ionization mass spectrometry. *Rapid Communications in Mass Spectrometry* 14, 585–589.

Hsu, H.-W.; Postberg, F.; Sekine, Y.; Shibuya, T.; Kempf, S.; Horányi, M.; Juhász, A.; Altobelli, N.; Suzuki, K.; Masaki, Y.; Kuwatani, T.; Tachibana, S.; Sirono, S.I.; Moragas-Klostermeyer, G.; Srama, R.; **2015**. Ongoing hydrothermal activities within Enceladus. *Nature* 519, 207–210.

Huang, Y.; Wang, Y.; Alexandre, M.R.; Lee, T.; Rose-Petruck, C.; Fuller, M.; Pizzarello, S.; **2005**. Molecular and compound-specific isotopic characterization of monocarboxylic acids in carbonaceous meteorites. *Geochimica et Cosmochimica Acta* 69, 1073–1084.

Huber, H.; Thomm, M.; König, H.; Thies, G.; Stetter, K.O.; **1982**. *Methanococcus thermolithotrophicus*, a novel thermophilic lithotrophic methanogen. *Archives of Microbiology* 132, 47–50.

Huguet, C.; Hopmans, E.C.; Febo-Ayala, W.; Thompson, D.H.; Sinninghe Damsté, J.S.; Schouten, S.; **2006**. An improved method to determine the absolute abundance of glycerol dibiphytanyl glycerol tetraether lipids. *Organic Geochemistry* 37, 1036–1041.

Jaeschke, A.; Jørgensen, S.L.; Bernasconi, S.M.; Pedersen, R.B.; Thorseth, I.H.; Früh-Green, G.L.; **2012**. Microbial diversity of Loki's Castle black smokers at the Arctic Mid-Ocean Ridge. *Geobiology* 10, 548–561.

Jaeschke, A.; Eickmann, B.; Lang, S.Q.; Bernasconi, S.M.; Strauss, H.; Früh-Green, G.L.; **2014**. Biosignatures in chimney structures and sediment from the Loki's Castle low-

temperature hydrothermal vent field at the Arctic Mid-Ocean Ridge. *Extremophiles* 18, 545–560.

Jones, W.J.; Leigh, J.A.; Mayer, F.; Woese, C.R.; Wolfe, R.S.; **1983**. *Methanococcus jannaschii* sp.nov., an extremely thermophilic methanogen from a submarine hydrothermal vent. *Archives of Microbiology* 136, 254–261.

Jones, W.J.; Stugard, C.E.; Jannasch, H.W.; **1989**. Comparison of thermophilic methanogens from submarine hydrothermal vents. *Archives of Microbiology* 151, 314–318.

Judge, P.; **2017**. A novel strategy to seek biosignatures at Enceladus and Europa. *Astrobiology* 17, 852–861.

Kaneshiro, S.M.; Clark, D.S.; **1995**. Pressure effects on the composition and thermal behavior of lipids from the deep-sea thermophile *Methanococcus jannaschii*. *Journal of Bacteriology* 177, 3668–3672.

Kato, S.; Kosaka, T.; Watanabe, K.; **2008**. Comparative transcriptome analysis of responses of *Methanothermobacter thermautotrophicus* to different environmental stimuli. *Environmental Microbiology* 10, 893–905.

Kelley, D.S.; Karson, J.A.; Blackman, D.K.; Früh-Green, G.L.; Butterfield, D.A.; Lilley, M.D.; Olson, E.J.; Schrenk, M.O.; Roe, K.K.; Lebon, G.T.; Rivizzigno, P.; Shipboard Party, AT3-60; **2001**. An off-axis hydrothermal vent field near the Mid-Atlantic Ridge at 30°N. *Nature* 412, 145–149.

Kendall, M.M.; Liu, Y.; Sieprawska-Lupa, M.; Stetter, K.O.; Whitman, W.B.; Boone, D.R.; **2006**. *Methanococcus aeolicus* sp. nov., a mesophilic, methanogenic archaeon from shallow and deep marine sediments. *International Journal of Systematic and Evolutionary Microbiology* 56, 1525–1529.

Keswani, J.; Orkand, S.; Premachandran, U.; Mandelco, L.; Franklin, M.J.; Whitman, W.B.; **1996**. Phylogeny and taxonomy of mesophilic *Methanococcus* spp. and comparison of rRNA, DNA hybridization, and phenotypic methods. *International Journal of Systematic Bacteriology* 46, 727–735.

Kitadai, N.; Maruyama, S.; **2018**. Origins of building blocks of life: A review. *Geoscience Frontiers* 9, 1117–1153.

Knappy, C.S., Chong, J.P.J., Keely, B.J., **2009**. Rapid discrimination of archaeal tetraether lipid cores by liquid chromatography – tandem mass spectrometry. *American Society for Mass Spectrometry* 20, 51–59.

Knappy, C.S.; **2010**. Mass spectrometric studies of ether lipids in Archaea and sediments. P.h.D thesis, University of York, Department of Chemistry, 406 p.

Knappy, C.S.; Nunn, C.E.M.; Morgan, H.W.; Keely, B.J.; **2011**. The major lipid cores of the archaeon *Ignisphaera aggregans*: Implications for the phylogeny and biosynthesis of glycerol monoalkyl glycerol tetraether isoprenoid lipids. *Extremophiles* 15, 517–528.

Knappy, C.S.; Keely, B.J.; **2012**. Novel glycerol dialkanol triols in sediments: transformation products of glycerol dibiphytanyl glycerol tetraether lipids or biosynthetic intermediates? *Chemical Communications* 48, 841–843.

Knappy, C.S.; Barillà, D.; Chong, J.; Hodgson, D.; Morgan, H.; Suleman, M.; Tan, C.; Yao, P.; Keely, B.; **2015**. Mono-, di- and trimethylated homologues of isoprenoid tetraether lipid cores in archaea and environmental samples: Mass spectrometric identification and significance. *Journal of Mass Spectrometry* 50, 1420–1432.

Koga, Y.; Nishihara, M.; Morii, H.; Akagawa-Matsushita, M.; **1993**. Ether polar lipids of methanogenic bacteria: Structures, comparative aspects, and biosyntheses. *Microbiological Reviews* 57, 164–182.

Koga, Y.; Morii, H.; Akagawa-Matsushita, M.; Ohga, M.; **1998**. Correlation of polar lipid composition with 16S rRNA phylogeny in methanogens. Further analysis of lipid component parts. *Bioscience, Biotechnology, and Biochemistry* 62, 230–236.

Koga, Y.; Morii, H.; **2005**. Recent advances in structural research on ether lipids from archaea including comparative and physiological aspects. *Bioscience, Biotechnology, and Biochemistry* 69, 2019–2034.

Koga, Y.; Morii, H.; **2007**. Biosynthesis of ether-type polar lipids in Archaea and evolutionary considerations. *Microbiology and Molecular Biology Reviews* 71, 97–120.

Koga, Y.; **2012**. Thermal adaptation of the archaeal and bacterial lipid membranes. *Archaea* 789652, 1–6.

Koga, T.; Naraoka, H.; **2017**. A new family of extraterrestrial amino acids in the Murchison meteorite. *Scientific Reports* 7, 636.

Kon, T.; Nemoto, N.; Oshima, T.; Yamagishi, A.; **2002**. Effects of a squalene epoxidase inhibitor, terbinafine, on ether lipid biosyntheses in a thermoacidophilic archaeon, *Thermoplasma acidophilum*. *Journal of Bacteriology* 184, 1395–1401.

Kral, T.A.; Goodhart, T.H.; Harpool, J.D.; Hearnsberger, C.E.; McCracken, G.L.; McSpadden, S.W.; **2016**. Sensitivity and adaptability of methanogens to perchlorates: Implications for life on Mars. *Planetary and Space Science* 120, 87–95.

Kramer, J.K.G.; Sauer, F.D.; **1991**. Changes in the diether-to-tetraether-lipid ratio during cell growth in *Methanobacterium thermoautotrophicum*. *FEMS Microbiology Letters* 83, 45–50.

Krömer, J.O.; Fritz, M.; Heinzle, E.; Wittmann, C.; **2005**. In vivo quantification of intracellular amino acids and intermediates of the methionine pathway in *Corynebacterium glutamicum*. *Analytical Biochemistry* 340, 171–173.

Kuan, Y.; Charnley, S.B.; Huang, H.; Tseng, W.; Kisiel, Z.; **2003**. Interstellar glycine. *The Astrophysical Journal* 593, 848–867.

Kushwaha, S.C.; Kates, M.; Sprott, G.D.; Smith, I.C.P.; **1981**. Novel polar lipids from the methanogen *Methanospirillum hungatei* GP1. *Biochimica et Biophysica Acta – Lipids and Lipid Metabolism* 664, 156–173.

Kvenvolden, K.; Lawless, J.; Pering, K.; Peterson, E.; Flores, J.; Ponnamperuma, C.; Kaplan, I.R.; Moore, C.; **1970**. Evidence for extraterrestrial amino-acids and hydrocarbons in the murchison meteorite. *Nature 228*, 923–926.

Langworthy, T.A.; **1977**. Long-chain diglycerol tetraethers from *Thermoplasma acidophilum*. *Biochimica et Biophysica Acta* 487, 37–50.

Lees, R.M.; Haque, S.S.; **1974**. Microwave double resonance study of collision induced population transfer between levels of interstellar methanol lines. *Canadian Journal of Physics* 52, 2250–2271.

Lengger, S.K., Hopmans, E.C., Sinninghe Damsté, J.S., Schouten, S.; **2014**. Fossilization and degradation of archaeal intact polar tetraether lipids in deeply buried marine sediments (Peru Margin). *Geobiology* 12, 212-220.

Li, K.; Xu, E.; **2008**. The role and the mechanism of γ-aminobutyric acid during central nervous system development. *Neuroscience Bulletin* 24, 195–200.

Liu, Y.; Whitman, W.B.; **2008**. Metabolic, phylogenetic, and ecological diversity of the methanogenic archaea. *Annals of the New York Academy of Sciences* 1125, 171–189.

Liu, X.-L.; Lipp, J.S.; Simpson, J.H.; Lin, Y.-S.; Summons, R.E.; Hinrichs, K.-U.; **2012a**. Mono- and dihydroxyl glycerol dibiphytanyl glycerol tetraethers in marine sediments: Identification of both core and intact polar lipid forms. *Geochimica et Cosmochimica Acta* 89, 102–115.

Liu, X.-L.; Lipp, J.S.; Schröder, J.M.; Summons, R.E.; Hinrichs, K.-U.; **2012b**. Isoprenoid glycerol dialkanol diethers: A series of novel archaeal lipids in marine sediments. *Organic Geochemistry* 43, 50–55.

Liu, X.-L.; Summons, R.E.; Hinrichs, K.-U.; **2012c**. Extending the known range of glycerol ether lipids in the environment: Structural assignments based on tandem mass spectral fragmentation patterns. *Rapid Communications in Mass Spectrometry* 26, 2295–2302.

Liu, X.-L.; Birgel, D.; Elling, F.J.; Sutton, P.A.; Lipp, J.S.; Zhu, R.; Zhang, C.; Könneke, M.; Peckmann, J.; Rowland, S.J.; Summons, R.E.; Hinrichs, K.-U.; **2016**. From ether to acid: A plausible degradation pathyway of glycerol dialkyl glycerol tetraethers. *Geochimica et Cosmochimica Acta* 183, 138–152.

Lu, Z.; Hegemann, W.; **1998**. Anaerobic toxicity and biodegradation of formaldehyde in batch cultures. *Water Research* 32, 209–215.

Lu, Y.; Freeland, S.; **2006**. On the evolution of the standard amino acid alphabet. *Genome Biology* 7, 102.

Makula, R.A.; Singer, M.E.; **1978**. Ether-containing lipids of methanogenic bacteria. *Biochemical and Biophysical Research Communications* 82, 716–722.

Manoharan, L.; Kozlowski, J.A.; Murdoch, R.W.; Löffler, F.E.; Sousa, F.L.; Schleper, C.; **2019**. Metagenomes from coastal marine sediments give insights into the ecological role and cellular features of Loki- and Thorarchaeota. *mBio* 10, 1–15.

Martin, W.; Baross, J.; Kelley, D.; Russell, M.; **2008**. Hydrothermal vents and the origin of life. *Nature Reviews Microbiology* 6, 805–814.

McCartney, C.A.; Dewhurst, R.J.; Bull, I.D.; **2014**. Changes in the ratio of tetraether to diether lipids in cattle feces in response to altered dietary ratio of grass silage and concentrates. *Journal of Animal Science* 92, 4095–4098.

Meador, T.B.; Zhu, C.; Elling, F.J.; Könneke, M.; Hinrichs, K.-U.; **2014**. Identification of isoprenoid glycosidic glycerol dibiphytanol diethers and indications for their biosynthetic origin. *Organic Geochemistry* 69, 70–75.

Méhay, S.; Früh-Green, G.L.; Lang, S.Q.; Bernasconi, S.M.; Brazelton, W.J.; Schrenk, M.O.; Schaeffer, P.; Adam, P.; **2013**. Record of archaeal activity at the serpentinite-hosted Lost City Hydrothermal Field. *Geobiology* 11, 570–592.

Miller, S.L.; **1953**. A production of amino acids under possible primitive Earth conditions. *Science* 117, 528–529.

Miller, J.F.; Shah, N.N.; Nelson, C.M.; Ludlow, J.M.; Clark, D.S.; **1988**. Pressure and temperature effects on growth and methane production of the extreme thermophile *Methanococcus jannaschii*. *Applied and Environmental Microbiology* 54, 3039–3042.

Moissl-Eichinger, C.; Cockell, C.; Rettberg, P.; **2016**. Venturing into new realms? Microorganisms in space. *FEMS Microbiology Reviews* 40, 722–737.

Morii, H.; Koga, Y.; **1993**. Tetraether type polar lipids increase after logarithmic growth phase of *Methanobacterium thermoautotrophicum* in compensation for the decrease of diether lipids. *FEMS Microbiology Letters* 109, 283–288.

Morii, H.; Koga, Y.; **1994**. Asymmetrical topology of diether- and tetraether-type polar lipids in membranes of *Methanobacterium thermoautotrophicum* cells. *The Journal of Biological Chemistry* 269, 10492–10497.

Morii, H.; Eguchi, T.; Nishihara, M.; Kakinuma, K.; König, H.; Koga, Y.; **1998**. A novel ether core lipid with H-shaped C_{80}-isoprenoid hydrocarbon chain from the hyperthermophilic methanogen *Methanothermus fervidus*. *Biochimica et Biophysica Acta* 1390, 339–345.

Naafs, B.D.A.; McCormick, D.; Inglis, G.N.; Pancost, R.D.; T-GRES peat database collaborators; **2018**. Archaeal and bacterial H-GDGTs are abundant in peat and their relative abundance is positively correlated with temperature. *Geochimica et Cosmochimica Acta* 227, 156–170.

Nemoto, N.; Shida, Y.; Shimada, H.; Oshima, T.; Yamagishi, A.; **2003**. Characterization of the precursor of tetraether lipid biosynthesis in the thermoacidophilic archaeon *Thermoplasma acidophilum*. *Extremophiles* 7, 235–243.

Nichols, D.S.; Miller, M.R.; Davies, N.W.; Goodchild, A.; Raftery, M.; Cavicchioli, R.; **2004**. Cold adaptation in the Antarctic archaeon *Methanococcoides burtonii* involves membrane lipid unsaturation. *Journal of Bacteriology* 186, 8508–8515.

Niemann, H.; Elvert, M.; **2008**. Diagnostic lipid biomarker and stable carbon isotope signatures of microbial communities mediating the anaerobic oxidation of methane with sulphate. *Organic Geochemistry* 39, 1668–1677.

Offre, P.; Spang, A.; Schleper, C.; **2013**. Archaea in biogeochemical cycles. *Annual Review of Microbiology* 67, 437–457.

Park, M.H.; **2006**. The post-translational synthesis of a polyamine-derived amino acid, hypusine, in the eukaryotic translation initiation factor 5A (eIF5A). *The Journal of Biochemistry* 139, 161–169.

Patel, G.; Sprott, G.D.; **1999**. Archaeobacterial ether lipid liposomes (archaeosomes) as novel vaccine and drug delivery systems. *Critical Reviews in Biotechnology* 19, 317–357.

Paul, K.; Nonoh, J.O.; Mikulski, L.; Brune, A.; **2012**. "*Methanoplasmatales*," *Thermoplasmatales*-related archaea in termite guts and other environments, are the seventh order of methanogens. *Applied and Environmental Microbiology* 78, 8245–8253.

Perner, M.; Kuever, J.; Seifert, R.; Pape, T.; Koschinsky, A.; Schmidt, K.; Strauss, H.; Imhoff, J.F.; **2007**. The influence of ultramafic rocks on microbial communities at the Logatchev hydrothermal field, located 15°N on the Mid-Atlantic Ridge. *FEMS Microbiology Ecology* 61, 97–109.

Postberg, F.; Khawaja, N.; Abel, B.; Choblet, G.; Glein, C.R.; Gudipati, M.S.; Henderson, B.L.; Hsu, H.-W.; Kempf, S.; Klenner, F.; Moragas-Klostermeyer, G.; Magee, B.; Nölle, L.; Perry, M., Reviol, R.; Schmidt, J.; Srama, R.; Stolz, F.; Tobie, G.; Trieloff, M.; Waite, J.H.; **2018**. Macromolecular organic compounds from the depths of Enceladus. *Nature* 558, 564–568.

Poulter, C.D.; Aoki, T.; Daniels, L.; **1988**. Biosynthesis of isoprenoid membranes in the methanogenic archaebacterium *Methanospirillum hungatei*. *Journal of the American Chemical Society* 110, 2620–2624.

Reeves, E.P.; Yoshinaga, M.Y.; Pjevac, P.; Goldenstein, N.I.; Peplies, J.; Meyerdierks, A.; Amann, R.; Bach, W.; Hinrichs, K.-U.; **2014**. Microbial lipids reveal carbon assimilation patterns on hydrothermal sulfide chimneys. *Environmental Microbiology* 16, 3515–3532.

Rittmann, S.; Seifert, A.; Herwig, C.; **2015**. Essential prerequisites for successful bioprocess development of biological CH_4 production from CO_2 and H_2. *Critical Reviews in Biotechnology* 35, 141–151.

Robertson, D.E.; Roberts, M.F.; Belay, N.; Stetter, K.O.; Boone, D.R.; **1990**. Occurrence of beta-glutamate, a novel osmolyte, in marine methanogenic bacteria. *Applied and Environmental Microbiology* 56, 1504–1508.

Robertson, D.E.; Noll, D.; Roberts, M.F.; **1992**. Free amino acid dynamics in marine methanogens. Beta-amino acids as compatible solutes. *Journal of Biological Chemistry* 267, 14893–14901.

Rossel, P.E.; Lipp, J.S.; Fredricks, H.F.; Arnds, J.; Boetius, A.; Elvert, M.; Hinrichs, K.-U.; **2008**. Intact polar lipids of anaerobic methanotrophic archaea and associated bacteria. *Organic Geochemistry* 39, 992–999.

Russell, M.J.; Hall, A.J.; Martin, W.; **2010**. Serpentinization as a source of energy at the origin of life. *Geobiology* 8, 355–371.

Rütters, H.; Sass, H.; Cypionka, H.; Rullkötter, J.; **2002**. Phospholipid analysis as a tool to study complex microbial communities in marine sediments. *Journal of Microbiological Methods* 48, 149–160.

Schinteie, R.; Brocks, J.J.; **2017**. Paleoecology of Neoproterozoic hypersaline environments: Biomarker evidence for haloarchaea, methanogens, and cyanobacteria. *Geobiology* 15, 641–663.

Schlesinger, G.; Miller, S.L.; **1983**. Prebiotic synthesis in atmospheres containing CH_4, CO, and CO_2. *Journal of Molecular Evolution*, 19, 376–382.

Schouten, S.; Van Der Maarel, M.J.E.C.; Huber, R.; Sinninghe Damsté, J.S.; **1997**. 2,6,10,15,19-Pentamethylicosenes in *Methanolobus bombayensis*, a marine methanogenic archaeon, and in *Methanosarcina mazei*. *Organic Geochemistry* 26, 409–414.

Schouten, S.; Baas, M.; Hopmans, E.C.; Reysenbach, A.-L.; Sinninghe Damsté, J.S.; **2008a**. Tetraether membrane lipids of *Candidatus* "*Aciduliprofundum boonei*", a cultivated obligate thermoacidophilic euryarchaeote from deep-sea hydrothermal vents. *Extremophiles* 12, 119–124.

Schouten, S.; Hopmans, E.C.; Baas, M.; Boumann, H.; Standfest, S.; Könneke, M.; Stahl, D.A.; Sinninghe Damsté, J.S.; **2008b**. Intact membrane lipids of "*Candidatus Nitrosopumilus maritimus*," a cultivated representative of the cosmopolitan mesophilic Group I Crenarchaeota. *Applied and Environmental Microbiology* 74, 2433–2440.

Schouten, S.; Baas, M.; Hopmans, E.C.; Sinninghe Damsté, J.S.; **2008c**. An unusual isoprenoid tetraether lipid in marine and lacustrine sediments. *Organic Geochemistry* 39, 1033–1038.

Schouten, S.; Hopmans, E.C.; Sinninghe Damsté; J.S.; **2013**. The organic geochemistry of glycerol dialkyl glycerol tetraether lipids: A review. *Organic Geochemistry* 54, 19–61.

Schrenk, M.O.; Kelley, D.S.; Bolton, S.A.; Baross, J.A.; **2004**. Low archaeal diversity linked to subseafloor geochemical processes at the Lost City Hydrothermal Field, Mid-Atlantic Ridge. *Environmental Microbiology* 6, 1086–1095.

Schulze-Makuch, D.; Irwin, L.N.; **2018**. Building blocks of life: "The uniqueness of carbon"; "An alien carbon biochemistry?" In chapter 6 of *Life in the universe – Expectations and constraints*. *Springer Praxis Books*, *Springer Nature Switzerland AG*; 3rd edition, pp. 101–106.

Shimada, H.; Nemoto, N.; Shida, Y.; Oshima, T.; Yamagishi, A.; **2008**. Effects of pH and temperature on the composition of polar lipids in *Thermoplasma acidophilum* HO-62. *Journal of Bacteriology* 190, 5404–5411.

Siliakus, M.F.; van der Oost, J.; Kengen, S.W.M.; **2017**. Adaptations of archaeal and bacterial membranes to variations in temperature, pH and pressure. *Extremophiles* 21, 651–670.

Sinninghe Damsté, J.S.; Rijpstra, W.I.C.; Hopmans, E.C.; Jung, M.-Y.; Kim, J.G.; Rhee, S.-K.; Stieglmeier, M.; Schleper, C.; **2012**. Intact polar and core glycerol dibiphytanyl glycerol

tetraether lipids of Group I.1a and I.1b Thaumarchaeota in Soil. *Applied and Environmental Microbiology* 78, 6866–6874.

Snyder, L.E.; Buhl, D.; Zuckerman, B.; Palmer, P.; **1969**. Microwave detection of interstellar formaldehyde. *Physical Review Letters* 22, 679–681.

Sollich, M.; Yoshinaga, M.Y.; Häusler, S.; Price, R.E.; Hinrichs, K.-U.; Bühring, S.I.; **2017**. Heat stress dictates microbial lipid composition along a thermal gradient in marine sediments. *Frontiers in Microbiology* 8, 1550: 1–19.

Sorokin, D.Y.; Abbas, B.; Merkel, A.Y.; Rijpstra, W.I.C.; Sinninghe Damsté, J.S.; Sukhacheva, M.V.; Van Loosdrecht, M.C.M.; **2015**. *Methanosalsum natronophilum* sp. nov., and *Methanocalculus alkaliphilus* sp. nov., haloalkaliphilic methanogens from hypersaline soda lakes. *International Journal of Systematic and Evolutionary Microbiology* 65, 3739–3745.

Sprott, G.D.; Meloche, M.; Richards, J.C.; **1991**. Proportions of diether, macrocyclic diether, and tetraether lipids in *Methanococcus jannaschii* grown at different temperatures. *Journal of Bacteriology* 173, 3907–3910.

Stadnitskaia, A.; Baas, M.; Ivanov, M.K.; Van Weering, T.C.E.; Sinninghe Damsté, J.S.; **2003**. Novel archaeal macrocyclic diether core membrane lipids in a methane-derived carbonate crust from a mud volcano in the Sorokin Trough, NE Black Sea. *Archaea* 1, 165–173.

Sturt, H.F.; Summons, R.E.; Smith, K.; Elvert, M.; Hinrichs, K.-U.; **2004**. Intact polar membrane lipids in prokaryotes and sediments deciphered by high-performance liquid chromatography/electrospray ionization multistage mass spectrometry – new biomarkers for biogeochemistry and microbial ecology. *Rapid Communications in Mass Spectrometry* 18, 617–628.

Sugai, A.; Uda, I.; Itoh, Y.H.; Itoh, T.; **2004**. The core lipid composition of the 17 strains of hyperthermophilic archaea, *Thermococcales*. *Journal of Oleo Science* 53, 41–44.

Summons, R.E.; Powell, T.G.; Boreham, C.J.; **1988**. Petroleum geology and geochemistry of the Middle Proterozoic McArthur Basin, Northern Australia: III. Composition of extractable hydrocarbons. *Geochimica et Cosmochimica Acta* 52, 1747–1763.

Summons, R.E.; Albrecht, P.; McDonald, G.; Moldowan, J.M.; **2008**. Molecular biosignatures. *Space Science Reviews* 135, 133–159.

Sutherland, J.D.; **2016**. The Origin of Life – Out of the Blue. *Angewandte Chemie International Edition* 55, 104–121.

Takai, K.; Horikoshi, K.; **2000**. *Thermosipho japonicus* sp. nov., an extremely thermophilic bacterium isolated from a deep-sea hydrothermal vent in Japan. *Extremophiles* 4, 9–17.

Takai, K.; Inoue, A.; Horikoshi, K.; **2002**. *Methanothermococcus okinawensis* sp. nov., a thermophilic, methane-producing archaeon isolated from a Western Pacific deep-sea hydrothermal vent system. *International Journal of Systematic and Evolutionary Microbiology* 52, 1089–1095.

Tan, J.; Lewis, J.M.T.; Sephton, M.A.; **2018**. The fate of lipid biosignatures in a Mars-analogue

sulfur stream. *Scientific Reports* 8, 7586: 1–8.

Taubner, R.-S.; Schleper, C.; Firneis, M.G.; Rittmann, S.K.-M.R.; **2015**. Assessing the ecophysiology of methanogens in the context of recent astrobiologcial and planetological studies. *Life* 5, 1652–1686.

Taubner, R.-S.; Rittmann, S.K.-M.R.; **2016**. Method for indirect quantification of CH_4 production via H_2O production using hydrogenotrophic methanogens. *Frontiers in Microbiology* 7, 532: 1–11.

Taubner, R.-S.; Pappenreiter, P.; Zwicker, J.; Smrzka, D.; Pruckner, C.; Kolar, P.; Bernacchi, S.; Seifert, A.H.; Krajete, A.; Bach, W.; Peckmann, J.; Paulik, C.; Firneis, M.G.; Schleper, C.; Rittmann, S.K.-M.R.; **2018**. Biological methane production under putative Enceladus-like conditions. *Nature Communications* 9, 748: 1–11.

Taubner, R. An interdisciplinary approach: On the habitability of Enceladus' potential subsurface water reservoir. P.h.D thesis, *University of Vienna*, **2018**.

Taubner, R.-S.; Baumann, L.M.F.; Bauersachs, T.; Clifford, E.L.; Mähnert, B.; Reischl, B.; Seifert, R.; Peckmann, J.; Rittmann, S.K.-M.R; Birgel, D.; **2019**. Membrane lipid composition and amino acid excretion patterns of *Methanothermococcus okinawensis* grown in the presence of inhibitors detected in the Enceladian plume. *Life* 9, 85, 1–19.

Taubner, R.-S.; Olsson-Francis, K.; Vance, S.D.; Ramkissoon, N.K.; Postberg, F.; de Vera, J.-P.; Antunes, A.; Camprubi Casas, E.; Sekine, Y.; Noack, L.; Barge, L.; Goodman, J.; Jebbar, M.; Journaux, B.; Karatekin, Ö.; Klenner, F.; Rabbow, E.; Rettberg, P.; Rückriemen-Bez, T.; Saur, J.; Shibuya, T.; Soderlund, K.M.; **2020**. Experimental and simulation efforts in the astrobiological exploration of exooceans. *Space Science Reviews* 216, 9: 1–41.

Teixidor, P.; Grimalt, J.O.; Pueyo, J.J.; Rodriguez-Valera, F.; **1993**. Isopranylglycerol diethers in non-alkaline evaporitic environments. *Geochimica et Cosmochimica Acta* 57, 4479–4489.

Timmers, P.H.A.; Welte, C.U.; Koehorst, J.J.; Plugge, C.M.; Jetten, M.S.M.; Stams, A.J.M.; **2017**. Reverse methanogenesis and respiration in methanotrophic archaea. *Archaea* 1654237, 1–22.

Thauer, R.K.; Kaster, A.-K.; Seedorf, H.; Buckel, W.; Hedderich, R.; **2008**. Methanogenic archaea: Ecologically relevant differences in energy conservation. *Nature Reviews Microbiology* 6, 579–591.

Tornabene, T.G.; Langworthy, T.A.; **1979**. Diphytanyl and dibiphytanyl glycerol ether lipids of methanogenic archaebacterial. *Science* 203, 51–53.

Tornabene, T.G.; Langworthy, T.A.; Holzer, G.; Oró, J.; **1979**. Squalenes, phytanes and other isoprenoids as major neutral lipids of methanogenic and thermoacidophilic "Archaebacteria". *Journal of Molecular Evolution* 13, 73–83.

Trincone, A.; Nicolaus, B.; Palmieri, G.; De Rosa, M.; Huber, R.; Huber, G.; Stetter, K.O.; Gambacorta, A.; **1992**. Distribution of complex and core lipids within new hyperthermophilic members of the *Archaea* domain. *Systematic and Applied Microbiology* 15, 11–17.

Uda, I.; Sugai, A.; Itoh, Y.H.; Itoh, T.; **2001**. Variation in molecular species of polar lipids from *Thermoplasma acidophilum* depends on growth temperature. *Lipids* 36, 103–105.

Uda, I.; Sugai, A.; Itoh, Y.H.; Itoh, T.; **2004**. Variation in molecular species of core lipids from the order Thermoplasmales strains depends on the growth temperature. *Journal of Oleo Science* 53, 399–404.

Ueno, Y.; Yamada, K.; Yoshida, N.; Maruyama, S.; Isozaki, Y.; **2006**. Evidence from fluid inclusions for microbial methanogenesis in the early Archaean era. *Nature* 440, 516–519.

Van de Vossenberg, J.L.C.M.; Driessen, A.J.M.; Konings, W.N.; **1998**. The essence of being extremophilic: The role of the unique archaeal membrane lipids. *Extremophiles* 2, 163–170.

Villanueva, L.; Sinninghe Damsté, J.S.; Schouten, S.; **2014**. A re-evaluation of the archaeal membrane lipid biosynthetic pathway. *Nature* 12, 438–448.

Waite, J.H.; Lewis, W.S.; Magee, B.A.; Lunine, J.I.; McKinnon, W.B.; Glein, C.R.; Mousis, O.; Young, D.T.; Brockwell, T.; Westlake, J.; Nguyen, M.-J.; Teolis, B.D.; Niemann, H.B.; McNutt, R.L.Jr.; Perry, M.; Ip, W.-H.; **2009**. Liquid water on Enceladus from observations of ammonia and ^{40}Ar in the plume. *Nature* 460, 487–490.

Wasserfallen, A.; Nölling, J.; Pfister, P.; Reeve, J.; de Macario, E.C.; **2000**. Phylogenetic analysis of 18 thermophilic *Methanobacterium* isolates supports the proposals to create a new genus, *Methanothermobacter* gen. nov., and to reclassify several isolates in three species, *Methanothermobacter thermautotrophicus* comb. nov., *Methanothermobacter wolfeii* comb. nov., and *Methanothermobacter marburgensis* sp. nov.. *International Journal of Systematic and Evolutionary Microbiology* 50, 43–53.

Weber, A.L.; Miller, S.L.; **1981**. Reasons for the occurrence of the twenty coded protein amino acids. *Journal of Molecular Evolution* 17, 273–284.

Woodman, J.H.; Trafton, L.; Owen, T; **1977**. The abundances of ammonia in the atmospheres of Jupiter, Saturn, and Titan. *Icarus* 32, 314–320.

Yoshinaga, M.Y.; Gagen, E.J.; Wörmer, L.; Broda, N.K.; Meador, T.B.; Wendt, J.; Thomm, M.; Hinrichs, K.-U.; **2015**. *Methanothermobacter thermautotrophicus* modulates its membrane lipids in response to hydrogen and nutrient availability. *Frontiers in Microbiology* 6, 5: 1–9.

Zaia, D.A.M.; Zaia, C.T.B.V; De Santana, H.; **2008**. Which amino acids should be used in prebiotic chemistry studies? *Origins of Live and Evolution of Biospheres* 38, 469–488.

Zwicker, J.; Birgel, D.; Bach, W.; Richoz, S.; Smrzka, D.; Grasemann, B.; Gier, S.; Schleper, C.; Rittmann, S.K.-M.R.; Koşun, E.; Peckmann, J.; **2018**. Evidence for archaeal methanogenesis within veins at the onshore serpentinite-hosted Chimaera seeps, Turkey. *Chemical Geology* 483, 567–580.

7. Liste der aus der Dissertation hervorgegangenen Vorveröffentlichungen – List of previous publications emerged from this dissertation

Baumann, L.M.F.; Taubner, R.-S.; Bauersachs, T.; Steiner, M.; Schleper, C.; Peckmann, J.; Rittmann, S.K.-M.R.; Birgel, D., **2018**. Intact polar lipid and core lipid inventory of the hydrothermal vent methanogens *Methanocaldococcus villosus* and *Methanothermococcus okinawensis*. *Organic Geochemistry* 126, 33–42.

Taubner, R.-S.; Baumann, L.M.F.; Bauersachs, T.; Clifford, E.L.; Mähnert, B.; Reischl, B.; Seifert, R.; Peckmann, J.; Rittmann, S.K.-M.R; Birgel, D.; **2019**. Membrane lipid composition and amino acid excretion patterns of *Methanothermococcus okinawensis* grown in the presence of inhibitors detected in the Enceladian plume. *Life* 9, 85, 1–19.

8. Supplementary figures and tables

Table S1: Elution gradient applied for the separation of primary dissolved free amino acids by high performance liquid chromatography (HPLC). Eluent A (polar phase): 40 mM NaH_2PO_4 buffer (pH 7.8 adjusted with NaOH pellets in Milli-Q water; Sigma-Aldrich); B (non-polar phase): 1000/100/2 – Methanol (HPLC grade, Sigma-Aldrich)/Milli-Q water/Trifluoroacetic acid (HPLC grade, Roth); C: Tetrahydrofuran (HPLC grade; Sigma-Aldrich), total time: 90 min. Table from Taubner and Baumann et al. (2019).

Time (min)	A %	B %	C %
0	90	10	0
2	90	7.5	2.5
40	68	30	2.0
42	64	35	1.0
75	35	65	0
77	0	100	0
80	90	10	0
90	90	10	0

Figure S1: HPLC-Chromatograms of a 2.5 µmol/L standard (AAS18, Sigma Aldrich; the single amino acid tryptophane (Trp) is missing in that specific standard curve) in Milli-Q water compared with a sample (undiluted) analysed by the method published in Clifford et al., 2017. Injection volume 500 µL, gain factor 10, method duration 28 min. Figure from Taubner and Baumann et al. (2019).

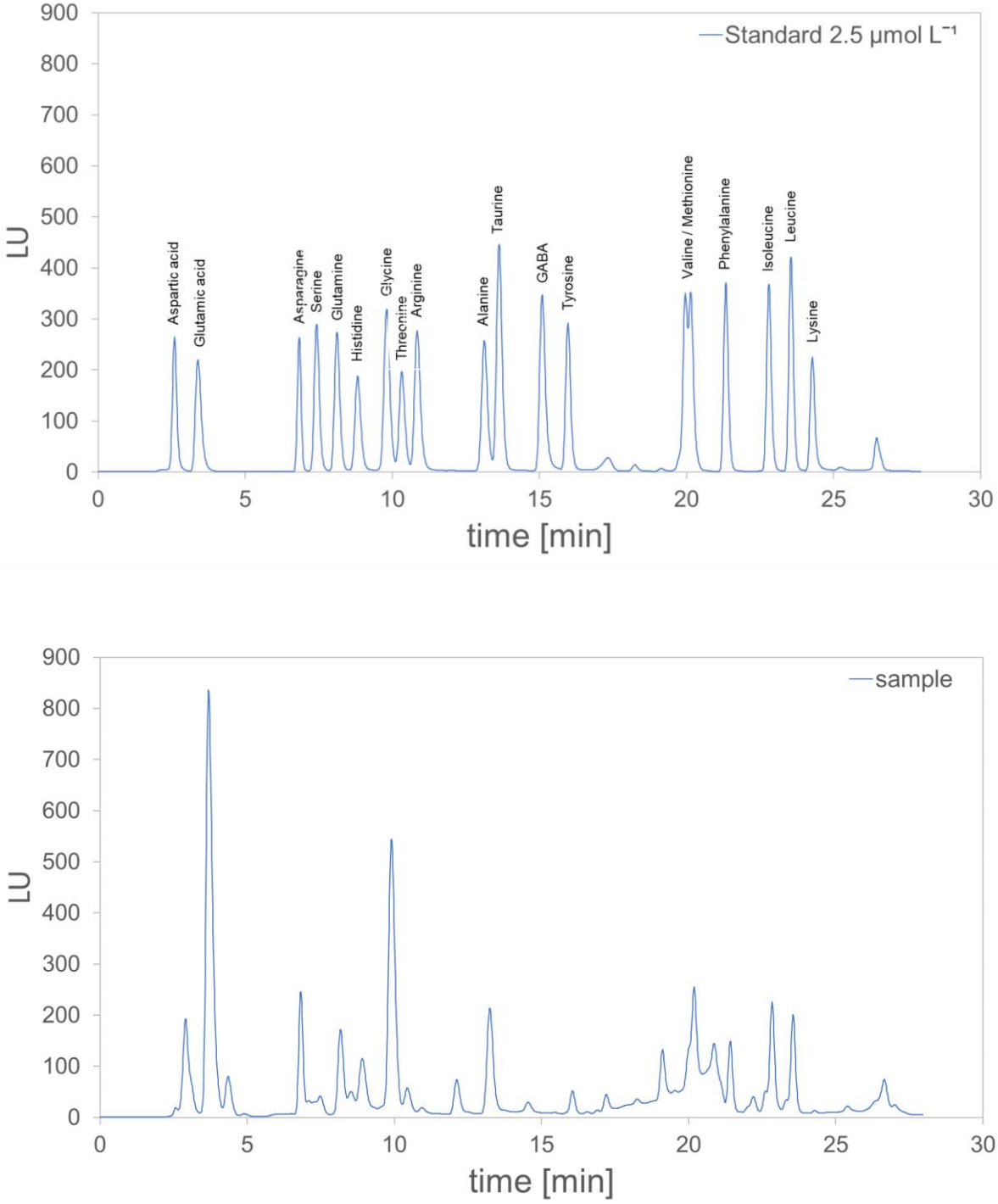

Figure S2: HPLC-Chromatograms of a 5 µmol/L standard (AAS18, Sigma Aldrich) in Milli-Q water compared with a sample (dilution 1:4, in Milli-Q water) analysed by the new method presented in this thesis. Injection volume 100 µL, gain factor 10, method duration 90 min. Figure from Taubner and Baumann et al. (2019).

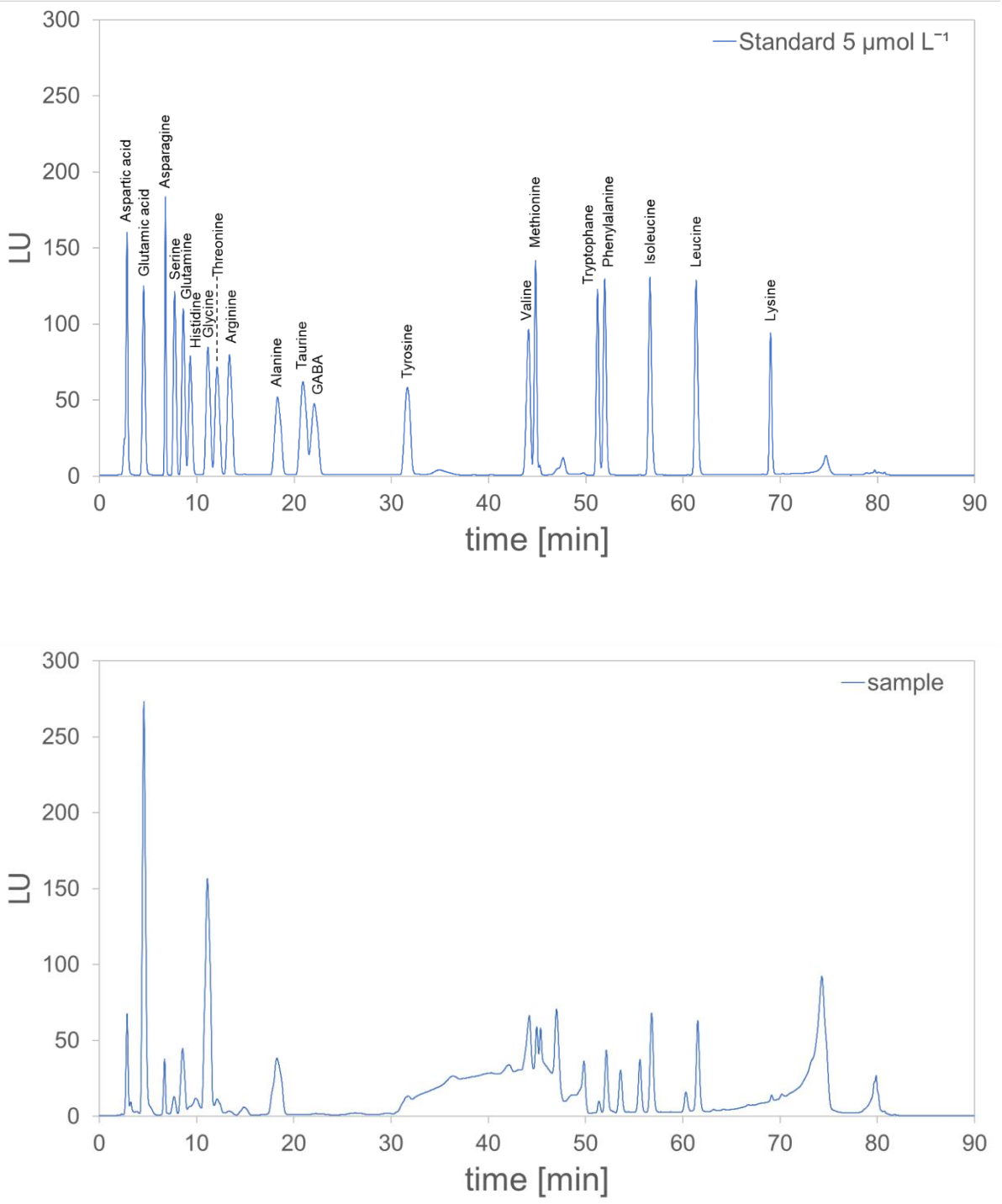

Figure S3: MS/MS spectra of (a) the first isomer of GMGT-0, $[M+H]^+$ at m/z 1300.2; and (b) the second isomer of GMGT-0, $[M+H]^+$ at m/z 1300.0; in a total lipid extract of *M. okinawensis*. Figure from Baumann and Taubner et al. (2018).

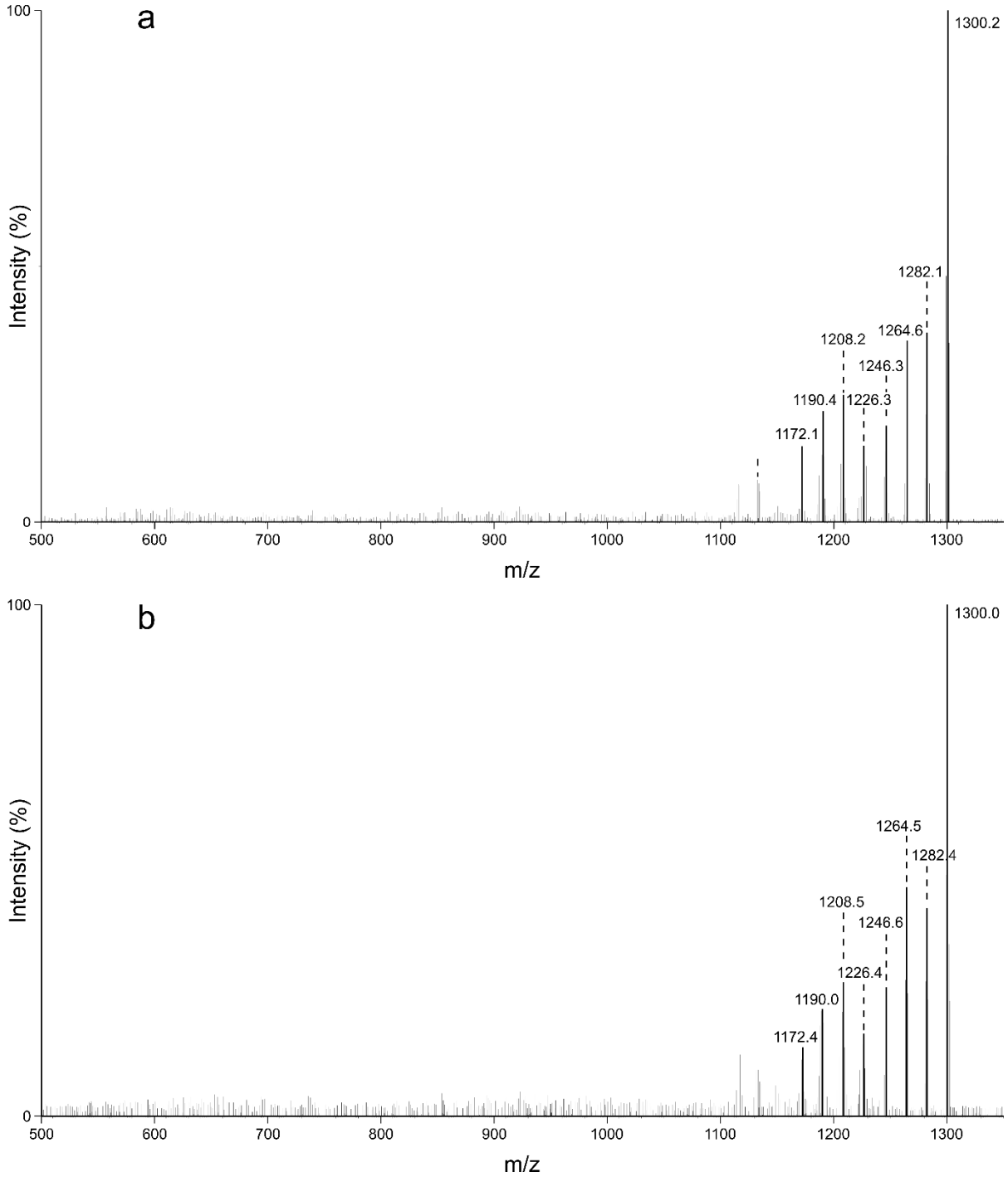

Table S2: Comparison of diether lipid contents of *M. villosus* and *M. okinawensis* in nanogram per milligram dry weight of biomass (ng/mg dw) and as ratios measured with GC-FID and with HPLC-APCI-MS. Table from Baumann and Taubner et al. (2018).

		Methanocaldococcus villosus			***Methanothermococcus okinawensis***		
		Vil-1	**Vil-2**	**Vil-3**	**Oki-1**	**Oki-2**	**Oki-3**
GC-FID:		[ng/mg dw]	[ng/mg dw]	[ng/mg dw]	[ng/mg dw]	[ng/mg dw]	[ng/mg dw]
	Archaeol	1158.7	2115.6	1425.2	945.8	1733.6	719.8
	Macrocyclic archaeol	2503.3	2577.9	2081.6	474.5	925.7	574.4
HPLC-APCI-MS:		[ng/mg dw]	[ng/mg dw]	[ng/mg dw]	[ng/mg dw]	[ng/mg dw]	[ng/mg dw]
	Archaeol	1045.7	1674.9	1120.6	711.5	1589.2	588.5
	Macrocyclic archaeol	1772.7	1958.4	1597.4	333.8	917.1	460.6
Ratio GC-FID / HPLC-APCI-MS		[ratio]	[ratio]	[ratio]	[ratio]	[ratio]	[ratio]
	Archaeol	1.11	1.26	1.27	1.33	1.09	1.22
	Macrocyclic archaeol	1.41	1.32	1.30	1.42	1.01	1.25

Table S3: Mean values of the OD_{max}, the turnover rate max, and of each lipid in % of total lipids of all samples of one experiment. For the OD_{max} and the turnover rate max triplicates (n = 3) were used except for "F" (n = 2). Further, for the lipid analysis, one datapoint of each setting "E", "J", and "N" had to be excluded (n = 2). Values of extreme value setting are mean values of four samples (n = 4). "Min" (all amounts at minimum); "Me" (high CH_3OH); "Am" (high in NH_4Cl); and "Fo" (high in H_2CO). Table modified from Taubner and Baumann et al. (2019).

DoE setting

	K	E	B	F	A	I	G	C	M	N	O	J	D	L	H
OD_{max}	1.71	1.62	1.53	1.52	1.51	1.27	1.17	1.16	1.13	1.11	1.10	0.59	0.21	0.20	0.20
Turnover rate max [h^{-1}]	0.096	0.096	0.096	0.095	0.096	0.098	0.098	0.098	0.096	0.097	0.093	0.086	0.031	0.028	0.029
Archaeol	64.5%	68.3%	63.8%	64.4%	63.0%	63.4%	75.4%	72.6%	71.0%	68.7%	72.9%	71.0%	69.1%	74.0%	68.6%
Macr. Ar.	29.7%	25.7%	30.2%	28.8%	29.2%	30.3%	19.3%	19.7%	21.4%	25.1%	18.0%	23.7%	23.5%	18.1%	23.3%
GTGT-0a	0.2%	0.3%	0.3%	0.3%	0.4%	0.3%	0.5%	0.7%	0.4%	0.5%	0.6%	0.4%	0.4%	0.8%	0.4%
GDGT-0a	3.9%	4.2%	4.1%	4.7%	5.1%	3.7%	3.5%	5.2%	4.7%	3.6%	5.6%	2.7%	4.8%	4.6%	4.5%
GMGT-0a	1.1%	1.1%	1.1%	1.2%	1.7%	1.6%	0.8%	1.2%	1.8%	1.5%	2.0%	1.6%	1.6%	1.8%	2.2%
GMGT-0a'	0.5%	0.5%	0.4%	0.5%	0.7%	0.8%	0.4%	0.6%	0.7%	0.6%	0.8%	0.7%	0.6%	0.6%	0.9%

Extreme value setting

	Min	Me	Am	Fo
OD_{max}	1.10	1.08	0.52	0.22
Turnover rate max [h^{-1}]	0.094	0.088	0.081	0.051
Archaeol	33.4%	33.5%	41.6%	73.5%
Macr. Ar.	42.3%	44.9%	43.0%	15.5%
GTGT-0a	0.3%	0.3%	0.4%	1.1%
GDGT-0a	12.6%	9.7%	7.8%	6.9%
GMGT-0a	7.6%	7.7%	4.8%	2.1%
GMGT-0a'	3.8%	4.0%	2.5%	0.8%

Figure S4: Average growth curves of the extreme value experiments (n = 4, the OD of the respective zero control was subtracted, error bars present respective standard deviations). “Min” (all amounts at minimum); “Me” (high CH_3OH); “Am” (high in NH_4Cl); and “Fo” (high in H_2CO). Figure from Taubner and Baumann et al. (2019).

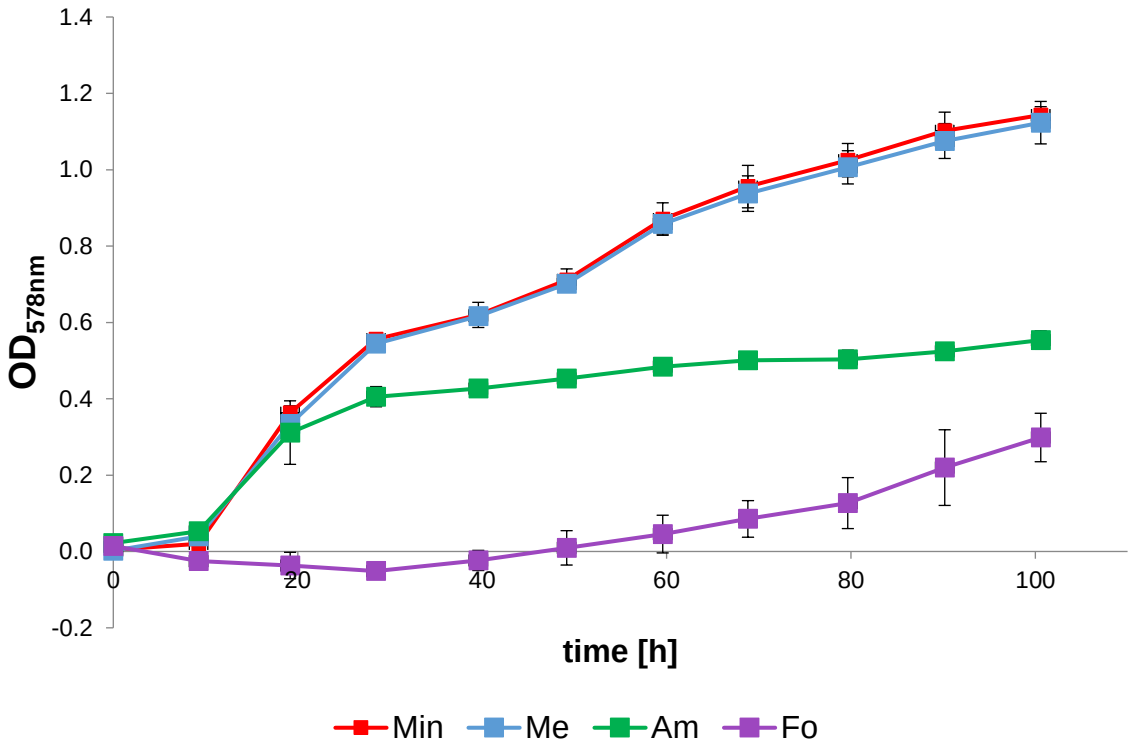

Figure S5: Concentrations of the different amino acids for the extreme value experiments (n = 4, error bars present respective standard deviations). “Min” (all amounts at minimum); “Me” (high CH_3OH); “Am” (high in NH_4Cl); and “Fo” (high in H_2CO). The high error of Gln for the “Fo”-setting is caused by a wide spreading of the data points between 4 and 46 µM. However, even the error is high, all single samples of the “Fo”-set showed a value far higher in Gln than in any other sample. Abbreviations of amino acids: Asp = aspartic acid; Glu = glutamic acid; Asn = asparagine; Ser = serine; Gln = glutamine; His = histidine; Gly = glycine; Thr = threonine; Arg = arginine; Ala = alanine; Tyr = tyrosine; Val = valine; Met = methionine; Trp = tryptophan; Phe = phenylalanine; Ile = isoleucine; Leu = leucine; Lys = lysine. Figure from Taubner and Baumann et al. (2019).

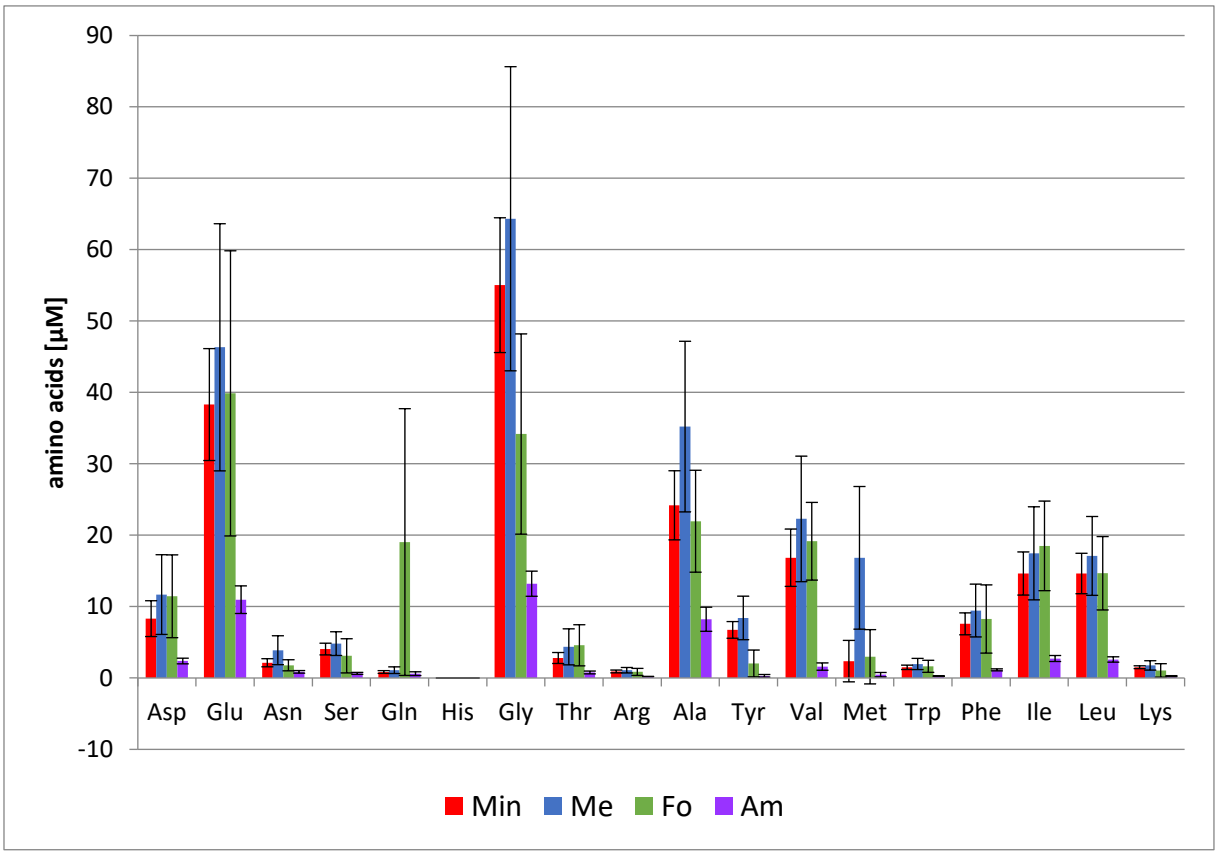

Methanothermobacter marburgensis

Table S4: Contents of core ether lipids in *Methanothermobacter marburgensis* in nanogram per milligram dry weight of biomass (ng/mg dw) and in % of total lipids at 65°C with and without carbonate in the liquid medium (Without carbonate: n = 23; With carbonate: n = 21). GTGT (glycerol trialkyl glycerol tetraether), GDGT (glycerol dialkyl glycerol tetraether), GMGT (glycerol monoalkyl glycerol tetraether), GDD (glycerol dialkyl diether), and GMD (glycerol monoalkyl diether).

	Carbonate in liquid medium – Mean values					
	Concentrations [ng/mg dw]		**Relative amounts [%]**		**Overall mean values**	
Carbonate	**Without**	**With**	**Without**	**With**	**ng/mg dw**	**%**
Archaeol	2281.4	2133.8	54.5%	52.4%	2076.3	52.6%
GTGT-0a	20.1	21.4	0.48%	0.52%	19.3	0.5%
GDGT-0a	1043.3	882.4	24.9%	21.7%	889.1	22.5%
GDGT-0b	543.3	678.5	13.0%	16.7%	593.3	15.0%
GDGT-0c	9.6	20.3	0.2%	0.5%	17.9	0.5%
GMGT-0a	1.7	1.5	0.041%	0.037%	1.8	0.05%
GMGT-0a‘	74.8	65.9	1.8%	1.6%	70.8	1.8%
GMGT-0b	0.1	0.7	<0.01%	0.018%	0.6	0.02%
GMGT-0b‘	174.6	180.5	4.2%	4.4%	202.4	5.1%
GMGT-0c	0.0	0.0	0.0%	0.0%	0.0	0.0%
GMGT-0c‘	35.3	85.1	0.8%	2.1%	76.1	1.9%
GDD-0a	1.5	0.9	0.035%	0.023%	1.1	0.03%
GDD-0b	0.8	0.7	0.019%	0.018%	0.7	0.02%
GMD-0a	0.0	0.0	0.0%	0.0%	0.0	0.0%
GMD-0a‘	0.02	0.0	<0.01%	0.0%	0.01	<0.01%
GMD-0b	0.0	0.0	0.0%	0.0%	0.0	0.0%
GMD-0b‘	0.1	0.1	<0.01%	<0.01%	0.1	<0.01%
Diethers	2283.8	2135.5	54.6%	52.4%	2078.2	52.6%
Tetraethers	1902.8	1936.3	45.4%	47.6%	1871.3	47.4%
Sum	4186.6	4071.8	100.0%	100.0%	3949.5	100.0%

Table S5: Contents of core ether lipids in *Methanothermobacter marburgensis* in nanogram per milligram dry weight of biomass (ng/mg dw) and in % of total lipids at three different temperatures (50°C: n = 7; 60°C: n = 8; 65°C: n = 8). GTGT (glycerol trialkyl glycerol tetraether), GDGT (glycerol dialkyl glycerol tetraether), GMGT (glycerol monoalkyl glycerol tetraether), GDD (glycerol dialkyl diether), and GMD (glycerol monoalkyl diether).

	Temperature; 50 mL with carbonate					
	Concentrations [ng/mg dw]			**Relative amounts [%]**		
	50°C	**60°C**	**65°C**	**50°C**	**60°C**	**65°C**
Archaeol	2323.3	1041.7	2040.7	56.1%	38.9%	61.9%
GTGT-0a	25.6	4.6	14.2	0.6%	0.2%	0.4%
GDGT-0a	921.1	414.6	600.6	22.2%	15.5%	18.2%
GDGT-0b	720.6	360.7	437.4	17.4%	13.5%	13.3%
GDGT-0c	19.3	34.4	11.2	0.5%	1.3%	0.3%
GMGT-0a	0.4	4.5	1.0	0.01%	0.17%	0.03%
GMGT-0a‘	30.4	114.2	43.8	0.7%	4.3%	1.3%
GMGT-0b	0.0	2.7	0.6	0.0%	0.1%	0.02%
GMGT-0b‘	77.2	476.6	104.2	1.9%	17.8%	3.2%
GMGT-0c	0.0	0.0	0.0	0.0%	0.0%	0.0%
GMGT-0c‘	21.9	225.5	41.1	0.5%	8.4%	1.2%
GDD-0a	1.1	0.2	0.0	0.03%	<0.01%	0.0%
GDD-0b	0.8	0.0	0.0	0.02%	0.0%	0.0%
GMD-0a	0.0	0.0	0.0	0.0%	0.0%	0.0%
GMD-0a‘	0.0	0.0	0.0	0.0%	0.0%	0.0%
GMD-0b	0.0	0.0	0.0	0.0%	0.0%	0.0%
GMD-0b‘	0.0	0.1	0.0	0.0%	<0.01%	0.0%
Diethers	2325.2	1042.0	2040.7	56.2%	38.9%	61.9%
Tetraethers	1816.5	1637.8	1254.1	43.8%	61.1%	38.1%
Sum	4141.7	2679.8	3294.8	100.0%	100.0%	100.0%

Table S6: Contents of core ether lipids in *Methanothermobacter marburgensis* in nanogram per milligram dry weight of biomass (ng/mg dw) and in % of total lipids at three different volumes of liquid medium (25 mL: n = 12; 50 mL: n = 16; 75 mL: n = 16). GTGT (glycerol trialkyl glycerol tetraether), GDGT (glycerol dialkyl glycerol tetraether), GMGT (glycerol monoalkyl glycerol tetraether), GDD (glycerol dialkyl diether), and GMD (glycerol monoalkyl diether).

	Volume of liquid medium – Mean values					
	Concentrations [ng/mg dw]			**Relative amounts [%]**		
	25 mL	**50 mL**	**75 mL**	**25 mL**	**50 mL**	**75 mL**
Archaeol	2612.5	2090.9	1919.3	53.5%	59.8%	47.8%
GTGT-0a	26.0	16.0	20.2	0.53%	0.46%	0.50%
GDGT-0a	1143.7	738.8	1005.9	23.4%	21.1%	25.1%
GDGT-0b	684.7	437.0	710.9	14.0%	12.5%	17.7%
GDGT-0c	20.3	9.0	15.4	0.42%	0.26%	0.38%
GMGT-0a	1.8	1.3	1.8	0.037%	0.036%	0.046%
GMGT-0a‘	76.3	52.4	82.4	1.6%	1.5%	2.1%
GMGT-0b	0.4	0.3	0.5	<0.01%	<0.01%	0.012%
GMGT-0b‘	225.3	114.8	192.5	4.6%	3.3%	4.8%
GMGT-0c	0.0	0.0	0.0	0.0%	0.0%	0.0%
GMGT-0c‘	88.1	32.6	60.0	1.8%	0.9%	1.5%
GDD-0a	1.4	0.6	1.6	0.03%	0.02%	0.04%
GDD-0b	0.9	0.3	1.1	0.02%	0.01%	0.03%
GMD-0a	0.0	0.0	0.0	0.0%	0.0%	0.0%
GMD-0a‘	0.0	0.0	0.0	0.0%	<0.01%	0.0%
GMD-0b	0.0	0.0	0.0	0.0%	0.0%	0.0%
GMD-0b‘	0.1	0.0	0.1	<0.01%	<0.01%	<0.01%
Diethers	2614.9	2091.8	1922.1	53.6%	59.9%	47.9%
Tetraethers	2266.6	1402.2	2089.6	46.4%	40.1%	52.1%
Sum	4881.5	3494.0	4011.7	100.0%	100.0%	100.0%

Methanocaldococcus villosus

Table S7: Contents of core ether lipids in *Methanocaldococcus villosus* in nanogram per milligram dry weight of biomass (ng/mg dw) and in % of total lipids at three different volumes of liquid medium (reliable results only: 25 mL: n = 13; 50 mL: n = 14; 75 mL: n = 14; all results: 25 mL: n = 29; 50 mL: n = 28; 75 mL: n = 30). "Macr. arch." = macrocyclic archaeol; GTGT (glycerol trialkyl glycerol tetraether), GDGT (glycerol dialkyl glycerol tetraether), GMGT (glycerol monoalkyl glycerol tetraether), GDD (glycerol dialkyl diether), and GMD (glycerol monoalkyl diether).

	Volume of liquid medium – Mean values of all samples							
	ng/mg dw (reliable concentrations only)			**% (all results)**			**Overall mean values**	
	25 mL	**50 mL**	**75 mL**	**25 mL**	**50 mL**	**75 mL**	**ng/mg dw**	**% (all results)**
Archaeol	1400.8	1590.3	1503.8	44.2%	36.6%	37.6%	1498.3	39.5%
Macr. arch.	1281.5	1952.4	1653.4	47.5%	57.2%	54.7%	1629.1	53.1%
GTGT-0a	17.9	18.4	18.6	0.6%	0.4%	0.5%	18.3	0.5%
GDGT-0a	173.9	204.2	220.7	6.3%	4.7%	5.9%	199.6	5.6%
GMGT-0a	3.2	4.0	3.3	0.1%	0.1%	0.1%	3.5	0.1%
GMGT-0a'	38.6	37.7	38.1	1.2%	1.0%	1.1%	38.1	1.1%
GDD-0a	0.0	0.2	1.4	<0.01%	<0.01%	0.04%	0.6	0.02%
GMD-0a	0.0	0.0	0.0	0.0%	<0.01%	0.0%	0.0	<0.01%
GMD-0a'	0.0	0.0	0.3	<0.01%	<0.01%	<0.01%	0.1	<0.01%
Diethers	2682.3	3542.9	3158.9	91.7%	93.8%	92.3%	3128.1	92.6%
Tetraethers	233.6	264.3	280.7	8.3%	6.2%	7.7%	259.5	7.4%
Sum	2915.9	3807.2	3439.6	100.0%	100.0%	100.0%	3387.6	100.0%

Table S8: Contents of core ether lipids in *Methanocaldococcus villosus* in % of total lipids at two temperatures and three different volumes of liquid medium (65°C: 25 mL: n = 15; 50 mL: n = 15; 75 mL: n = 15; 80°C: 25 mL: n = 14; 50 mL: n = 13; 75 mL: n = 15). "Macr. arch." = macrocyclic archaeol, GTGT (glycerol trialkyl glycerol tetraether), GDGT (glycerol dialkyl glycerol tetraether), GMGT (glycerol monoalkyl glycerol tetraether), GDD (glycerol dialkyl diether), and GMD (glycerol monoalkyl diether).

	Temperature – Mean values of all samples							
	65°C			**80°C**			**Overall mean values**	
	25 mL	**50 mL**	**75 mL**	**25 mL**	**50 mL**	**75 mL**	**65°C**	**80°C**
Archaeol	54.3%	36.3%	43.2%	34.2%	37.0%	32.0%	44.6%	34.4%
Macr. arch.	36.0%	56.5%	50.8%	59.0%	57.8%	58.6%	47.8%	58.5%
GTGT-0a	1.0%	0.5%	0.5%	0.3%	0.3%	0.5%	0.7%	0.3%
GDGT-0a	7.8%	5.4%	4.6%	4.8%	4.0%	7.2%	5.9%	5.3%
GMGT-0a	0.1%	0.1%	0.1%	0.1%	0.1%	0.1%	0.1%	0.1%
GMGT-0a'	0.9%	1.1%	0.8%	1.5%	0.9%	1.5%	0.9%	1.3%
GDD-0a	<0.01%	<0.01%	0.02%	<0.01%	0.01%	0.05%	<0.01%	0.02%
GMD-0a	0.0%	0.0%	0.0%	0.0%	<0.01%	0.0%	0.0%	<0.01%
GMD-0a'	0.0%	<0.01%	<0.01%	<0.01%	<0.01%	0.02%	<0.01%	<0.01%
Diethers	90.3%	92.8%	94.0%	93.2%	94.8%	90.7%	92.4%	92.9%
Tetraethers	9.7%	7.2%	6.0%	6.8%	5.2%	9.3%	7.6%	7.1%
Sum	100.0%	100.0%	100.0%	100.0%	100.0%	100.0%	100.0%	100.0%

Table S9: Contents of core ether lipids in *Methanocaldococcus villosus* in % of total lipids at a gas exchange once or twice per day and at three different volumes of liquid medium (1x: 25 mL: n = 15; 50 mL: n = 13; 75 mL: n = 15; 2x: 25 mL: n = 14; 50 mL: n = 15; 75 mL: n = 15). "Macr. arch." = macrocyclic archaeol, GTGT (glycerol trialkyl glycerol tetraether), GDGT (glycerol dialkyl glycerol tetraether), GMGT (glycerol monoalkyl glycerol tetraether), GDD (glycerol dialkyl diether), and GMD (glycerol monoalkyl diether).

	Gassing frequency – Mean values of all samples							
	1x daily gas exchange			**2x daily gas exchange**			**Overall mean values**	
	25 mL	**50 mL**	**75 mL**	**25 mL**	**50 mL**	**75 mL**	**1x**	**2x**
Archaeol	41.7%	40.3%	42.6%	46.7%	32.9%	32.6%	41.5%	37.4%
Macr. arch.	50.4%	53.5%	51.3%	44.7%	60.8%	58.1%	51.7%	54.5%
GTGT-0a	0.6%	0.4%	0.4%	0.7%	0.3%	0.5%	0.5%	0.5%
GDGT-0a	6.1%	4.7%	4.7%	6.5%	4.7%	7.1%	5.2%	6.1%
GMGT-0a	0.1%	0.1%	0.1%	0.1%	0.1%	0.2%	0.1%	0.1%
GMGT-0a'	1.1%	0.9%	0.9%	1.3%	1.1%	1.5%	0.9%	1.3%
GDD-0a	<0.01%	<0.01%	0.02%	<0.01%	0.01%	0.06%	<0.01%	0.02%
GMD-0a	0.0%	0.0%	0.0%	0.0%	<0.01%	0.0%	0.0%	<0.01%
GMD-0a'	<0.01%	<0.01%	<0.01%	<0.01%	<0.01%	0.02%	<0.01%	<0.01%
Diethers	92.1%	93.9%	93.9%	91.4%	93.8%	90.8%	93.3%	92.0%
Tetraethers	7.9%	6.1%	6.1%	8.6%	6.2%	9.2%	6.7%	8.0%
Sum	100.0%	100.0%	100.0%	100.0%	100.0%	100.0%	100.0%	100.0%

Table S10: Contents of core ether lipids in *Methanocaldococcus villosus* in % of total lipids without (Non-OD) and with optical density measurements (OD), at three different volumes of liquid medium (Non-OD: 25 mL: n = 15; 50 mL: n = 13; 75 mL: n = 15; OD: 25 mL: n = 14; 50 mL: n = 15; 75 mL: n = 15). "Macr. arch." = macrocyclic archaeol, GTGT (glycerol trialkyl glycerol tetraether), GDGT (glycerol dialkyl glycerol tetraether), GMGT (glycerol monoalkyl glycerol tetraether), GDD (glycerol dialkyl diether), and GMD (glycerol monoalkyl diether).

	OD measurements – Mean values of all samples							
	Non-OD			**OD**			**Overall mean values**	
	25 mL	**50 mL**	**75 mL**	**25 mL**	**50 mL**	**75 mL**	**Non-OD**	**OD**
Archaeol	41.0%	40.0%	38.9%	47.4%	33.3%	36.3%	40.0%	39.0%
Macr. arch.	51.2%	54.3%	54.2%	43.8%	60.1%	55.2%	53.2%	53.0%
GTGT-0a	0.5%	0.4%	0.4%	0.7%	0.4%	0.5%	0.4%	0.6%
GDGT-0a	5.7%	4.4%	5.3%	6.9%	5.0%	6.5%	5.1%	6.2%
GMGT-0a	0.1%	0.1%	0.1%	0.1%	0.1%	0.1%	0.1%	0.1%
GMGT-0a'	1.4%	0.9%	1.1%	1.0%	1.1%	1.3%	1.1%	1.1%
GDD-0a	<0.01%	0.01%	0.05%	0.0%	<0.01%	0.03%	0.02%	0.01%
GMD-0a	0.0%	0.0%	0.0%	0.0%	<0.01%	0.0%	0.0%	<0.01%
GMD-0a'	<0.01%	<0.01%	0.01%	0.0%	<0.01%	<0.01%	<0.01%	<0.01%
Diethers	92.2%	94.3%	93.2%	91.2%	93.4%	91.5%	93.2%	92.0%
Tetraethers	7.8%	5.7%	6.8%	8.8%	6.6%	8.5%	6.8%	8.0%
Sum	100.0%	100.0%	100.0%	100.0%	100.0%	100.0%	100.0%	100.0%

Methanothermococcus okinawensis

Table S11: Contents of core ether lipids in *Methanothermococcus okinawensis* in nanogram per milligram dry weight of biomass (ng/mg dw) and in % of total lipids of all samples cultured at 50 mL gas exchange once per day at four different temperatures (50°C: n = 8; 60°C: n = 8; 65°C: n = 8; 70°C: n = 8). "Macr. arch." = macrocyclic archaeol, GTGT (glycerol trialkyl glycerol tetraether), GDGT (glycerol dialkyl glycerol tetraether), GMGT (glycerol monoalkyl glycerol tetraether), GDD (glycerol dialkyl diether), and GMD (glycerol monoalkyl diether).

	50 mL; 1x daily gas exchange; different temperatures							
	Concentration [ng/mg dw]				**Relative amount [%]**			
	50°C	**60°C**	**65°C**	**70°C**	**50°C**	**60°C**	**65°C**	**70°C**
Archaeol	1461.1	632.0	773.1	697.2	75.9%	25.5%	62.1%	55.6%
Macr. arch.	391.5	1570.9	374.7	356.4	20.3%	63.3%	30.1%	28.4%
GTGT-0a	6.8	3.7	4.1	2.4	0.4%	0.1%	0.3%	0.2%
GDGT-0a	58.2	93.0	71.0	76.3	3.0%	3.8%	5.7%	6.1%
GMGT-0a	5.6	116.3	13.7	75.7	0.3%	4.7%	1.1%	6.0%
GMGT-0a'	1.5	51.9	6.2	43.2	0.1%	2.1%	0.5%	3.4%
GDD-0a	0.1	9.8	1.3	2.2	0.0%	0.4%	0.1%	0.2%
GMD-0a	0.0	2.2	0.0	1.0	0.0%	0.09%	0.0%	0.08%
GMD-0a'	0.0	0.0	0.0	0.0	0.0%	0.0%	0.0%	0.0%
Diethers	1852.7	2214.9	1149.1	1056.8	96.2%	89.3%	92.3%	84.3%
Tetraethers	72.1	264.9	95.0	197.6	3.8%	10.7%	7.6%	15.7%
Sum	1924.8	2479.8	1244.1	1254.4	100.0%	100.0%	100.0%	100.0%

Table S12: Contents of core ether lipids in *Methanothermococcus okinawensis* in nanogram per milligram dry weight of biomass (ng/mg dw) and in % of total lipids of all samples cultured at 65°C at three different volumes of liquid medium (25 mL: n = 16; 50 mL: n = 16; 75 mL: n = 16). "Macr. arch." = macrocyclic archaeol, GTGT (glycerol trialkyl glycerol tetraether), GDGT (glycerol dialkyl glycerol tetraether), GMGT (glycerol monoalkyl glycerol tetraether), GDD (glycerol dialkyl diether), and GMD (glycerol monoalkyl diether).

	65°C; different volumes of liquid medium					
	Concentration [ng/mg dw]			**Relative amount [%]**		
	25 mL	**50 mL**	**75 mL**	**25 mL**	**50 mL**	**75 mL**
Archaeol	889.0	764.9	638.4	70.5%	55.8%	46.8%
Macr. arch.	274.4	477.4	582.6	21.8%	34.8%	42.7%
GTGT-0a	4.3	4.2	3.3	0.34%	0.31%	0.25%
GDGT-0a	75.6	92.3	90.7	6.0%	6.7%	6.6%
GMGT-0a	12.1	21.3	32.8	1.0%	1.6%	2.4%
GMGT-0a'	4.8	8.5	13.8	0.4%	0.6%	1.0%
GDD-0a	0.2	1.7	3.1	0.0%	0.1%	0.2%
GMD-0a	0.0	0.0	0.5	<0.01%	<0.01%	0.04%
GMD-0a'	0.0	0.0	0.0	0.0%	0.0%	<0.01%
Diethers	1163.6	1244.0	1224.6	92.3%	90.8%	89.7%
Tetraethers	96.8	126.3	140.6	7.7%	9.2%	10.3%
Sum	1260.4	1370.3	1365.2	100.0%	100.0%	100.0%

Table S13: Contents of core ether lipids in *Methanothermococcus okinawensis* in nanogram per milligram dry weight of biomass (ng/mg dw) and in % of total lipids of all samples cultured at 65°C at three different volumes of liquid medium without (Non-OD) and with (OD) optical density measurements (Non-OD: 25 mL: n = 8; 50 mL: n = 8; 75 mL: n = 8; OD: 25 mL: n = 8; 50 mL: n = 8; 75 mL: n = 8). "Macr. arch." = macrocyclic archaeol, GTGT (glycerol trialkyl glycerol tetraether), GDGT (glycerol dialkyl glycerol tetraether), GMGT (glycerol monoalkyl glycerol tetraether), GDD (glycerol dialkyl diether), and GMD (glycerol monoalkyl diether).

	65°C; Non-OD vs. OD; different volumes of liquid medium											
	Concentration [ng/mg dw]						**Relative amount [%]**					
	Non-OD			**OD**			**Non-OD**			**OD**		
	25 mL	**50 mL**	**75 mL**	**25 mL**	**50 mL**	**75 mL**	**25 mL**	**50 mL**	**75 mL**	**25 mL**	**50 mL**	**75 mL**
Archaeol	943.8	669.2	561.0	834.2	860.6	715.8	71.6%	57.8%	42.1%	69.4%	54.3%	51.2%
Macr. arch.	282.2	387.5	611.9	266.7	567.3	553.2	21.4%	33.5%	45.9%	22.2%	35.8%	39.6%
GTGT-0a	4.3	3.5	3.3	4.3	4.9	3.3	0.3%	0.3%	0.3%	0.4%	0.3%	0.2%
GDGT-0a	71.7	72.2	99.0	79.4	112.3	82.4	5.4%	6.2%	7.4%	6.6%	7.1%	5.9%
GMGT-0a	11.9	16.1	37.0	12.2	26.5	28.6	0.9%	1.4%	2.8%	1.0%	1.7%	2.0%
GMGT-0a'	4.8	7.0	16.7	4.7	10.0	10.9	0.4%	0.6%	1.3%	0.4%	0.6%	0.8%
GDD-0a	0.0	1.5	3.4	0.5	1.9	2.9	0.0%	0.1%	0.3%	0.04%	0.1%	0.2%
GMD-0a	0.0	0.0	0.6	0.1	0.1	0.3	0.0%	0.0%	0.05%	<0.01%	<0.01%	0.02%
GMD-0a'	0.0	0.0	0.1	0.0	0.0	0.0	0.0%	0.0%	<0.01%	0.0%	0.0%	0.0%
Diethers	1226.0	1058.2	1177.0	1101.5	1429.9	1272.2	93.0%	91.5%	88.3%	91.6%	90.3%	91.0%
Tetraethers	92.7	98.8	156.0	100.6	153.7	125.2	7.0%	8.5%	11.7%	8.4%	9.7%	9.0%
Sum	1318.7	1157.0	1333.0	1202.1	1583.6	1397.4	100.0%	100.0%	100.0%	100.0%	100.0%	100.0%

Table S14: Contents of core ether lipids in *Methanothermococcus okinawensis* in nanogram per milligram dry weight of biomass (ng/mg dw) and in % of total lipids of all samples cultured at 65°C at three different volumes of liquid medium at a gas exchange once or twice per day (1x: 25 mL: n = 8; 50 mL: n = 8; 75 mL: n = 8; 2x: 25 mL: n = 8; 50 mL: n = 8; 75 mL: n = 8). "Macr. arch." = macrocyclic archaeol, GTGT (glycerol trialkyl glycerol tetraether), GDGT (glycerol dialkyl glycerol tetraether), GMGT (glycerol monoalkyl glycerol tetraether), GDD (glycerol dialkyl diether), and GMD (glycerol monoalkyl diether).

	65°C; 1x vs. 2x daily gas exchange; different volumes of liquid medium											
	Concentration [ng/mg dw]						**Relative amount [%]**					
	1x daily			**2x daily**			**1x daily**			**2x daily**		
	25 mL	**50 mL**	**75 mL**	**25 mL**	**50 mL**	**75 mL**	**25 mL**	**50 mL**	**75 mL**	**25 mL**	**50 mL**	**75 mL**
Archaeol	939.9	773.1	542.0	838.1	756.7	734.8	71.4%	62.1%	41.7%	69.6%	50.6%	51.4%
Macr. arch.	266.1	374.7	609.8	282.7	580.1	555.3	20.2%	30.1%	46.9%	23.5%	38.8%	38.8%
GTGT-0a	5.2	4.1	2.9	3.3	4.4	3.8	0.4%	0.3%	0.2%	0.3%	0.3%	0.3%
GDGT-0a	87.9	71.0	85.7	63.3	113.5	95.7	6.7%	5.7%	6.6%	5.3%	7.6%	6.7%
GMGT-0a	12.6	13.7	38.4	11.5	28.8	27.2	1.0%	1.1%	3.0%	1.0%	1.9%	1.9%
GMGT-0a'	5.0	6.2	16.2	4.5	10.8	11.4	0.4%	0.5%	1.2%	0.4%	0.7%	0.8%
GDD-0a	0.4	1.3	4.1	0.1	2.0	2.2	0.03%	0.11%	0.31%	0.01%	0.14%	0.15%
GMD-0a	0.0	0.0	0.7	0.1	0.1	0.2	0.0%	0.0%	0.06%	<0.01%	<0.01%	0.02%
GMD-0a'	0.0	0.0	0.1	0.0	0.0	0.0	0.0%	0.0%	<0.01%	0.0%	0.0%	0.0%
Diethers	1206.4	1149.1	1156.7	1121.0	1338.9	1292.5	91.6%	92.4%	89.0%	93.1%	89.5%	90.3%
Tetraethers	110.7	95.0	143.2	82.6	157.5	138.1	8.4%	7.6%	11.0%	6.9%	10.5%	9.7%
Sum	1317.1	1244.1	1299.9	1203.6	1496.4	1430.6	100.0%	100.0%	100.0%	100.0%	100.0%	100.0%

Table S15: Contents of core ether lipids in *Methanothermococcus okinawensis* in nanogram per milligram dry weight of biomass (ng/mg dw) and in % of total lipids of all samples cultured at 65°C at a gas exchange once or twice per day (1x: n = 24; 2x: n = 24). "Macr. arch." = macrocyclic archaeol, GTGT (glycerol trialkyl glycerol tetraether), GDGT (glycerol dialkyl glycerol tetraether), GMGT (glycerol monoalkyl glycerol tetraether), GDD (glycerol dialkyl diether), and GMD (glycerol monoalkyl diether).

	65°C; 1x vs. 2x daily gas exchange			
	Concentration [ng/mg dw]		**Relative amount [%]**	
	1x daily	**2x daily**	**1x daily**	**2x daily**
Archaeol	751.6	776.5	58.4%	56.4%
Macr. arch.	416.9	472.7	32.4%	34.3%
GTGT-0a	4.1	3.8	0,32%	0.28%
GDGT-0a	81.5	90.8	6.3%	6.6%
GMGT-0a	21.6	22.5	1.7%	1.6%
GMGT-0a'	9.1	8.9	0.7%	0.6%
GDD-0a	1.9	1.4	0.2%	0.1%
GMD-0a	0.2	0.1	0.02%	<0.01%
GMD-0a'	0.0	0.0	<0.01%	0.0%
Diethers	1170.6	1250.7	91.0%	90.8%
Tetraethers	116.3	126.0	9.0%	9.2%
Sum	1286.9	1376.7	100.0%	100.0%

9. Versicherung an Eides statt – Affirmation on oath

Hiermit versichere ich an Eides statt, dass ich die vorliegende Dissertation mit dem Titel:

„Membrane lipids of the (hyper)thermophilic, methanogenic archaea *Methanothermobacter marburgensis, Methanocaldococcus villosus* and *Methanothermococcus okinawensis* and their geobiological and astrobiological relevance“

selbstständig verfasst und keine anderen als die angegebenen Hilfsmittel – insbesondere keine im Quellenverzeichnis nicht benannten Internet-Quellen – benutzt habe. Alle Stellen, die wörtlich oder sinngemäß aus Veröffentlichungen entnommen wurden, sind als solche kenntlich gemacht. Ich versichere weiterhin, dass ich die Dissertation oder Teile davon vorher weder im In- noch im Ausland in einem anderen Prüfungsverfahren eingereicht habe und die eingereichte schriftliche Fassung der auf dem elektronischen Speichermedium entspricht.

I hereby declare an oath that I have written the present dissertation on my own with the title:

"Membrane lipids of the (hyper)thermophilic, methanogenic archaea *Methanothermobacter marburgensis, Methanocaldococcus villosus* and *Methanothermococcus okinawensis* and their geobiological and astrobiological relevance"

and have not used other than the acknowledge resources and aids. All passages taken literally or analogously from other publications are identified as such. I further declare that this thesis has not been submitted to any other German or foreign examination board and that the submitted written version corresponds to that on the electronic repository.

……. ……

Ort, Datum
Place, Date

Die Doktorandin
The doctoral student